Design of Experimental Facility for Kinetic Turbines

by

Qing Sun

A thesis

Submitted to the Faculty of Graduate Studies

in Partial Fulfillment of the Requirement

for the Degree of

Master of Science

in

Mechanical Engineering

Department of Mechanical & Manufacturing Engineering

University of Manitoba

Winnipeg, Canada

©Qing Sun, 2004

THE UNIVERSITY OF MANITOBA

FACULTY OF GRADUATE STUDIES

*****

COPYRIGHT PERMISSION PAGE

Design of Experimental Facility for Kinetic Turbines

BY

Qing Sun

A Thesis/Practicum submitted to the Faculty of Graduate Studies of The University of Manitoba in partial fulfillment of the requirements of the degree of

MASTER OF SCIENCE

QING SUN ©2004

Permission has been granted to the Library of The University of Manitoba to lend or sell copies of this thesis/practicum, to the National Library of Canada to microfilm this thesis and to lend or sell copies of the film, and to University Microfilm Inc. to publish an abstract of this thesis/practicum.

The author reserves other publication rights, and neither this thesis/practicum nor extensive extracts from it may be printed or otherwise reproduced without the author's written permission.

Abstract

This thesis develops an experimental facility for kinetic turbines. The facility can allow various design parameters to be investigated, such as blade performance, flow separation and loss analysis with entropy generation contours. A novel method of transmitting power through a magnetic coupling is developed. The flow energy is converted to electrical energy by a DC generator. Measured data is presented for rotational rpm at varying flow velocities. The experimental facility is considered to provide a useful basis from which other turbine data can be studied. This data includes calculations of the rotational speed of the turbine runners, maximum power that the turbines can extract from the water flow and mechanical efficiency of the equipment.

Also, turbine models are developed for testing of performance in a water tunnel. These efforts involve building test equipment, as well as constructing a turbine runner for a kinetic turbine hydro application. Another turbine with a 2-D NACA 4412 airfoil on its blade section is designed and manufactured, for purposes of conducting PIV experiment in a water tunnel and investigating the performance of the kinetic turbines.

Moreover, the thesis is concerned with the design of effective testing equipment as well as the representation of blade profiles in terms of NURBS functions and traditional NACA airfoils, which implicitly satisfy the design parameters and provide flexibility and accuracy to develop turbine blade shapes. The variation of the angle of attack of the incoming flow in the spanwise direction is then obtained directly from a parabolic function for the blade geometry. A case study involving the analysis of a turbine is given and results are discussed. It is shown that the blade design in this study is

effective and it saves computational time, as compared with other commonly used iterative procedures.

Using a facility of a laser surface scanner along with the application of 3-D CAD modeling programs, an existing wind turbine blade and propeller were remodeled with reverse engineering technology. A comparison between the original turbine blade shape and the newly developed blade with NURBS representation is then made. It demonstrates the NURBS accuracy and flexibility in capturing a target blade profile or a target blade curvature distribution.

Acknowledgements

I would like to express my sincere appreciation and gratitude to my advisors, Dr. Greg F. Naterer and Dr. Dan. W. Fraser for their great insight, encouragement and guidance. I really enjoy the opportunity to work with them in this challenging field of research. I have benefited from their suggestions. Their valuable guidance and continuous support was extremely helpful in completing this thesis.

My thanks are due to Dr. Eric Bibeau, who contributed through his suggestions and response. I also thank Irwin Penner for his assistance when I was working in the machine shop.

I would like to thank Dr. Kenneth Snelgrove for reviewing the thesis.

The financial assistance offered by my advisors is gratefully acknowledged. It supported me through the difficult times.

Finally, I would like to thank my wife, Hongling, and my daughter, Yujia for their patience and support throughout the course of this graduate study.

Nomenclature

A_{Rotor}	Area swept by rotor blade
B	Number of blade
C	Chord length
C_d	Drag coefficient
$C_{d\min}$	Minimum drag coefficient
C_l	Lift coefficient
$C_{l\max}$	Maximum lift coefficient
C_m	Moment coefficient
C_{mac}	Moment coefficient at aerodynamic center
C_N	Cavitation Number
$\vec{C}(u)$	X and Y coordinate of curve
L	Length of blade
M	Mach number
n	Number of control point
n^R	Unit vector in normal direction
$N_{i,p}(u)$	Basis function
P_r	Reference pressure
P_v	Vapor pressure
$\vec{P}_i$	Control point

P_∞	Power carried by uniform free-flow
Re	Reynolds number
t^R	Unit vector in tangential direction
t_{max}	Airfoil thickness
t_{Pr}	Correction factor
U_i	Fluid velocity
U_n	Normal component
U_t	Tangential component
u	Knot value
V	Flow velocity
V_∞	Uniform free-flow velocity
V_{rel}	Relative flow velocity
$\dot{W}$	Mechanical power
w_i	Weight
α	Angle-of-attack
β	Twist angle
δ	Airfoil camber
ε	Efficiency coefficient
ρ	Density
Ω	Rotational velocity
Ω^*	Turbine Domain

Contents

List of Figures

Chapter 1

Introduction

1.1 Preamble

In today's industrial world, power generation is based predominantly on oil, followed by natural gas and coal. Water power and nuclear energy contribute only small part to the total demand. Growth potential of technically feasible hydropower exists in the world today, mostly in countries where increased power supplies from clean and renewable sources are most urgently needed, in order to allow social and economic development [1].

Although development of the entire world's remaining hydroelectric potential could not fully meet the future world demand for electricity, it is clear that hydro has a substantial role in the world energy supply. It is a resource with the greatest capability to provide clean renewable energy to parts of the world which have the greatest need. It can also offer a number of environmental and technical advantages, in terms of reduced power generation based on fossil fuels. When implemented as part of a multipurpose water resource development scheme, hydro power can offer a number of other benefits and subsidize other valuable functions of a reservoir or river system. No other source of energy can offer such benefits.

The development of hydro-electricity in the 20th century was usually associated with building of large dams. Hundreds of massive barriers of concrete, rock and earth were placed across river valleys world-wide to create huge artificial lakes. While they created a major, reliable power supply, plus irrigation and flood control benefits, the dams necessarily flooded large areas of fertile land and displaced many thousands of

local inhabitants. In many cases, rapid silting of the dam has since reduced its productivity and lifetime. There are also numerous environmental problems that can result from such major interference with river flows.

Hydropower on a small-scale is one of the most cost-effective energy technologies to be considered for rural electrification in less developed countries. It is also a main prospect for future hydro developments in the world, where the large-scale opportunities have either been exploited, or would now be considered environmentally unacceptable. Hydropower on a small scale involves the exploitation of a river's hydro potential without significant damming or negative social and environmental effects. Whether for powering of a house or small community, proliferation of small hydro on a wide scale could provide one of the most significant and benign energy options available. Small hydro technology is extremely robust and it is one of the most environmentally benign energy technologies available. The systems can last for 50 years or more with little maintenance. Small hydro is thus becoming increasingly recognized as a serious alternative for future decentralized energy supply [2].

1.2 Definition of Small Hydro

Hydropower has various degrees of size. To date there is not internationally agreed definition of small hydro; the upper limit varies between 2.5 and 25 MW. A maximum of 10 MW is the most widely accepted value worldwide. In the terminology of the industry, mini hydro typically refers to schemes below 2 MW, micro-hydro below 500 kW and pico-hydro below 10 kW. These are arbitrary divisions and many of the principles apply to both smaller and larger schemes [2].

1.3 Historical Background

Hydropower started with the wooden waterwheel. Waterwheels of various types have been in use in many parts of Europe and Asia for about 2,000 years, mostly for milling grain. By the time of the Industrial Revolution, waterwheel technology had been developed to a fine art, and efficiencies approaching 70% were being achieved in many tens of thousands of waterwheels that were in regular use. Improved engineering skills during the 19th century, combined with the need to develop smaller and higher speed devices to generate electricity, led to the development of modern-day turbines. Towards the end of that century, many mills were replacing their waterwheels with turbines, and governments were beginning to focus on how they could exploit hydropower for a large-scale supply of electricity.

The golden age of hydropower was the first half of the 20th century, before oil became the dominant force in power generation. Europe and North America built dams and hydropower stations at a rapid rate, exploiting up to 50% of the technically available potential. Hundreds of equipment suppliers sprung up to supply this booming market. Whereas the large hydro manufacturers have managed to maintain their business on export markets, particularly to developing countries, the small hydro industry has been in decline since the 1960's. A few countries have boosted this sector in recent years with attractive policies favoring green electricity supply, but small hydro in general cannot compete with existing fossil fuel or nuclear power stations. Without environmental incentives to use non-polluting power sources, there has been no firm market for small hydropower in developed countries for many years [2].

1.4 Current Status

Hydropower remains the most important renewable resource for electrical power production worldwide. The World Hydropower Atlas 2000 [3], published by the International Journal of Hydropower and Dams, reported that the world's technically feasible hydro potential is estimated at 14,370 TWh/year, which equates to 100% of today's global electricity demand. The economically feasible proportion of this amount is currently considered to be 8080 TWh/yr [2].

The hydropower potential exploited as of 1999 was 2650 TWh/yr, providing 19% of the planet's electricity from an installed capacity of 674 GW. It is expected that 135 GW of new hydro capacity will be commissioned in the period 2001–10. All other renewable energy source combined provided less than 2% of global consumption [2].

Small hydro (up to10 MW) currently contributes over 40 GW of world capacity. The global small hydro potential is believed to be in excess of 100 GW. China alone has developed more than 15 GW. It plans to develop a further 10 GW in the current decade [2].

1.5 Motivation of Developing Kinetic Turbine

Most hydraulic turbines that are presently used for hydropower generation have been developed for installation in water dams across streams. This conventional design is the most economical and energy efficient for river hydropower plants because it provides a maximum water head and forces all of the water to flow through the turbines under maximum hydraulic pressure. However, dams damage the environment and interfere with fish migration. They also cannot be used for power systems extracting energy from other

potential sources, such as ocean currents or low-grade rivers. Interest in low-head hydro electrical power generation, operating without water storage, has increased with the design of small efficient hydro-power generators and development agreement among government, manufacturers and utilities. A part of the impetus for these agreements is to promote the development of hydro power, which is observed to have less impact on migratory fish production than traditional high-head hydro power.

The opening in 1996 of a low –head hydro facility, operated by Morgan Falls Power Company and located on the LaHave River at Morgan Falls, Nova Scotia, provided an opportunity to assess the impact of a low-head hydro facility on downstream migration of Atlantic salmon smolts. Based on an assumption that all mortality was attributed to the turbine effect and not impingement on the temporary nets, the mortality was estimated as 60% [4], which represents a significant effect.

Thus, new hydraulic turbines are needed to operate efficiently in free flow without dams. For decades, scientists and engineers have tried unsuccessfully to utilize conventional turbines for free flow hydro. The very efficient hydraulic turbines in high heads become too expensive in applications with low and ultra low-head hydroelectric stations. For example, the unit cost of the Kaplan turbine jumps by a factor of 4 when the water head falls from 5 to 2 m [5]. The principal difference between exploiting high-head and free flow turbines is that the latter needs large flow openings to capture as much water mass as possible with low velocities and pressure. Conventional turbines, in contrast, are designed for high pressure and relatively small water ducts, where water cannot escape the turbine installed in the dam structure. According to the Bernoulli theorem, the density of potential energy of a fluid flow is proportional to the pressure,

while the density of the kinetic energy is proportional to the square of velocity. Conventional water turbines mainly utilize the potential component at the expense of the kinetic portion. In this capacity, they need ''high solidity'', where turbine blades cover most of the inside flow passage, while resisting water flow and building up water head. This causes the fluid velocity to fall and the kinetic component of Bernoulli's equation to become negligibly small, compared to the potential component. This is the reason why the higher water heads correspond to a higher efficiency of hydraulic turbines. The efficiency comes close to 90 percent in some cases. However, the situation is completely reversed for free water flows. In this case, the kinetic part dominates, and conventional turbines perform poorly, while becoming very expensive. For a free flow turbine, the main problem is that any attempt to use the flow passing through the turbine more effectively would result in an increase of streamlining flow and it might eventually decrease the net efficiency.

The purpose of this thesis is to examine the characteristics of a kinetic turbine in a free flow. This can be accomplished with experimental measurements of the fluid velocity and the rpm of the turbine runner. In order to achieve these goals, experimental equipment has been designed and constructed. Relevant studies have been performed in blade profile analysis for both 3-D and 2-D curvature surfaces. These measurements can reveal the performance of a run-of-the turbine in a water tunnel.

An important aspect of the design is the development of performance prediction methods. Another purpose of this study is to present analytical and direct procedures for evaluating the performance characteristics of kinetic turbines. The mathematical formulation of a run-of –the-river turbine power output problem is discussed in this thesis.

An explicit solvable model describing a certain procedure of blade design is proposed in this thesis.

Chapter 2

Literature Review and Turbine Technology

2.1 Turbine Theory Overview

Turbine performance is an essential element in the economic feasibility of renewable energy systems, namely wind and water energy. In such systems, blade aerodynamics, turbine design and wake flows are important design issues when striving to improve system efficiency.

An overview of historical developments and the current status of turbines for wind power generation are given by Ackermann and Soder [6]. Power grid integration, economics, environmental impact and offshore wind energy are discussed. It is reported that worldwide wind power generation has doubled approximately every three years. Due to these rapid advances, turbine technology has experienced appreciable evolutions over time.

The most effective utilization of renewable energy resources can be predicted from the Optimal Renewable Energy Model (OREM; Iniyan, Jagaeesan [7]). The cost / efficiency ratio can be minimized, so that existing energy resources can be optimally allocated. Factors including social acceptance, demand and reliability are incorporated in the model. A reliability factor of 0.5 during 10,000 hours of operation is determined for wind turbines of 200 kW capacities. In addition, the model is applicable to solar and biomass energy systems.

Hysteresis characteristics of a Wells turbine (see Figure 2.1) in reciprocating flows during wave power conversion are addressed by Setoguchi et al. [8]. Based on 3-D simulations of the Navier-Stokes equations, it is described how the hysteresis loop is

opposite to the phenomenon of dynamic stall of an airfoil. It arises predominantly with stream wise vertical flows appearing near the blade suction surface. Effects of setting angle and blade thickness on the Wells turbine performance are described by Setoguchi et al. [8].

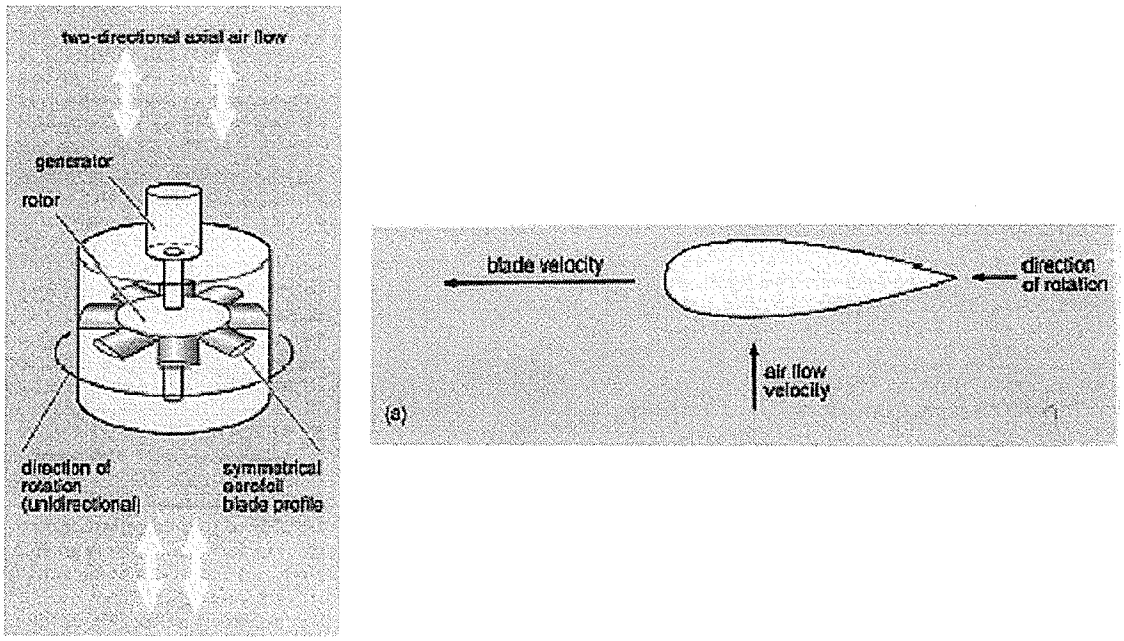

Figure 2.1 Wells Turbine [9]

Effects of blade sweep angle on Wells turbine performance are reported by Kim et al. [10]. NACA0020 and CA9 blade profiles were investigated. In the former case, an optimum blade sweep ratio of 0.35 was determined from 3-D numerical simulations. This produced better overall performance than optimal performance for the CA9 case. But a Wells turbine encounters lower efficiency and poor starting characteristics. Setoguchi et al. [11] suggest that guide vanes on either side of the rotor can overcome such limitations. Both numerical and experimental studies were performed by the authors, while confirming that 3-D guide vanes exhibit better performance than 2-D guide vanes.

A direct method of predicting aerodynamic performance of horizontal axis turbines is described by Maalawi and Badawy [12]. The optimum chord distribution is obtained from an exact trigonometric function method and Gluer's solution of an ideal windmill. Based on a given rotor size and turbine blade geometry, the calculation procedure gives the variation of angle of attack for the relative wind velocity. The predicted results are successfully validated for a case involving an existing turbine blade configuration.

Fluid mechanics of partially static and shrouded turbines is outlined by Grassmann et al. [13]. A rotating impeller extracts energy from the fluid motion, without fluid passing through the propeller itself. Such impellers may have promising capabilities for preventing cavitation in water turbines. Additional studies by Grassmann et al. [14] show that small wing profiled structures placed in the vicinity of turbines can augment their power output appreciably.

Thakker and Dhanasekaran [15] apply a numerical formulation for analyzing impulse turbines with fixed guide vanes for wave energy conversion. Three-dimensional effects of tip clearance are considered in the turbine performance. The numerical analysis is successfully validated against experimental data. Results suggest that a turbine with 0.25% tip clearance performs similarly to cases without tip clearance. But turbine efficiency is reduced by about 4% due to tip clearance flows at high flow coefficients.

Dimensional analysis for performance characteristics of impulse turbines is developed by Thakker and Hourigan [16]. The formulation is applied to different turbines under varying axial and angular velocities. Also, the optimum rotational speed for

maximum power output is predicted over a range of input power levels. It is shown how the optimal operating point can be achieved within the design range.

Mansouri et al. [17] examine an energy conversion system consisting of a wind turbine, speed multiplier and asynchronous generator. The generator is connected to a power network. It is observed that a large variation of power output leads to step-out operation of the generator, when the wind speed changes significantly. A control strategy is developed to reduce power variations, based on feed forward control and methods of conventional feedback control.

In contrast, Bahaj and Myers [18] examine marine current turbines for electric power generation from marine tidal currents. The marine current turbine is like submerged windmills (see Figure 2.2). It is installed in the sea at places with high tidal current velocities, to take out energy from the huge volumes of flowing water. These flows have the major advantage of being an energy resource as predictable as the tides that cause them. The turbine shown in Figure 2.2 consists of twin axial flow rotors, each driving a generator via a gearbox like a hydro-electric turbine or a wind turbine. The twin power units of each system are mounted on wing-like extensions either side of a tubular steel pole which is set into a hole drilled into the seabed from a jack-up barge.

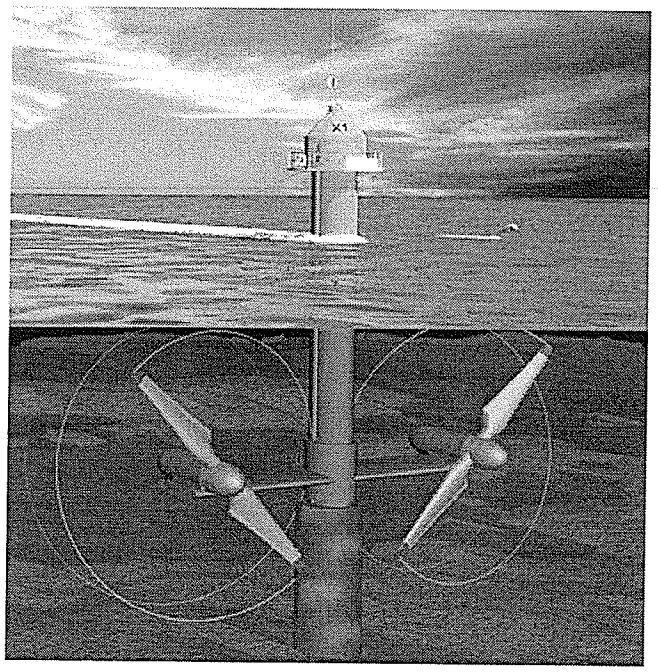

Figure 2.2 Marine Current Turbine [19]

High load factors are encountered in these systems. Bahaj and Myers suggest that virtually no previous work has been carried out to determine performance characteristics of turbines running in water for kinetic energy conversion. This article considers such systems. Technical challenges involving harsh marine environments, cavitation and high stresses on marine current turbines are addressed by Bahaj and Myers [18]. Unlike marine currents, a floating platform, enclosed generators and submerged turbines have been documented by Hartono [20] for generating energy from ocean currents.

A method of wave energy conversion, based on an OWC (Oscillating Water Column), is documented by Setoguchi et al. [21]. Wave energy is converted into low-pressure pneumatic energy of a bi-directional airstreams. A Wells turbine with zero blade pitch is used to convert this pneumatic power into unit-directional mechanical shaft power. A higher efficiency can be realized when the rotor blade pitch is set asymmetrically to a positive pitch. The performance characteristics of a turbine with

different blade setting angles were documented by the authors. Variations over time exhibit a pseudo-sinusoidal variation, whereby the amplitude of a half sine wave is greater than the corresponding negative half sine wave. A rotor blade setting angle of 2 degree was reported to be the optimal setting angle.

Self-rectifying turbines can extract mechanical shaft power in OWC energy conversion [22]. Optimum parameters for fixed guide vane turbines have been outlined by Setoguchi et al. [22]. This thesis develops a new experimental facility for investigating related turbine performance parameters, particularly for applications to small hydro. As discussed previously, there has been renewed emphasis worldwide in small hydro (1 to 10 MW) to harness energy from rivers using kinetic concepts.

An accurate estimate of the theoretical power limit of turbines in free fluid flows is important because of growing interest in the development of wind power and zero-head water power resources. The latter resource includes the large kinetic energy of ocean currents, tidal streams, and rivers without dams. Knowledge of turbine efficiency limits helps to optimize the design of hydro and wind power farms. An efficiency limit of 59.3 percent was obtained by Betz back in the 1920s for propeller-type turbines in free flow. It became common practice to use this limit for estimating the maximum efficiency of such turbines. The derivation of the Betz limit can be found in many textbooks and other publications on fluid mechanics.

A new model (called the GGS model) for a plane turbine in free flow with curvilinear streams was suggested by Gorban [5]. The most interesting result of the analysis shows that the maximum efficiency of the plane propeller is about 30 percent for free fluids. This is a sharp contrast to 60 percent given by the Betz limit. The model also

indicates that the three-dimensional helical turbine is more efficient than the two-dimensional propeller and it has an efficiency of 35 percent, thereby making it preferable for free water currents [5].

2.2 Renewable Energy Developments

In order to counter the effects of global warming from the combustion of fossil fuels, a rapid shift towards renewable energy development is now underway. As discussed previously, economic projections indicate that this trend will continue to accelerate rapidly into the 21st Century. Wind and solar power developments have been leading the way with annual capacity increases of 25.7% and 16.8% respectively, between 1990 and 1997 [23]. Planning renewable energy projects requires many stages of technical and financial study to determine if a site is technically and economically feasible. The viability of each potential project is very site specific. Power output depends on the flow rate of water (or wind) and its associated head. The amount of energy that can be generated depends on the seasonal availability of these flow rates and flow variability throughout the year.

The economics of a site depends on the power (capacity) and energy that a project can produce, if the power can be sold and the price paid for the power sold. In a remote community, the value of power generated for consumption is generally significantly more than for systems that are connected to a central grid. However, remote communities may not be able to use all of the available energy from a small hydro plant, or may be unable to use the energy when it is available because of seasonal variations in flow rate and energy consumption.

Work on the selected site or sites would require site mapping and geological investigations (with drilling confined to areas where foundation uncertainty would have a major effect on costs); a reconnaissance for suitable borrow areas (i.e., for sand and gravel); a preliminary layout based on materials known to be available; preliminary selection of the main project characteristics (installed capacity, type of development, etc.); a cost estimate based on major quantities; the identification of possible environmental impacts; and production of a single volume report on each site.

Such work would include studies and final design of the transmission system; integration of the transmission system; integration of the project into the power network to determine the precise operating mode; production of tender drawings and specifications; analysis of bids and a detailed design of the project; production of detailed construction drawings and a review of manufacturer's equipment drawings. However, the scope of this phase would not include site supervision or project management, since this work would form part of the project execution costs.

For example, Blue Energy Canada is commercializing the Davis Hydro Turbine, which is a technological breakthrough that can generate high-density renewable and emission-free electricity from ocean currents and tides at prices competitive with the cheapest conventional sources of energy today. For example, over an 11-year period, Blue Energy has leveraged $300 million of Intellectual Property development into a world-class renewable energy system. Designed by eminent Canadian aeronautic and hydrodynamic engineer Barry Davis, the development lineage of the Davis turbine is directly linked to two engineering marvels that preceded its development. These marvels are the famous Avro Arrow and the D'Havilland Bras D'Or 400 naval destroyer produced

by the Canadian navy. The Davis turbine is supported by 6 successful prototypes funded by the Canadian National Research Council [24].

In another example, since 1981, UEK (Underwater Electric Kite) Corporation has developed a practical way to harness river, tidal and ocean currents with Hydro Kinetic turbines. After exploring many configurations and constructing and testing several prototypes, UEK has a design which is efficient and competitive with other sources of energy, plus no fuel costs, no pollution and no environmental disturbance. UEK's renewable technology is now ready for applications where a lack of grid infrastructure makes conventional sources of electric power expensive, especially in rural areas where the cost of transmission lines is an unacceptable burden to power generation access. The UEK turbine is positively buoyant or mounted at the seabed by a single anchorage system. Keeping a controlled operational depth, the turbines are not affected by the surface effect of large waves or navigation. Lateral positioning controls permit the turbines to stay in the core of the current, making the turbine efficient and cost effective [25].

UEK's niche lies in the range between 0.5 Megawatts to hundreds of Megawatts, when sites are developed in underwater groups of twelve units or more. Furthermore, since there is no civil engineering such as dams or impoundments, patented free flow hydro kinetic turbines can be installed quickly. They can produce power within months after "Turn Key" contracts are signed. In conjunction with Ontario Power Generation, UEK is testing Twin turbines (see Figure 2.3). The 10 ft. Twin is designed for rural electrification in river setting for small agglomerations where grid interconnection is prohibitive due to the economics of distance [26]. Since there is no civil engineering such as dams or impoundments and the turbines require no support structures, these free flow

hydro kinetic turbines are installed quickly and can produce power within months. This technology is for applications where lack of grid infrastructure makes conventional sources of electric power expensive, especially in rural areas where the cost of transmission lines is an unacceptable burden to power generation access [25].

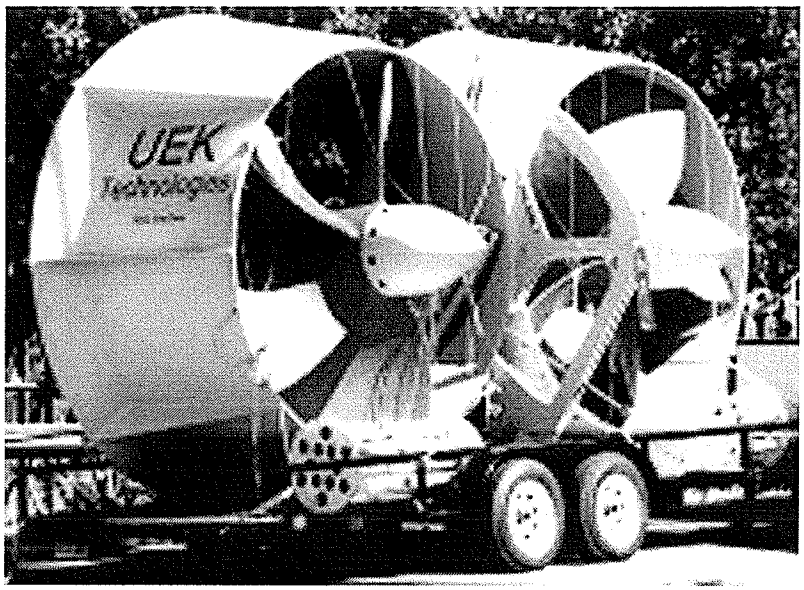

Figure 2.3 UEK 10 ft. Twin Turbines [25]

2.3 Technology of Low Head Hydraulic Turbines

2.3.1 Kaplan Turbine

The increasing need for more power during the early years of the twentieth century led to the invention of the Kaplan turbine. The idea is based on a propeller, similar to an airplane propeller (see Figure 2.4). The design has been improved by means of swiveling blades that improve the efficiency of the turbine in accordance with the prevailing conditions. Its invention allowed efficient power production in low head applications. Therefore, it has been developed to be the most popular type of turbine for low heads and comparatively large discharges.

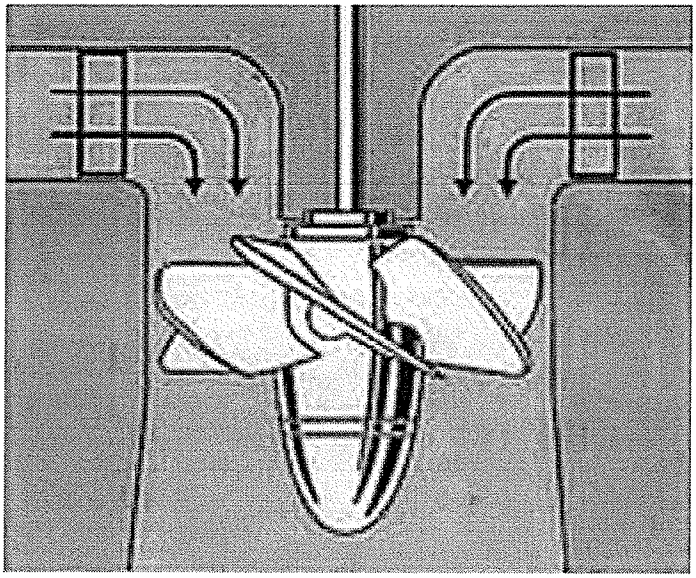

Figure 2.4 Kaplan Turbine [27]

The Kaplan turbine is an inward flow reaction turbine, which means that the working fluid changes pressure as it moves through the turbine and sets free its energy. The turbine design combines radial and axial features.The inlet is a variable cross section scroll shaped tube that wraps around the turbine's wicket gate. Water is directed tangentially, through the wicket gate, and spirals on to a propeller shaped runner, causing it to spin.The outlet is a specially shaped draft tube that helps decelerate the water and further reduces the kinetic energy of the water flow, thereby increases ΔP across the turbine.

The runner has only a few blades radial oriented on the hub and without an outer rim. The runner blades have a slight curvature and cause relatively low flow losses. This allows for higher flow velocities without great loss of efficiency. Accordingly, the runner diameter becomes relatively small and the rotational speed is more than two times higher than for a Francis turbine at the same head and discharge. In this way, the generator dimensions as well become comparatively smaller and cheaper.

The runner's blades are movable. The guide vanes can also be turned and automatically adjusted to any angle suitable to the flow conditions. The comparatively high efficiencies at partial loads and the ability of overloading are obtained by a co-ordinate regulation of the guide vanes and the runner blades to obtain optimal efficiency for all operations, so the turbine is efficient at different work-loads.

The turbine does not need to be at the lowest point of water flow, as long as the draft tube remains full of water. The higher the turbine is located, however, the more suction is imparted by the draft tube and cavitation becomes possible.

Variable geometry of the wicket gate and turbine blades allow efficient operation for a range of flow conditions. Kaplan turbine efficiencies are typically over 90%, but may be lower in very low head applications.

Kaplan turbines are widely used throughout the world for electrical power production. They cover the lowest head hydro sites and are especially suited for high flow conditions.Inexpensive microturbines are manufactured for individual power production with as little as two feet of head.Large Kaplan turbines are individually designed for each site to operate at the highest possible efficiency, typically over 90%. They are very expensive to design, manufacture and install, but operate for decades.

2.3.2 Bulb Turbine

The bulb turbine is a reaction turbine of Kaplan type in which the entire generator is mounted inside the water passageway as an integral unit with the turbine. These installations can offer significant reductions in the size of the powerhouse. The bulb turbine is an axial flow unit, i.e. the flow runs parallel with the centerline of the set. This

centerline is horizontal or sloping slightly downstream (see Figure 2.5). The water thus passes through the set in a straight line from the intake of the water chamber to the draft tub outlet.

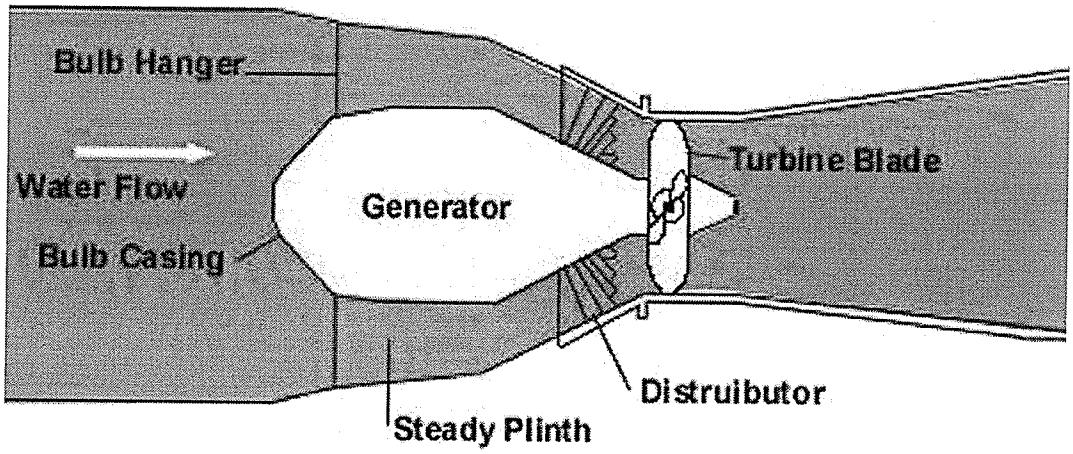

Figure 2.5 Bulb Turbine [28]

The Bulb turbine runner is of the same design as for the Kaplan turbine, and it may also have a different numbers of blades depending on the head and water flow. A bulb set consists of a horizontal shaft Kaplan turbine with fixed or movable distributor (guide wheel), driving an alternator mounted in a watertight bulb. A main difference from the Kaplan turbine is that the water flows with a mixed axial-radial direction into the guide vane cascade and not through a scroll casing. The guide vane spindles are inclined (normally 60°) in relation to the turbine shaft. A straight water passage instead of usual spiral case and the draft tube elbow of a Kaplan turbine results in better utilization of the primary energy and reduced powerhouse dimensions.

Most bulb turbines are supported by two bearings placed in the bulb casing. One arrangement is to have the turbine runner and generator rotor mounted on one common shaft and overhang on both sides of the bearings. Another arrangement uses separate

shafts for the turbine and generator, with the generator rotor situated between the turbine guide bearing and upstream combined thrust guide bearing. The construction employing one main shaft with overhang runner and rotor has been widely used in large capacity bulb units of recent manufacture.

Alternator (bulb casing) may be located either upstream or downstream of turbine runner and it is even possible to use two alternators on either side of runner. This arrangement considerably increase the specific output of this type of machine, for the capacity is limited only by that of the alternator that can be accommodated within the dimensions imposed by hydraulic circuit. The bulb diameter must not be more that 20 percent large than runner diameter, as beyond this , the length of the conic transition in front of the runner hub becomes excessive as regards the civil works and equipment. On the other hand, minimum bulb diameter seems to be limited to 20 percent less than runner diameter for reasons of electrical design.

The bulb is filled with air, oil or compressed gas, whatever the medium, the circulation of the fluid carries the heat to be dissipated to the wall of the unit. This bulb is situated within the stream of water, and guide vanes of the distributor serve as a support for bulb assembly.

Since the bulb set is completely submerged under pressure, water leakage into the generator chamber and condensation are source of trouble. A shaft seal box can be used for the bulb turbine with the sealing purpose (see Figure 2.6).

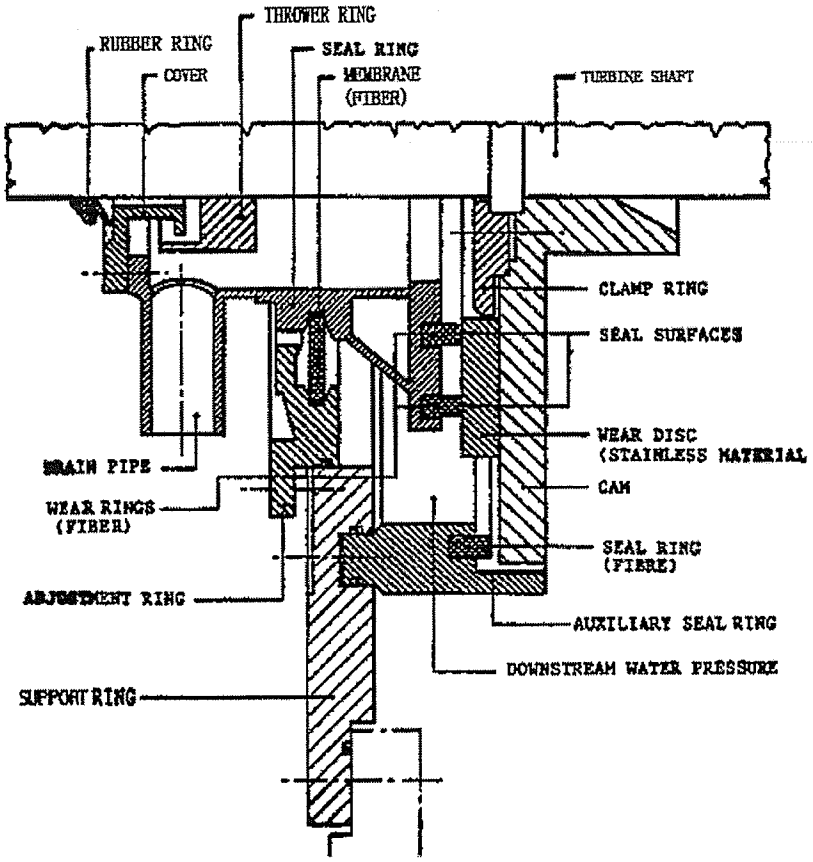

Figure 2.6 Shaft Seal Box [29]

This box has radial seal surfaces consisting of a stainless hardened wear disk and two wear rings made of Teflon type fibers. The wear disk is bolted to a cam fixed to the shaft. The wear rings are glued to the seal ring. This is movable and supported in the adjustment ring by means of a membrane. The membrane allows the seal ring to move axially 5-6 mm. This is necessary for the shaft movement in the downstream direction when the unit is loaded. In addition allowance must be made for wear of the seal surfaces. The adjustment ring is bolted to the support ring and may be axially adjusted by means of double acting jacking screws. According to the wear range of wear rings the adjustment range of the seal box should be 8-10 mm.

The auxiliary seal is located in the support ring. This may be pushed against/pulled away from the cam by means of push/pull jacking screws. When this ring is in contact with the cam the wear seal rings may be dismantled without draining the unit. Possible water leakage into the seal box is drained through a pipe to the pump sump. A thrower ring is mounted on the shaft to prevent water leakage along the shaft. A rubber ring is mounted on the upstream end of the shaft and seals against the seal box cover. The seal box is provided with four springs which are pressing the wear seal rings against the seal surface to prevent leakage when the balance system is out of operation, e.g., when filling the turbine [29].

Although improvements in waterproofing and sealing techniques have reduced this problem considerably, this can still become maintenance problem due to high humidity inside the chamber resulting in gradual deterioration of electrical insulation. Since the generator is to be mounted in restricted space, this is certainly not favorable from electric point of view.

2.4 Kinetic Turbine

Kinetic power generation technology is also called free-flow hydropower technology or kinetic hydro energy system, which generates electricity power from the kinetic energy present in flowing water. The basic technology is really applying what has been learned in the wind-power industry to water currents.

For a free flow turbine, the main attempt is to use the flow passing through the turbine more effectively or increase the net efficiency. Its power output can be formulated

in terms of free-flow velocity, V_∞, an efficiency ε, fluid density ρ and the area swept by the rotator blade, A_{Rotor}.

Suppose that the turbine is placed in a straight, uniform laminar current flowing towards the positive x-axis at velocity V_∞. Denote the region where the turbines are located by Ω^*, and assume that Ω^* is an open domain with a smooth or piecewise smooth boundary. Clearly, the projection of Ω^* onto the yz-plane is equal to the area A_{Rotor} (see Figure 2.7).

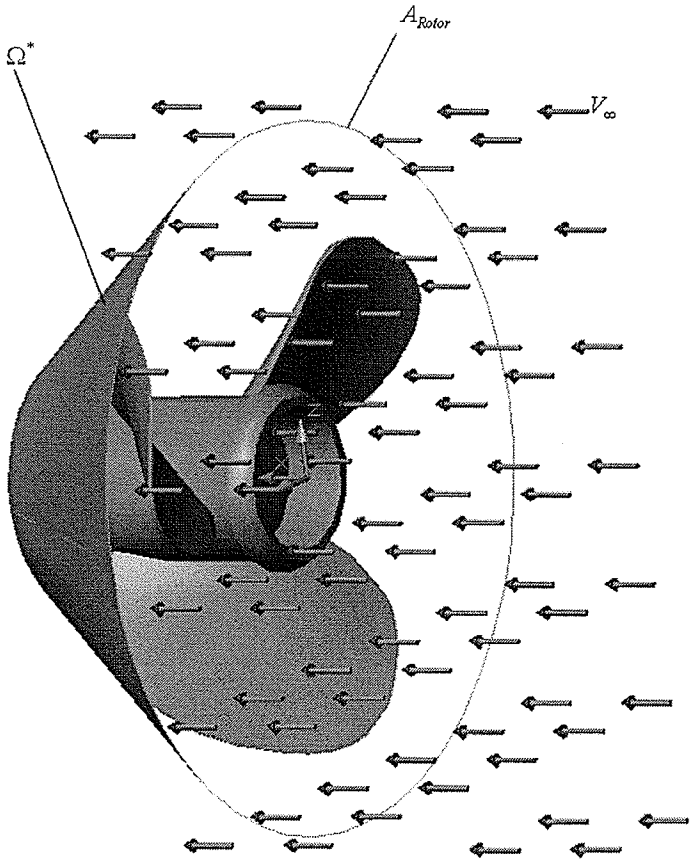

Figure 2.7 Description of Model for Kinetic Turbine in Uniform Laminar Flow

The power carried by the flow through Ω^* is given by

$$P_{\infty} = \frac{1}{2}\rho A_{Rotor} V_{\infty}^{3} \tag{2.1}$$

The power consumed by the turbine can be determined by

$$P = \varepsilon P_{\infty} = \frac{1}{2}\varepsilon \rho A_{Rotor} V_{\infty}^{3} \tag{2.2}$$

The efficiency coefficient ε of a free-flow turbine is the ratio of the consumed power P to the power P_{∞} carried by the flow through the projection of the turbine section region onto the plane perpendicular to it. The expression for the efficiency is given by

$$\varepsilon = \frac{\int_{\Omega^*} \nabla p \cdot V \, d\Omega^*}{\frac{1}{2}\rho A_{Rotor} V_{\infty}^{3}} \tag{2.3}$$

where p and V denote the pressure and the velocity of the flow, respectively [5]. Setting $\varepsilon = 0.3$, $\rho = 1000 kg/m^3$ and $A_{Rotor} = 1\, m^2$, the corresponding curve is plotted in Figure 2.8.

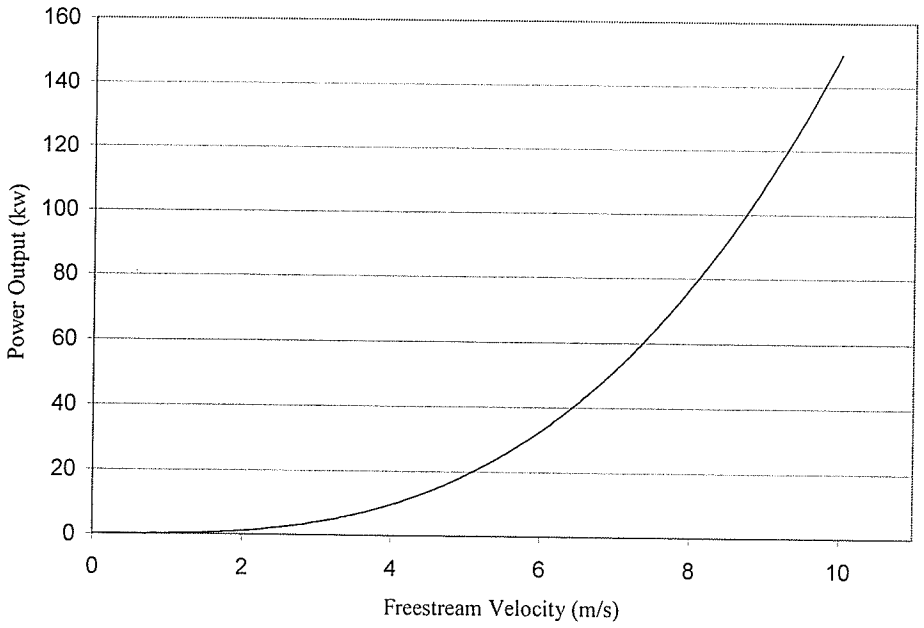

Figure 2.8 Power Output vs. Velocity

2.4.1 Axial-Flow Rotor Turbine

The design of these turbines consists of a concentric hub with radial blades, similar to that of a windmill (see Figure 2.9). Mechanical power is applied directly through a speed increaser to internal electric generator, or through a hydraulic pump that in turn drives an onshore electric generator.

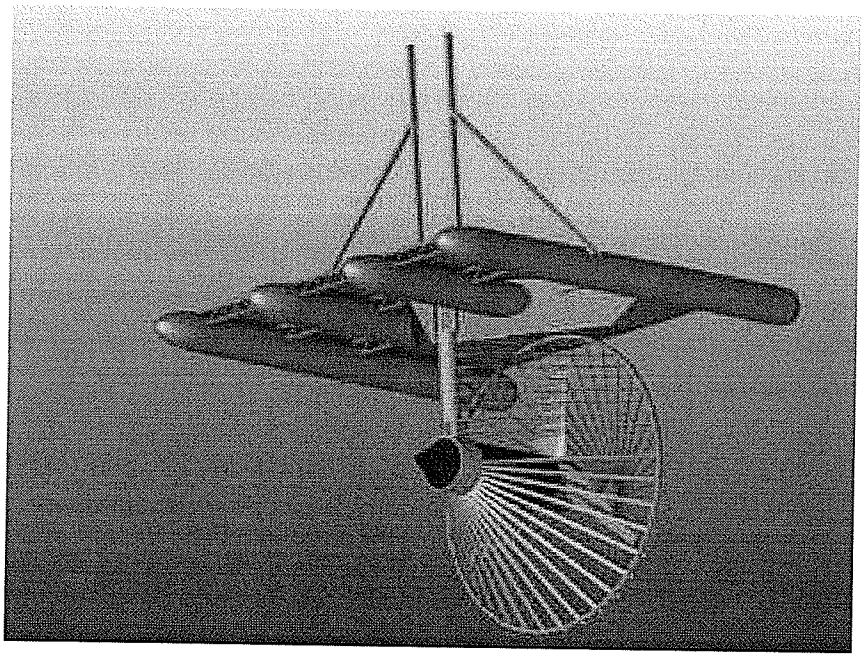

Figure 2.9 Axial-Flow Rotor Turbine [30]

2.4.2 Helical Turbine

This turbine is a low head, reaction cross-flow hydraulic turbine. The blades have hydrofoil sections that provide tangential pulling forces in the cross water flow (see Figure 2.10). These forces rotate the turbine in the direction of the leading edge of the blades. Thus, the direction of turbine rotation depends only on orientation of blades and not on direction of the fluid flow.

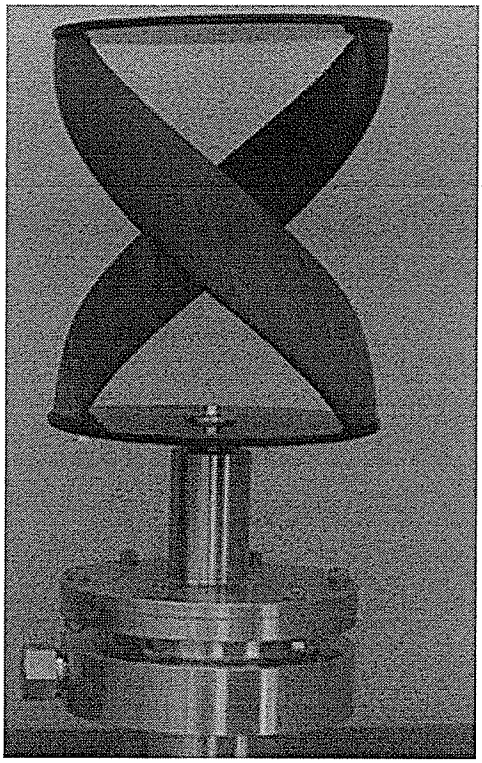

Figure 2.10 Helical Turbine [31]

2.4.3 Cycloid Turbine

It is a paddle wheel with articulating blades. The turbine works by placing a blade broadside to the flow while the opposing blade is feathered to the local flow (see Figure 2.11).

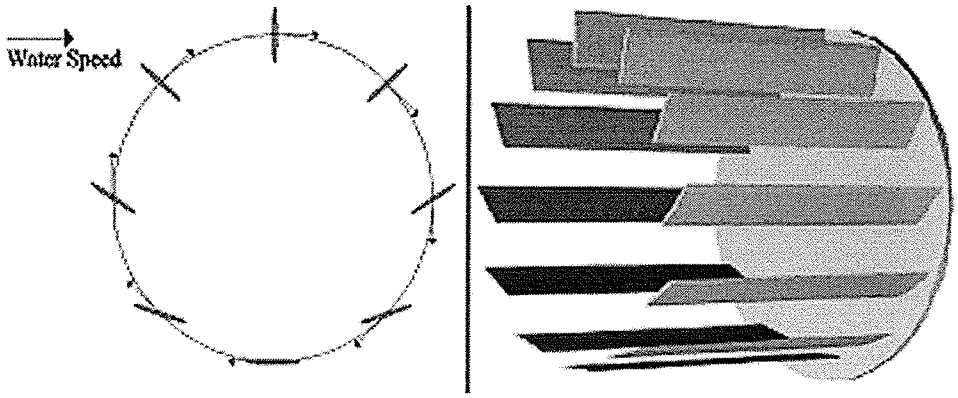

Figure 2.11 Cycloid Turbine [30]

2.4.4 Tyson Turbine

The Tyson turbine extracts power from the flow of water, as opposed to the fall of water which powers most hydropower systems(see Figure 2.12). It consists of a large propeller mounted below a raft, driving a generator, on top of the raft by belt or gear. The turbine is towed into the middle of a river or stream, where the flow is the fastest, and tied off to shore to keep it there. It requires no local engineering, and can easily be moved to other locations.

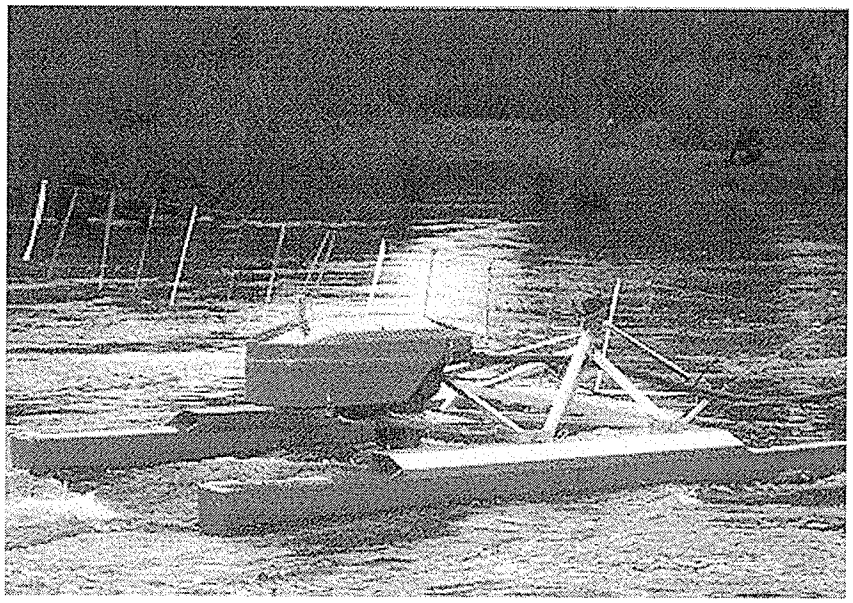

Figure 2.12 Tyson Turbine [32]

2.5 Turbine Design and Development

The ability to economically derive benefits from small hydro power systems leads to a substantial reduction of civil structures like dams to reduce costs and environmental impact. For low head applications with high flow rates, a larger cross-sectional area for the hydraulic equipment must be used to obtain the required power densities. However, since the power is proportional to the velocity cubed, an increase in flow velocity can

cause a significant increase in power density across the same flow cross-section. Therefore, maximizing flow velocities will minimize the diameter of the turbine impeller for a given output. Flows with significant velocities contain a large amount of energy without the requirement of substantial head (kinetic versus potential energy are equivalent from an availability standpoint).

However, conventional turbine designs require head for performance, mainly to avoid cavitation across the blades. There are still significant technology gains to be made in this area and the opportunity exists to develop a new class of turbines for low to high-speed flows. This requires searching for novel ways to deploy low head turbines in a channel with minimum environmental impact and without requiring a dam. The turbine/generator could be made submersible. Hence, the environmental impact would be almost negligible. Such concepts already exist (hermetically sealed units), although such turbine generator units are not able to perform at higher velocities. Most current designs are meant for tidal flows where the velocity rarely exceeds 5 ft/s.

Hydraulic turbine runners are considered by many experts in turbomachinery to be the most crucial component in hydraulic generators. There are many types that vary in shape, construction, size, and number of blades. Designers often try to achieve the following goals, while considering and combining different factors simultaneously: highly efficient performance, wide ranging capabilities, low costs of manufacturing and maintenance, as well as a long lifespan. However, these constructions can encounter more difficulties than initially expected during the design process.

For example, a technical challenge is the determination of parameters for the curved-face of the blades. Designers often take advantage of existing design theories and

experiences in an attempt to determine suitable parameters such as diameter, pitch, width and outline of the turbine runner. Those theories are often based on ideal conditions, such as laminar flow or a small Reynolds number. These idealizations can be inadequate when dealing with practical situations involving highly turbulent and complex flows.

Another important factor that designers must consider in small hydro systems is cavitation, which can occur behind the turbine runners under conditions of low pressure and high speed. This type of cavitation has significance because it restricts the speed at which the turbine runners may be operated.

If cavitation becomes severe, it lowers efficiency and produces significant noise and vibrations. It can also cause rapid erosion of the surfaces, even though those surfaces usually consist of cast iron, bronze or other hard and normally durable materials. For an effective design, highly efficient performance should be achieved. On the other hand, cavitation must not occur while the turbine is operating. Turbine designers have struggled with this dilemma. As a result, they usually take a compromised efficiency of the turbine in order to reduce the occurrence of cavitation.

Establishing suitable equipment for turbine testing is an effective method that turbine designers can utilize. In this thesis, such testing is developed in a water tunnel at the University of Manitoba. In this way, a set of useful data can be provided for the turbine design. From analysis of this data, the key parameters of a curved-face blade in turbine runners can be determined.

In addition, experiments to determine the cavitation number can be made on models geometrically similar to the prototype installation. The water tunnel testing has the advantage of lower cost and more precise control than field testing. Also, it permits

correction of undesirable characteristics of a design before the prototype machine is actually constructed. For instance, if it is found in a model test that a given turbine runner design cavitates heavily at a design operating value, then different combinations of diameter and pitch, revolutions, blade width and outline, or section shape may be tested to eliminate or alleviate the observed cavitation.

Moreover, hydraulic turbines must be designed individually according to the local operating conditions, such as discharge, and given geometrical situations. This requires a tailor-made design mainly for the turbine runners. The shapes of the runners are complicated and the understanding of the complex geometry and spatial structures of the flow is very difficult to analyze by two-dimensional display tools. Many different views and cuts must be prepared and analyzed, which is quite uneconomical and time consuming. A design tool based on virtual reality techniques has been developed at the Institute for Fluid Mechanics and the Hydraulic Machinery (IHS) and the Computing Center (RUS) at the University of Stuttgart in Germany.

In a virtual reality environment, however, the complex geometry and flow behavior can be controlled much faster, with more detail. The software for the VR system integrates visualization and simulation tasks across heterogeneous hardware platforms in a seamless manner. The user interface is based on a visual programming paradigm. Distributed applications can be built by combining modules from different application categories on different hosts to form more or less complex module networks. At the end of such networks, the rendering step usually completes the final visualization. A special feature allows several users to work in a collaborative way, thereby providing online consulting to end users at remote sites.

Chapter 3

Fluid Dynamics of a Hydro Turbine

3.1 Definitions

Fluid dynamics involves the study of physical laws of the behavior of fluid flow and the forces that are produced by the fluid. The front and rear sides of a hydro turbine blade have a shape similar to a sector or fan-shape with the edges bounded by the leading edge, the trailing edge, blade tip and blade root. The blade root is blended together with the hub (see Figure 3.1).

The radius of the blade is the distance from the centre of the rotor shaft to the outer edge of the blade tip. The cross section of a blade usually has a streamlined shape, with the flattest side facing the oncoming incoming water flow.

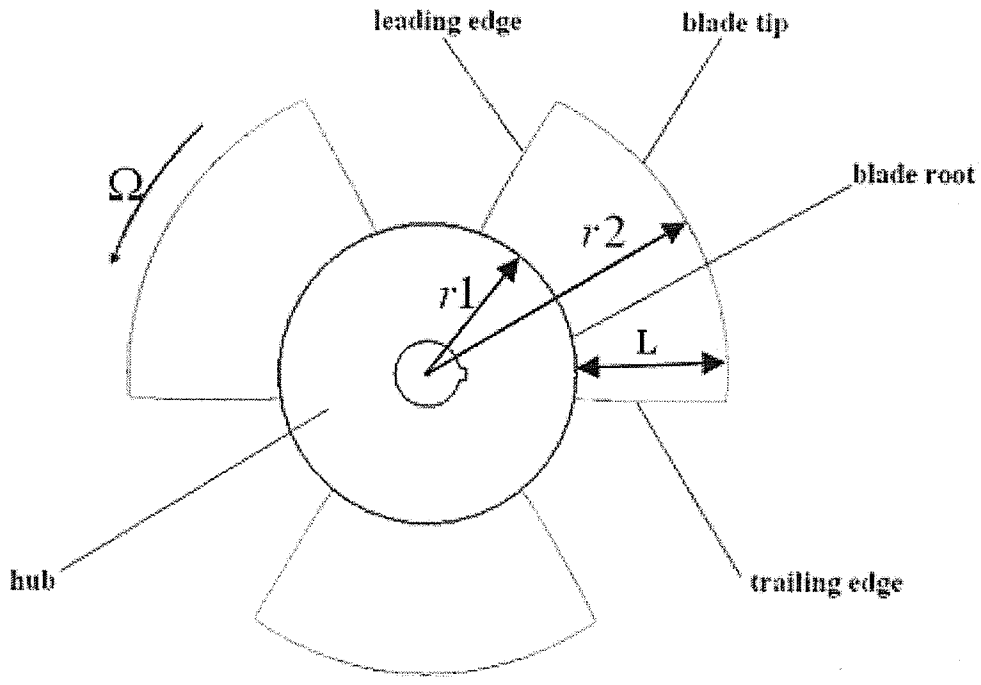

Figure 3.1 Different Parts of Hydro Turbine Blade

3.2 Airfoil

If the blade is sliced with a plane vertical to the spanwise direction, the intersection of the blade surfaces with that plane is called an airfoil. The airfoil shape can vary if the slice is taken at different locations on the blade (see Figure 3.2). However, for any given slice, we have a given airfoil. An assumption can be made that the airfoil has an infinitely long span with the same cross-sectional shape. Such an airfoil is called a two-dimensional airfoil.

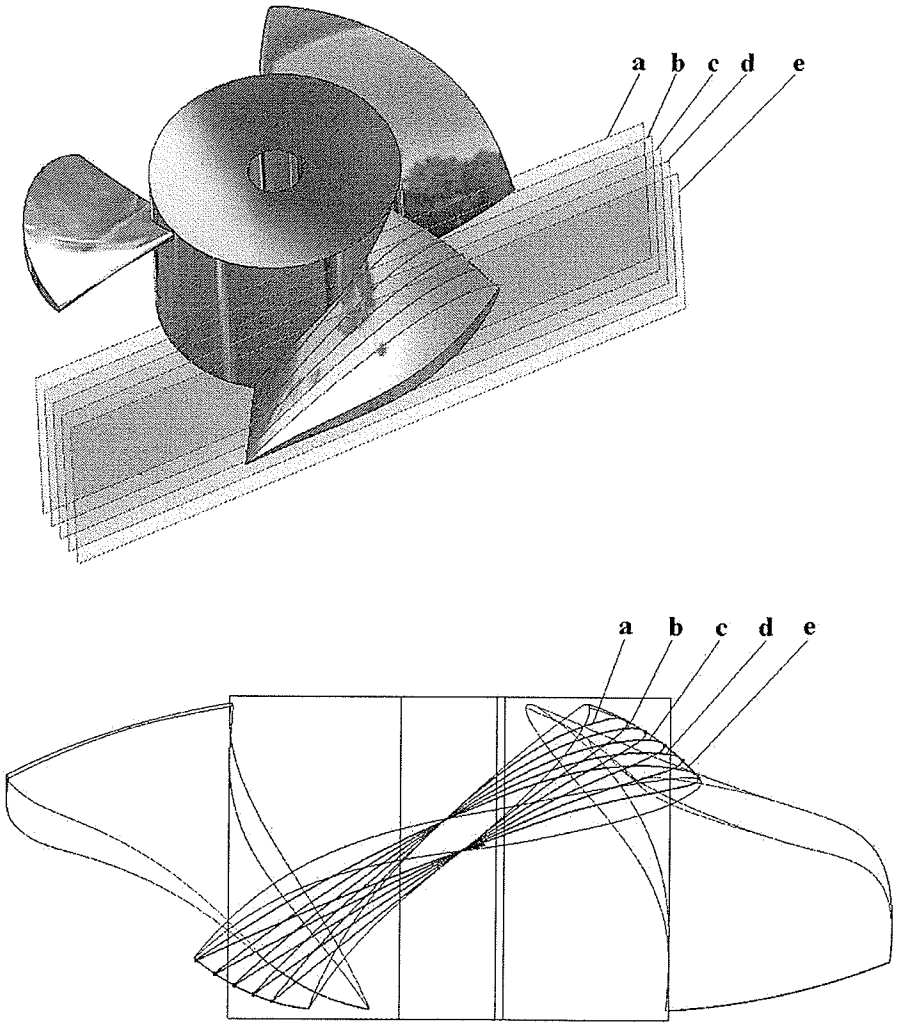

Figure 3.2 Different Airfoil Shapes on Different Intersecting Planes

Since the calculation of lift and drag coefficients with a reference area of infinity would not be feasible, we calculate airfoil lift and drag coefficients for airfoils based on the planform area, assuming a unit span. In practice, it is approached on the interior portion of an extremely long airfoil or an airfoil mounted wall-to-wall in a wind tunnel or water tunnel testing section. The exterior portions of the airfoil are excluded to avoid tip effects caused by the trailing tip vortices, which result from the three-dimensional flow over a finite airfoil and wall boundary layer effects. Two-dimensional airfoil properties are an integral part of the analysis of the three-dimensional flow characteristics over a finite airfoil.

3.3 Airfoil Terminology

Figure 3.3 shows a 2-D airfoil section. It consists of the leading edge (LE), trailing edge (TE) and the line joining the two edges called the chord (C). The angle-of-attack is generally measured between the velocity vector, V (or relative velocity vector, V_{rel}), and the chord line C.

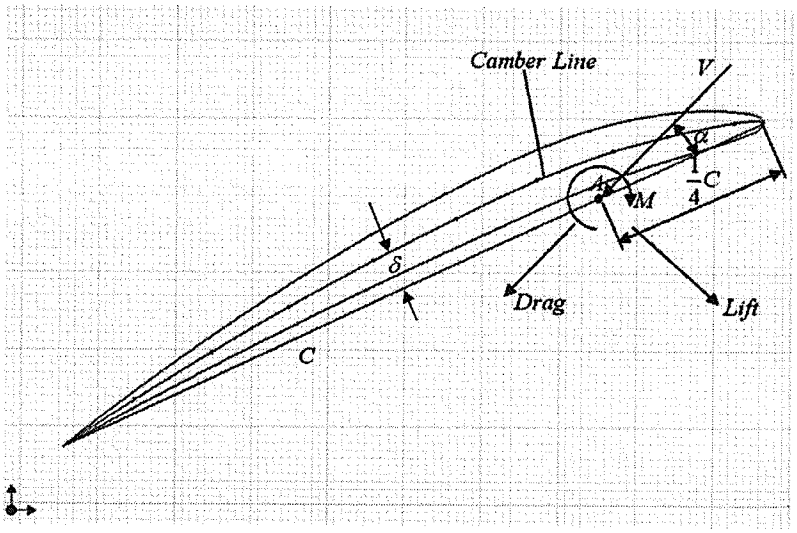

Figure 3.3 2-D Airfoil Section

The camber line is midway between the upper surface and lower surface. The maximum distance from the chord line to the camber line is designated as the airfoil camber (δ). It is generally expressed as a percent of the chord line. The maximum distance between the upper and lower surface is the airfoil thickness, t_{max}. It is designated as a percent of chord length [33]. Then,

$$\frac{\delta}{C} \times 100 = \%\, camber \qquad \frac{t_{max}}{C} \times 100 = \%\, thickness \tag{3.1}$$

3.3.1 Lift Characteristics

The aerodynamic properties of most interest for performance considerations are associated with lift and drag. A typical graph of lift coefficient vs. angle-of-attack is plotted in Figure 3.4.

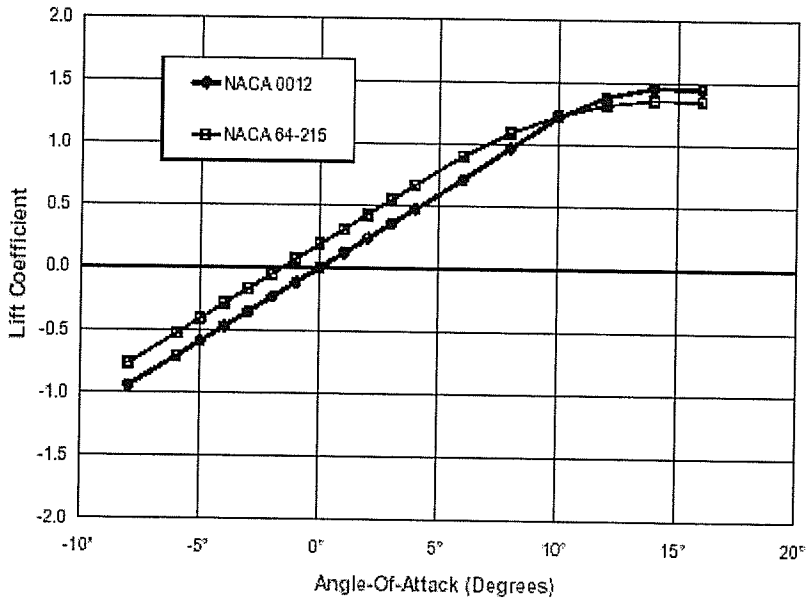

Figure 3.4 Lift Coefficients versus Angle-of-Attack [34]

From Figure 3.4, for small angles-of-attack, the lift curve is approximately a straight line. We will use this assumption and deal mainly with "linear" aerodynamics. For high attack angles (called the stall angle-of-attack), the lift coefficient reaches a maximum. Also, there are two intercepts that we can designate: the alpha (α) axis for zero lift, designated as the zero-lift angle-of-attack, and the intercept at zero angle-of-attack, designated as the lift at zero angle-of-attacks [33].

3.3.2 2-D Moment Characteristics

A reference point is defined to calculate an aerodynamic moment for an airfoil. Typical reference points are the leading edge of the airfoil and the 1/4 chord location of the airfoil. The force and moment system on an airfoil is shown in Figure 3.3. The drag is parallel to the relative flow, and the lift is perpendicular to the flow velocity, V. The dynamic moment is positive, nose up. Here we are taking the moment about point A. Once we pick the point, we can represent the force and moment system by assuming that the forces act thorough a given point and that there is a pure moment about that point.

3.3.3 Drag Characteristics

The drag on a 2-D airfoil is primarily due to viscous effects at low speed and compressibility effects (wave drag) at high speed. In addition, at high angles of attack, the flow can separate from the upper surface and cause additional drag. Hence the drag coefficient depends on two quantities, namely the Reynolds number and the angle-of-attack. Typically the Reynolds number is important at low speeds and the angle-of attack at all speeds.

3.4 Effects on Aerodynamic Coefficients

Airfoil theory shows that aerodynamic forces and moments can be expressed in terms of the free stream dynamic pressure, a characteristic length of the chord and a dimensionless coefficient, which is a function of the angle of attack, camber, and Reynolds number. For lift, drag and moment, these become, respectively [32].

$$\frac{L}{b} = \left(\frac{1}{2}\right)\rho V^2 c C_l \tag{3.2}$$

$$\frac{D}{b} = \left(\frac{1}{2}\right)\rho V^2 c C_d \tag{3.3}$$

$$\frac{M}{b} = \left(\frac{1}{2}\right)\rho V^2 c^2 C_m \tag{3.4}$$

$$C_l = f_l(\alpha, camber, \mathrm{Re}) \tag{3.5}$$

$$C_d = f_d(\alpha, camber, \mathrm{Re}) \tag{3.6}$$

$$C_m = f_m(\alpha, camber, \mathrm{Re}) \tag{3.7}$$

Aerodynamic theory shows that lift and moment are little affected by viscous effects below stall. Thus they are nearly independent of Reynolds number. Therefore, the theory used to predict lift and moment effects at angles of attack below stall are for incompressible flow, in which the only stress is the hydrostatic pressure. This pressure, related to the velocity by the well-known Bernoulli equation, gives the section lift and moment.

Drag, on the other hand, requires consideration of viscous effects. Even for angles of attack below stall, it is dependent on the Reynolds number. Summarizing, lift is affected by the angle of attack and camber. Only camber affects the moment about the

aerodynamic center (the aerodynamic center is the location about which the moment is independent of angle of attack) and drag is affected by the angle of attack, camber and thickness.

3.4.1 Effects on Lift

Theory predicts and past experiment verify that the relationship between C_l and α is essentially linear, below stall. Viscous effects have a secondary influence. As Re increases, the lift curve slope increases slightly, while if Re decreases, the lift curve slope decreases significantly if Re drops below approximately 500,000.

Stall is dependent on viscous effects and therefore dependent on Re. For most airfoils, it occurs between approximately 12 and 16 degrees angle of attack. Stall occurs at the point at which the upper surface boundary layer has significantly separated, thereby resulting in a reduction of the upper surface suction and hence a decrease in the lift. This condition defines $C_{l\max}$, the maximum lift coefficient. Operation much beyond stall is not generally useful. Past experiments show that $C_{l\max}$ increases with Re. Both $C_{l\max}$ and α (at which $C_{l\max}$ occurs) are significantly reduced at Reynolds numbers less than about 500,000.

Camber effects are generally limited to effects on the angle of zero lift. This is the angle through which the chord line must be rotated to produce zero lift. Zero lift is the reference level for aerodynamic performance. It is usually a negative angle, seldom less than about 4 degrees. Positive camber produces a negative angle of zero lift. Camber is generally less than about 6% of the chord. Positive camber results in a shift in the lift

curve to the left. Consequently the angle of attack referenced to the chord line is reduced. Camber also increases $C_{l\max}$, but the angle at which $C_{l\max}$ occurs may be reduced.

3.4.2 Effects on Moment

Camber also determines the pitching moment coefficient about the aerodynamic center, C_{mac}. At a larger camber, we find a more negative angle of zero lift and more negative moment coefficient about the aerodynamic center. Neither of these quantities is significantly dependent on the Reynolds number for Reynolds numbers above 500,000.

Airfoil theory shows that the aerodynamic center is located at the quarter chord, which is a good easy-to-find reference point. The variation of C_m about c/4 with α is linear with a small slope below stall. In equation form, these results appear as

$$C_l = a_0(\alpha - \alpha_{0L}) \tag{3.8}$$

$$C_{mac} = function\ of\ camber \tag{3.9}$$

Here, a_0 is the section lift curve slope with a theoretical value of 2π/radians. Also notice the linear relation between C_l and the angle-of-attack α, in Figure 3.5. Figure 3.5 shows a comparison of lift characteristics between a symmetrical and cambered airfoil of the same thickness to chord ratio. The lift curve slope, angle of zero lift, maximum lift coefficient and Reynolds number effects are also shown.

Figure 3.6 shows a comparison of moment characteristics of a symmetrical and cambered airfoil of the same thickness to chord ratio. Recall that a symmetrical airfoil has zero camber.

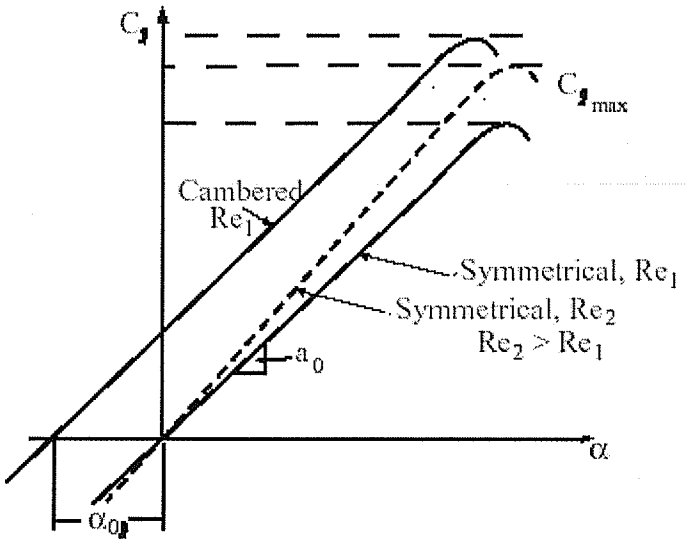

Figure 3.5 Effects of Camber and Reynolds Number on Airfoil Lift Characteristics [35]

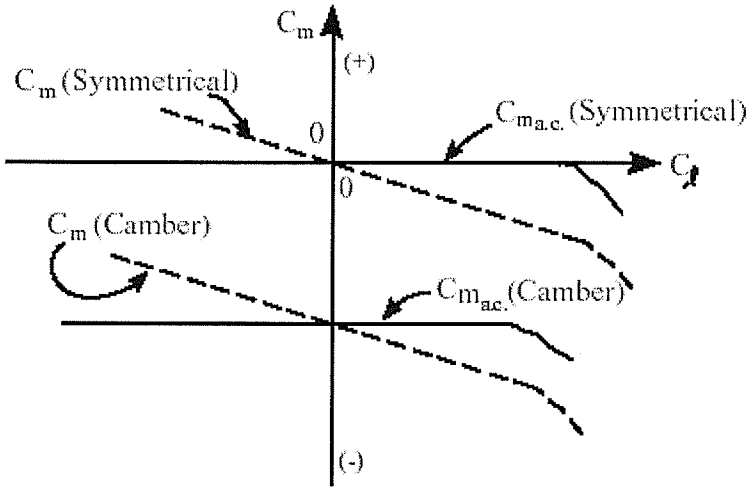

Figure 3.6 Effect of Camber on Airfoil Moment Characteristics [35]

3.4.3 Effects on Drag

The drag coefficient is heavily dependent on viscous effects and the pressure distribution on the airfoil. Hence, it depends heavily on the Reynolds number. Section drag is about equally dependent on skin friction and the pressure distribution. Skin friction drag arises due to the viscous shear stress created by the boundary layer on the

airfoil surface. It is affected by the viscosity of the fluid, roughness of the surface, whether the boundary layer is laminar or turbulent, etc. Pressure drag is a result of the fore and aft difference in the pressure distribution on the airfoil. Skin friction drag results from the momentum loss in the boundary layer. At low angles of attack, skin friction drag dominates, while at high angles of attack, boundary layer separation beginning at the trailing edge and moving forward causes the pressure drag to dominate. At stall and beyond, when the boundary layer has fully separated, the drag is almost entirely pressure drag [34].

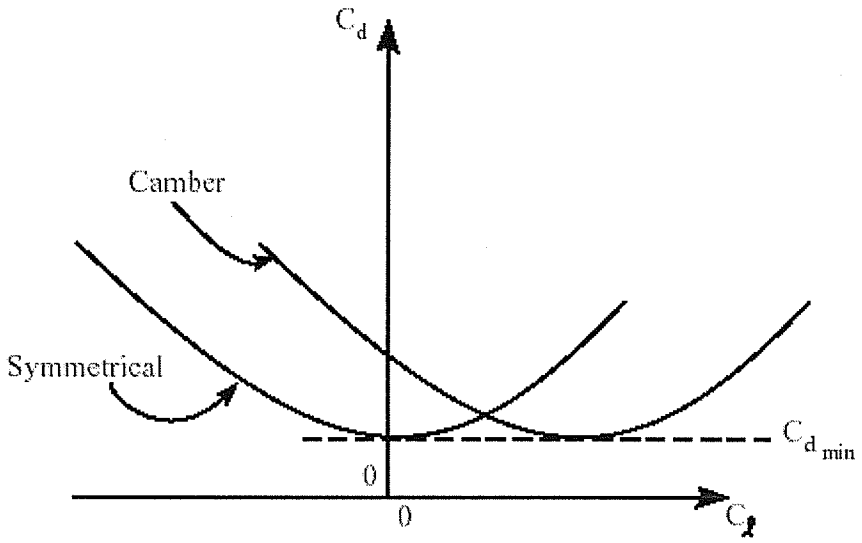

Figure 3.7 Effect of Camber on Airfoil Drag Coefficient [35]

Camber effects on drag coefficient are most significant at the lower angles of attack (or lift coefficients). The effect of positive camber is generally a shift in the minimum drag coefficient, $C_{d\min}$, to a positive angle of attack, α. The drag coefficient has a roughly parabolic variation with lift coefficient centered around $C_{d\min}$. Figure 3.7 shows

a comparison of drag characteristics of a symmetrical and cambered airfoil of the same thickness to chord ratio. This graph of C_d against C_l is called the drag polar [35].

3.5 Blade Element Theory

The turbine runner is composed of B blades and a length L having a rotational velocity of Ω. The blade chord, C, and its twist angle, β, can vary in the radial direction. Define the y axis as the axis of rotation of the turbine. Figure 3.1 shows a representation of the blade for a given azimuth position. Close analysis of the forces, due to lift and drag over a blade section at a given radial position, is required for the calculation of torque.

For a wind turbine blade, the arbitrary blade section can be taken via an intersection plane perpendicular to the spanwise direction. It is based on an assumption that there is equivalent circumference velocity over the airfoil (see Figure 3.8). The approximation is accurate enough for this wind blade study, due to its low aspect ratio shape.

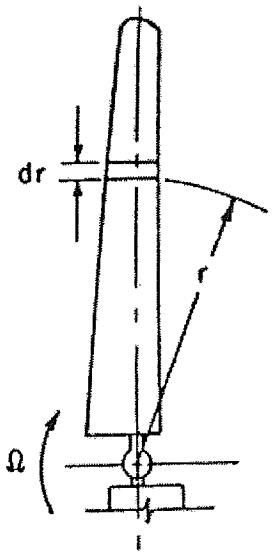

Figure 3.8 Wind Turbine Blade Geometry

However, the fan-shaped runner of a hydro turbine presents a high aspect ratio. If we still use the intersection plane as a blade section cutting surface, the assumption would result in significant errors. Instead, a cylindrical surface, whose axis coincides with the runner's axis, must be taken as the slice surface. On the cylindrical surface, the circumference velocities at every point on the blade curve are identical. A closed traverse 3-D curve is unfolded on a plane as a quasi-blade airfoil. The distinctive features between the unfolded curve and the plane section curve can be seen in Figure 3.9.

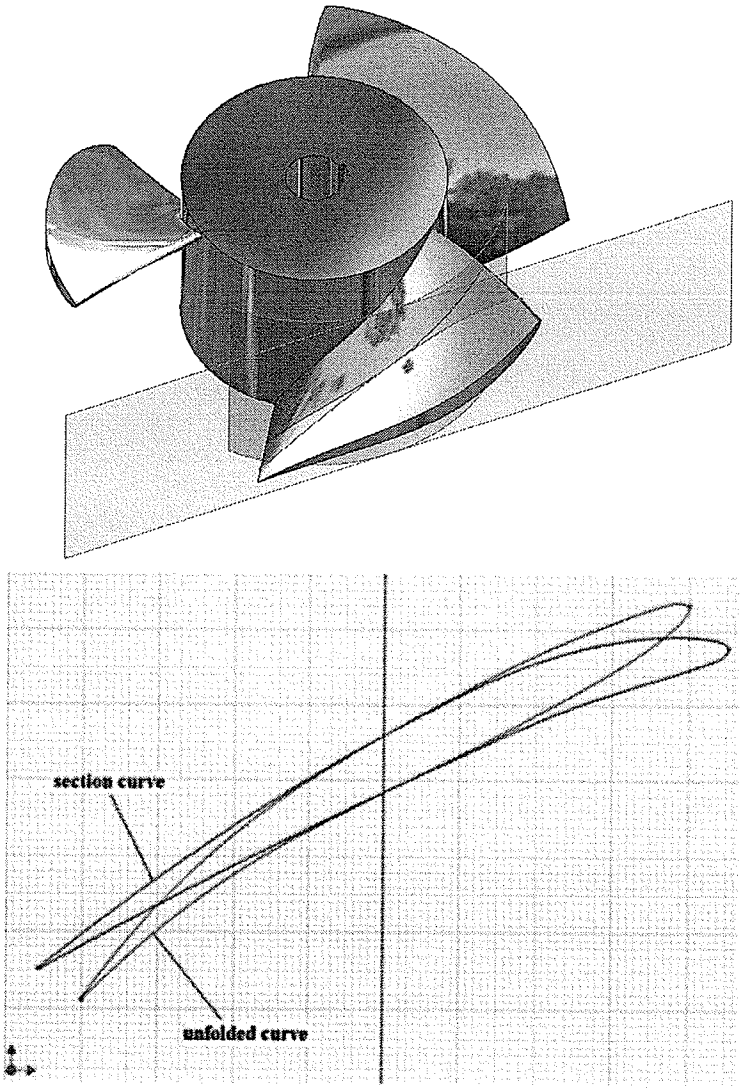

Figure 3.9 Comparisons of Two Different Curves

The theory of surface intersection algorithms predicts that a 3-D curve created by the intersection of two 3-D surfaces with both curvature and continuous features would keep the curvature and continuity on the incising surface. A cylindrical surface would be the incising surface and it can be unfolded to a flat surface without any lumpy features. Consequently, the 3-D curve would be unfolded along with the unfolded surface and it becomes a 2-D curve. The 2-D curve retains curvature and continuity, thus it can be considered a quasi-airfoil for aerodynamic analysis (see Figure 3.10).

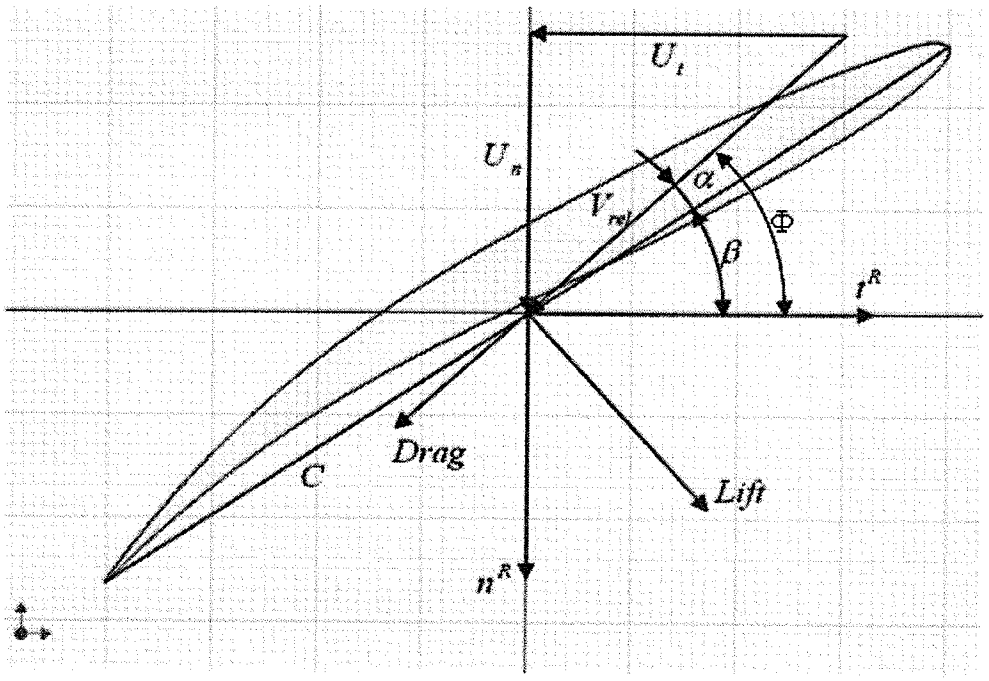

Figure 3.10 Forces on Quasi-Airfoil

The fluid velocity relative to the blade, V_{rel}, is decomposed (in the unfolded plane of the section) into a normal component, U_n, and a tangential component, U_t, which are both functions of the rotational velocity, Ω, and the fluid velocity, U_i. Blade-element theory implies that the local forces exerted on the blades by the flow are dependent only

on airfoil aerodynamic properties and the relative fluid velocity [36]. Decomposing these forces on the n^R and t^R axes and performing time –averaging of the forces exerted by the blades on the flow during one period of rotation, yields the following expression for the normal and tangential components of the surface force per unit area, exerted by the blade on the flow,

$$f_n = +\frac{B}{2\pi r}\rho\frac{V_{rel}A}{2}(U_t C_l - U_n C_d) \tag{3.10}$$

$$f_t = -\frac{B}{2\pi r}\rho\frac{V_{rel}A}{2}(U_n C_l - U_t C_d) \tag{3.11}$$

where

$$V_{rel} = \sqrt{U_n^2 + U_t^2} \tag{3.12}$$

$$U_n = -U_i n_i^R \tag{3.13}$$

$$U_t = r\Omega - U_i t_i^R \tag{3.14}$$

and n_i^R and t_i^R are the appropriate cosine directions of the unit vectors n^R and t^R, respectively. Also, C_l and C_d are the dynamic lift and drag coefficients of the quasi-airfoil, respectively. Furthermore, in order to take into account of the blade tip vortex effects, the lift of the two-dimensional airfoil must be corrected. The correction factor, $t_{\Pr}$, derived by Prandtl is used. This correction factor is introduced into Equations (3.10) and (3.11) by replacing C_l with $C_l/t_{\Pr}$.

The objective of bringing in the Prandtl factor in the blade element concept as a representation of hydro turbine fluid dynamics is to convey that a certain amount of momentum change along the streamline crossing the runner disk surface must be

imparted to tip vortices. However, it should not be introduced into the expression of the mechanical power produced by the turbine. It is given by the following Equation (3.15)

$$\dot{W} = \frac{B}{2\pi} \iint_{A_{Rotor}} \frac{\rho C V_{rel}}{2} [U_n C_l - U_t C_d] \Omega \, dA \tag{3.15}$$

where A_{Rotor} is the area swept by the rotor blades [36]. This equation gives an important way of characterizing the power output of upcoming turbine blade developments.

3.6 Cavitation Number

Cavitation is the phenomenon of liquid-to-gas and gas-to-liquid phase changes that occur when the local fluid dynamic pressures in areas of accelerated flow drop below the vapor pressure of the local fluid. The liquid-to-gas phase change is similar to the boiling of water, except that it occurs at ambient temperatures. The gas-to-liquid phase change produces extremely high local pressures as vapor cavities implode on themselves. According to the Bernoulli Equation this may happen when the fluid accelerates around a turbine runner. The vaporization itself does not cause the damage - the damage happens when the vapor almost immediately collapses after evaporation when the velocity is decreased and pressure increased.

The Cavitation Number is useful for analyzing fluid flow dynamics problems where cavitation may occur. It is normally defined in the following form:

$$C_N = \frac{P_r - P_v}{\frac{1}{2}\rho V^2} \tag{3.16}$$

where P_v is vapor pressure, P_r, reference pressure, ρ, water density, and V, velocity.

Chapter 4

Geometric Representation of an Airfoil Section

4.1 Introduction

Past efforts have been undertaken by many researchers [37, 38] to alleviate the labor in designing good blade profiles for hydro turbines. This interest is often focused on the development of blade cross sections which maximize the overall kinetic energy extracted from the flowing water. This problem is similar to the optimization of airfoil cross sections.

Turbine blades have their own unique characteristics. They can have very diverse surface contours, depending on the design requirements. Also, they can have large twist angles. The leading edge (LE) and trailing edge (TE) can be either sharp or rounded. The profiles can also vary drastically in the spanwise direction. It is a challenge to successfully develop a representation that is simple, yet highly flexible to allow an aerodynamic shape optimization to explore all possible regions of the design space.

Various techniques have been developed throughout the years in order to develop airfoils. These include the NACA airfoil. The Joukowski airfoil, Bézier representation, B-splines, single polynomial blade shapes and NURB curve. They usually deal with a set of geometric design parameters, which designers use to establish 2-D airfoils, such as the leading and trailing edge radii, blade angles, wedge angles and axial and tangential chords. The coefficients of such representations are used as design variables in the aerodynamic optimization problem. These techniques have been shown to be suitable for representing a turbine blade and effective in certain aspects of the turbine design.

4.2 Design Parameters

The first requirement of the section representation is flexibility. The surface approximation must be flexible enough to represent a wide variety of blade shapes, therefore allowing for a good initial guess to start an optimization. Also, the model must be relatively simple to apply and it must use a minimum set of design parameters to completely define a unique blade profile [39].

The Rapid Axial Turbine Design model (RATD), developed by Pritchard in1985 [38], is considered by many engineers in turbomachinery analysis to be a rather simplistic but realistic and practical approach for turbine blade geometry representation. It appears to be a promising alternative to traditional methods mentioned previously. It is straightforward and easy to use. Also, it provides a minimum set of design parameters that can be used to obtain an extensive family of turbine blade profiles.

In this model, eleven geometric parameters that are necessary and sufficient, in order to describe an axial turbine blade using circular arcs and cubic polynomials, are identified. These eleven parameters include the airfoil radial location, axial and tangential chords, inlet blade and wedge angles, exit blade angle, LE and TE radii, unguided turning, number of blades and throat area. The model sub-divides the blade into five distinct regions composed of the leading and trailing edge arcs, suction and pressure side surfaces (both modeled with a cubic polynomial) and a circular arc for the uncovered part of the blade suction surface. With the eleven parameters mentioned previously, it is possible to determine the locations of the five key points shown in Fig. 4.1, which represent intersection points between the five regions of the blade. Moreover, by imposing C1-

continuity of the blade profile at the intersection points, it is possible to determine uniquely the blade shape [39].

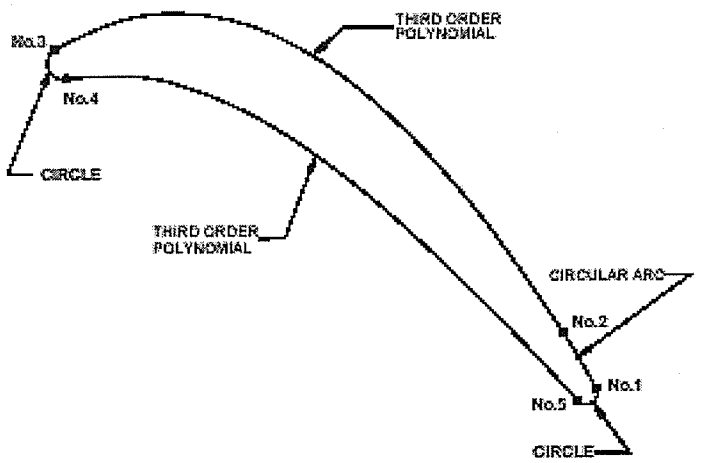

Figure 4.1 Five Key Points for RATD Model [36]

Dennis et al. (1999) examined the suitability of Pritchard's model (1985) for aerodynamic optimization and how the addition of a B-spline to the original model could improve the performance of the optimization. In their work, the authors clearly demonstrate the limitations of Pritchard's model (1985) and how a B-spline addition can significantly add to its flexibility and convenience when dealing with optimization.

4.3 NACA Airfoil

An implicit representation of the RATD model, using a minimum number of design parameters, becomes essential in order to reduce aerodynamic optimization efforts, while maintaining a high level of accuracy and flexibility of the representation. Past work

was performed by NACA in the early 1930's to create a family of airfoils known as NACA sections.

NACA (National Advisory Committee for Aeronautics) was established in 1915. It later became NASA (National Aeronautics and Space Administration). A few years afterwards, the Langley Aeronautical Research Center established a unique variable density wind tunnel which made it possible to test models with full-size aircraft sections.

The effect of Reynolds number became better understood. Langley researchers had determined that the thickness distributions, after straightening the mean lines, were nearly identical. They derived a formidable fifth order polynomial equation to describe the shape:

$$y = 5t\,(0.2969x^{0.5} - 0.1260x - 0.3516x^2 + 0.2843x^3 - 0.1015x^4) \qquad (4.1)$$

This function established the basis for a related family of airfoils. Two more parabolic equations were developed for the mean line, about which this basic symmetrical airfoil would be formed (one forward and the other aft of the center of camber):

$$y = m[(1 - 2p) + 2px - x^2](1 - p)^2 \qquad (4.2)$$

which is forward of the center of camber and

$$y = m\,(2px - x^2)p^2 \qquad (4.3)$$

aft of it [40]. The variables m and p refer to the maximum camber in percentage of the chord and the position of the maximum camber in tenths of chord, respectively.

A NACA airfoil can be characterized by the coordinates of the upper and lower surface. It is often summarized by a few parameters such as the maximum thickness, maximum camber, position of maximum thickness, position of maximum camber and the nose radius. A reasonable airfoil section can be generated, given these parameters. All

parameters are expressed in terms of the chord. The first digit represents the amount of camber in percent of the chord. The second digit is the center of camber in tenths of the chord and the last two digits are the thickness in percent of the chord. A NACA 4412 therefore has 4% camber centered 40% back and it is 12% thick.

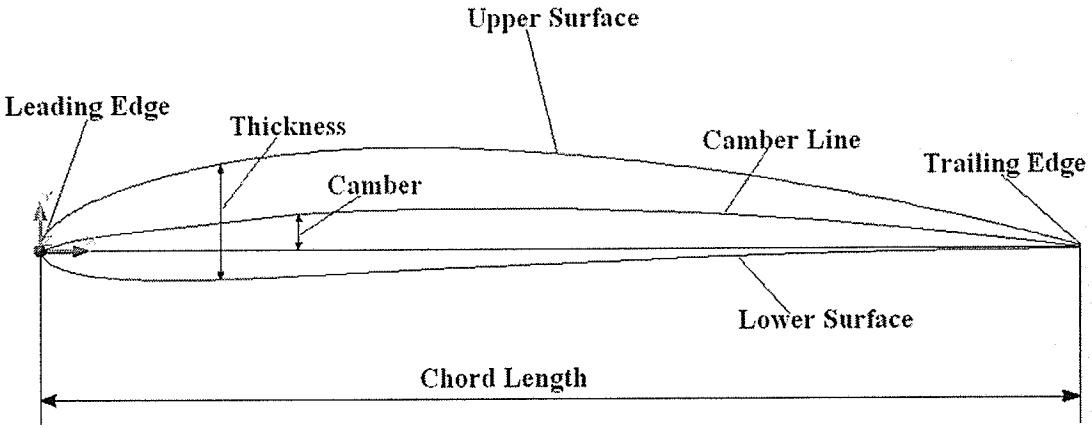

Figure 4.2 NACA Airfoil Geometrical Construction

A team led by Eastman Jacobs at Langley investigated these parameters in great detail and they published a document in 1933 reporting the measured characteristics of 78 airfoils [41]. The amount of labor required to accomplish this task is astonishing, since the calculations used tables of logarithms and trigonometric functions determined from mechanical adding machines. The wind tunnel models all used five inch chords and 30 inch spans. They were made of duralumin (typical aircraft material at that time), machined to close tolerances and finished to a high polish. It is unlikely that much electronic instrumentation was available, but the instrumentation was nevertheless precise and the measurements were repeatable. The landmark 1933 document was considered to be so significant that it was re-published recently as a part of the 75th anniversary celebrations at NACA Langley.

The development of efficient (low-drag) airfoils was the subject of intense experimental investigation in the 1930s. These airfoils were standardized by the National Advisory Committee for Aeronautics (NACA, which is now NASA) and extensive lists of data on lift coefficients were reported.

Many software packages have been developed to assist designers in applying NACA airfoils to their products. Some of them can be used to perform tests on blade sections and predict aerodynamic performance.

4.4 NURBS

Although the NACA airfoil maintains a high level of accuracy of representation, the lack of a high level of flexibility of modification makes the attempt of optimization difficult. Since the NACA airfoil used in the RATD model for upper and lower sides is too restrictive, it does not allow for exploring the entire design space. Therefore, an implicit representation of the RATD model using a minimum number of design parameters becomes essential, in order to reduce aerodynamic optimization efforts, while maintaining both a high level of accuracy and flexibility of the representation. Non-Uniform Rational B-Splines (NURBS) represent a flexible, powerful geometrical curve and a good choice for this purpose.

4.4.1 Using NURBS

A general representation given by NURBS will be considered. This inspiration is based on several factors. A powerful feature of NURBS is its ability to work with curves and surfaces of complex geometrical features, such as conic shapes, unlike other methods. Another advantage of NURBS is that it offers a way to represent arbitrary

shapes, while maintaining mathematical exactness and resolution independence. When conducting aerodynamic analysis on the blade profile, this level of accuracy at the leading and trailing edges is crucial for good results. Other useful properties are summarized below [39].

- They can represent virtually any desired shape, from points, straight lines and polylines to conic sections (circles, ellipses, parabolas and hyperbolas) and free-form curves with arbitrary shapes.
- They give great control over the shape of a curve. A set of control points and knots, which guide the curve's shape, can be directly manipulated to control its smoothness and curvature.
- They can represent very complex shapes with remarkably little data. For instance, approximating a circle (3 ft. diameter) with a sequence of line segments would require tens of thousands of segments to make it look like a circle, instead of a polygon. Defining the same circle with a NURBS representation requires only seven control points.

Ghaly and Mengitsu (2003) demonstrated the advantage of using NURBS for the representation of gas turbine blades when dealing with shape optimization. In their work, they were able to obtain results, which are accurate to within the machining tolerance, when approximating a target geometry using NURBS with as low as nine control points. Furthermore, the aerodynamic performance of the geometric approximation was nearly identical to the target geometry, thus corroborating for accuracy of the approximation [39].

4.4.2 NURBS Definition

For a more detailed understanding of NURBS, Piegel (1995) provided a useful discussion of this topic. NURBS, or Non-Uniform Rational B-Splines, are defined as:

$$\vec{C}(u) = \frac{\sum_{i=0}^{n} N_{i,p}(u) w_i \vec{P}_i}{\sum_{j=0}^{n} N_{j,p}(u) w_j} \tag{4.3}$$

where $\vec{C}(u)$ are x- and y-coordinates of the curve generated, n is the number of control points $\vec{P}_i$, w_i are the weights and $N_{i,p}(u)$ is the basis function computed based on the knots, u. The value of $N_{i,p}(u)$ is based on two variables, namely the knot value, u, and the degree of the function, p.It is defined as:

$$\begin{aligned} N_{i,1}(t) &= \begin{cases} 1 & if\ x_i \le t < x_{i+1} \\ 0 & otherwise \end{cases} \\ N_{i,k}(t) &= \frac{(t - x_i) N_{i,k-1}(t)}{x_{i+k-1} - x_i} + \frac{(x_{i+k} - t) N_{i+1,k-1}(t)}{x_{i+k} - x_{i+1}} \end{aligned} \tag{4.4}$$

The key feature of a NURBS curve is that its shape is determined or controlled by the set of control points and the corresponding weights. Moreover, after placing and moving either one or more of the control points, the knots or the weights can accomplish either a local or a global change of the target shape. A NURBS curve exactly represents conics, e.g. circles, ellipses, cylinders, cones. This implies that NURBS functions can represent a much wider family of curves, compared with B-splines or Bézier curves, while simultaneously ensuring profiles smoothness [42].

4.4.3 NURBS Representation

The advantages of using NURBS for optimization are apparent. Essentially, they offer flexibility, accuracy and efficiency simultaneously. The next task is to determine the best way that NURBS can be implemented, in order to represent the initial geometric model described in the previous section. For a proper representation of the geometric model, it seemed reasonable to conserve the five original sections of the RATD method using five distinct NURBS functions for the leading edge, trailing edge, uncovered surface, suction side and pressure side. This decision is based on the fact that each section holds distinct properties for a turbine blade. In order to have better control over the shape, especially during optimization, it becomes simpler to collapse the blade profile into several logical sections. In this way, a section of the blade can be optimized, but that section profile is constrained by its adjacent sections. Since NURBS can represent circular arcs exactly, the leading edge, trailing edge and uncovered surfaces are each fitted with individual NURBS functions. These NURBS functions are calculated analytically given the information on the circular arc segments.

For the case of the suction and pressure side regions, a B-spline is fitted through several points generated from the original cubic polynomial curve. A minimum of five control points on each of the suction and pressure sides is necessary to obtain a coarse fitting. Two control points are needed at each end point, in order to impose G0 and G1 continuity and one point in the middle to set the level of the curve. More details on the method used to fit the B-spline function and to impose G0 and G1 continuity are given by Piegel (1995).

Figure 4.3 shows a sample blade shape and control polygon for a turbine blade, where the five distinct NURBS functions representing the five regions of the profile are shown. Note that the profile is smooth, after imposing G0 and G1 continuity at all of the intersection points. Also, the LE and TE circles and the uncovered part of the suction surface are given by an exact NURBS representation.

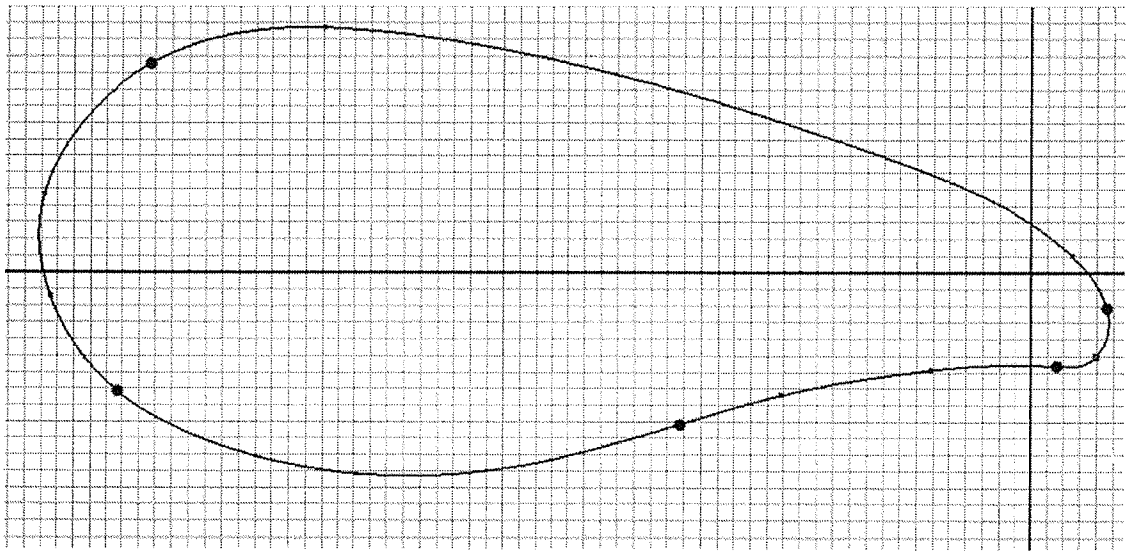

Figure 4.3 NURBS Representation of Five Sections Composing Blade

Chapter 5

Construction of 3-D Blade Profiles

5.1 Introduction

A prototype turbine runner will be constructed with blades for extracting energy from various fluid streams. In its application, the blade design is critical for realizing the best possible overall performance. Since the main function of blades is to efficiently change the velocity of fluid flow, they normally consist of parametric sculptured surface models. The multi-faceted interaction between the fluid mechanics and blade geometry has essential importance in the blade profile design.

In turbomachinery, a 3-D blade profile is usually determined from several 2-D blade sections. The features of the cross sections are represented by special reference geometries, defined by a series of closed loops, which are required to go smoothly through a number of predetermined points. The resulting curves should be smooth. Also, they vary in curvature depending on the position of the control points. These multiple closed loops with varying shapes on separate planes will be stacked in the spanwise direction and blended together from hub to shroud, in order to create a complex and smooth shape of the blade profile.

Since the NACA airfoils have been widely used in wing sections of airplanes, the performance of many NACA airfoils has been investigated experimentally. Technical data and specifications are available for aerodynamics research. Those technologies are used for defining wing sections of airplanes, and the design of blades of wind turbines and hydro turbines. In this chapter, NACA airfoils are introduced for blade section development for blade profiles.

Mechanical Desktop will be used for 3-D blade profile design and interaction. The final output is a standard IGES (Initial Graphics Exchange Specification) file (NIST, 1990). The blade surface geometry can then be analyzed by existing computational fluid dynamics packages.

5.2 Blade Design Methodology

A new design methodology is introduced and motivated by the need to define and modify blade sections on multiple separate planes, while providing flexible interaction techniques. A direct description and adjustment of a three-dimensional blade profile, involving both the shape of the blade cross section and the surface contour, would be extremely complicated. Furthermore, blade designers are familiar with blade sections using normalized two-dimensional coordinates. The objective of this effort is to provide two- dimensional closed loop construction tools that permit the definition and modification of blade sections precisely within general planes.

Almost every 3-D CAD modeling package recognizes any general closed loop for a blade section. The only requirement is to stack all blade sections to the blade surfaces (called LOFT in 3-D CAD programs). A loft is a complex shape created through a series of planar closed loops. These sections, which are distributed on multiple planes, can be connected with a loft feature. There is no maximum number of sections for a loft. If more sections are defined, the blade profile can be constructed more accurately. When loft sections are identified, the loft feature is created in the order of the selection. Two different types of lofts can be created: linear and cubic. If a loft is created using profiles,

a designer has the most flexibility for modifying the loft feature later. The loft is modified only if the sections are modified.

5.3 Application of 3-D CAD Modeling

In order to effectively work on 3-D curve modeling, 3-D CAD is a necessary tool for designers to show, describe and communicate their developments. The CAD principles of 3-D modeling can be applied to almost any geometric features. We can refine, change and modify designs until the blade contour meets the entire requirements of an optimization. The simulation also lets a designer see the prototype model in action prior to its physical construction.

In modeling of the blade profile, an advantage of the 3-D software is its ability to precisely describe any three-dimensional surfaces, which was impossible with the 2-D approach (see Figures 5.1 and 5.2). Using the full 3-D approach, the design, calculations and manufacturing can be performed relatively easily, regardless of the geometrical complexity of the case.

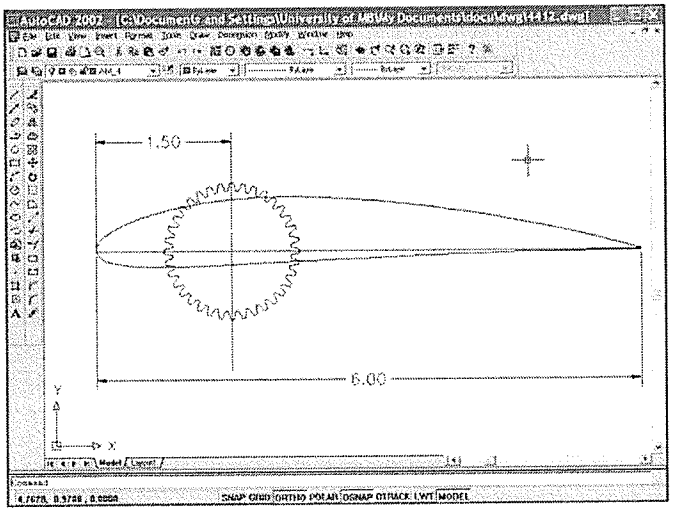

Figure 5.1 AutoCAD (2-D) Program in Application

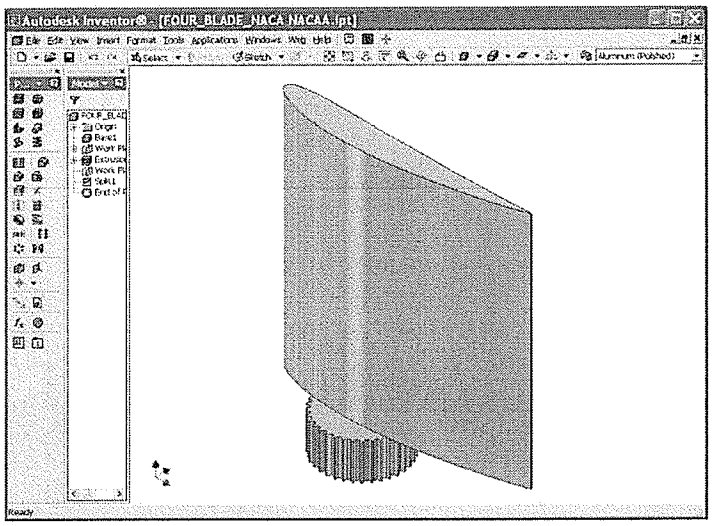

Figure 5.2 AutoDesk Inventor (3-D) in Application

The modern visualization possibilities offered by the 3-D CAD software allow realistic images of the virtual models of the blade profile. The visualization is especially important in evaluation of the design, particularly if no physical prototype exists. With the increasing availability of rapid prototyping, an exact geometrical model of the product can be created quickly and automatically.

Another advantage of 3-D CAD is the total associability. In 3-D, the blade entity itself is modeled, not its views. If a 2-D drawing is necessary, it can be obtained automatically, based on the 3-D geometry. Any future modifications are reflected everywhere where the part appears. This means that a 2-D drawing of the part is updated, as well as every assembly which contains the modified part. The associability ensures that all changes made to the part are reflected in the assembly and assembly drawings.

Parametric representation is also a very useful innovative feature of 3-D CAD. It means that the main numerical values for modeling of entities are stored and they can be modified directly by the user. The parametric approach makes the 3-D CAD software a

more suitable tool for design customization, as small logical changes are easy to implement. In non-parametric software, even a logically small modification may require could mean a large amount of routine work.

In addition, with the growing use of numerically controlled (NC) manufacturing tools, the 3-D software often allows parts to be produced without machine drawings. This eliminates many possible undefined details and the human factor, an easy source of mistakes. The role of machine drawing now becomes a derivative of the three-dimensional object. The engineer can concentrate more on the object under design, and less on the way to describe it. The product becomes much easier to evaluate in the early design stage.

5.4 Design of a Propeller Turbine Runner

As mentioned previously, the key to effectively designing a turbine runner is to establish the profile of the blade. The blade profile is defined by several cross sections with varying shapes and attack angles. Therefore, determining a series of 2-D closed loops distributed on separate planes along the spanwise direction becomes crucial. In this section, the process of designing the propeller turbine runner using 3-D CAD will be documented.

5.4.1 Obtain Data Files from NACA Airfoils

Many programs to generate NACA airfoils are available on the Internet [43, 44]. For example, NACA 4 Digits Series is an easy-to-use shareware program developed by the German Aerospace Centre. It was originally intended for use in model airplane design.

It can generate NACA airfoils data online with high precision. Figure 5.3 shows the window of the program application.

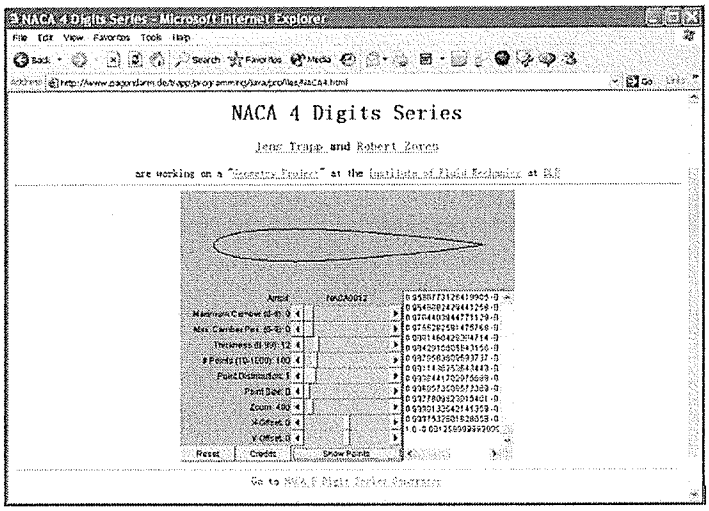

Figure 5.3 Online Program NACA 4 Digits Series

By running the online program, data for a NACA airfoil is obtained. It provides the coordinates in both X and Y directions for points on the closed loop. This data can be captured and saved in two data files (one file for the X coordinate and another file for Y, respectively).

5.4.2 Create NACA Airfoils

After saving these data files, designers seek an appropriate method for application of a CAD program to create the NACA closed curves, as required for construction of the blade profiles. A methodology is needed to establish the functional performance economically and efficiently with high resolution.

Experienced blade designers attempt to establish the best blade geometries. They characterize the geometry of closed curves with a grid of points on the loop. In order to

manufacture the blade using modern computer-aided manufacturing technology, those curves must be represented in a convenient format. For this reason, the blade is typically stimulated using a CAD package based on point data or other primitive input. However, this process may lead to misreading of the data by the CAD operator, who fundamentally alters the blade. Eventually, errors maybe commence and the original proposed performance is given up.

Like any CAD program, MDT (Mechanical Desk Top), one of the 3-D modeling software developed by AutoDesk, offers low-level geometric primitives for objects such as lines, points and triangles. The low-level primitives can also be used to define arbitrarily shaped objects. For example, a NACA airfoil will be approximated by a sequence of line segments. Because the representations of these objects are mathematically exact, that is, lines will be defined by their two endpoints, the resolution of the NACA curve depends on the number of points the curve goes through. It is estimated that at least one hundred points are required for the representation of a NACA curve with relative high resolution and accuracy at this level. As a result, manual data input for generating curves is impractical.

AutoLisp, an Autodesk's implementation of the lisp programming language, allows a designer to rapidly and accurately acquire data from the data files to design and produce highly reliable and accurate arbitrary curves, greatly reducing repeatedly tedious labor and save research and development time. This program is used with AutoCAD for automation and customization purposes. AutoCAD was early on given an open architecture that makes it possible to access almost any feature programmatically.

5.4.3 Turbine Runner Modeling

Appendix illustrates the process of creating a blade profile using 3-D CAD.

After the blade profile is modeled the rest is to construct a hub cylinder and join it together with the blade. At this stage, we need to define the diameter and the length of the hub as well as the location matching the blade. The operations of these procedures are relative straightforward for every 3-D CAD modeling program. Figure 5.4 demonstrates a primitive model having a blade and a hub cylinder.

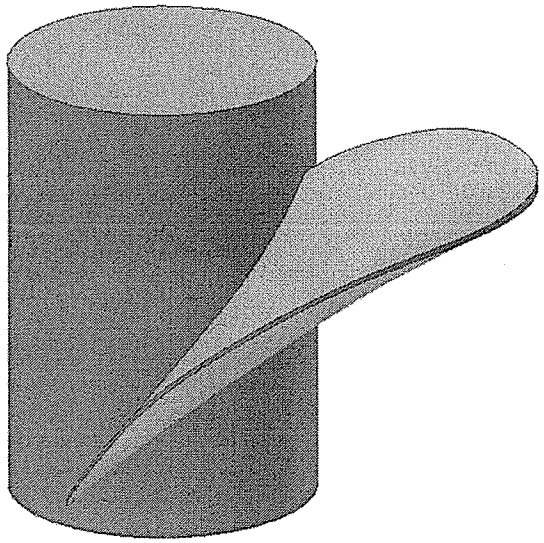

Figure 5.4 Combinations of Blade and Hub Cylinder

The three-bladed rotor is the most visible part of the hydro turbine. Other two copies of the blade can be created in a polar pattern. Adding features required for the conventional mechanical engineering design including a splined hole, an arc-swept rim, and a hole for weight cutting and so on. The final turbine runner can then be completed as shown below, in Figure 5.5.

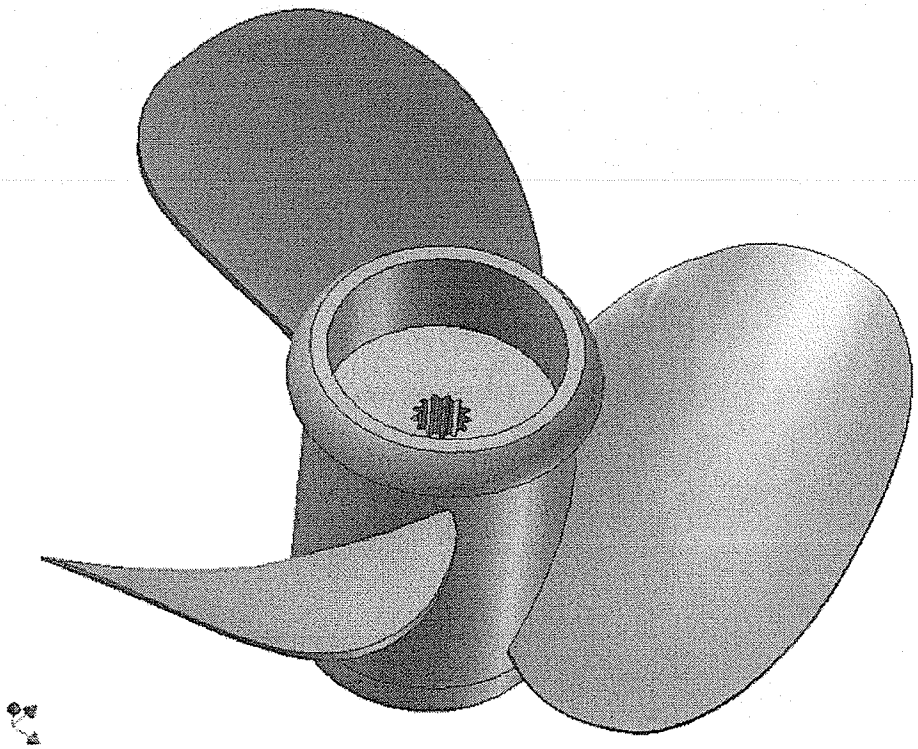

Figure 5.5 Three-bladed Turbine Runner

Chapter 6

Reverse Engineering in Blade Design

6.1 Introduction

An inspection of existing blade's profiles has played an important role in the proposed development of a new turbine runner. A designer can reverse engineer designs from models of original blades to either manufacture replacements or, for the reengineering and manufacture of blades which may offer improved performance over the original design.

The measurement of blade profiles requires data to define the geometric shape. Sometimes multifaceted forms of blade profiles are too intricate to reverse engineer in practice. Accurately defining the geometric shape of a blade profile requires the measurement of a large number of points over the blade surface. The ShapeGrabber laser scanners system, which is equipped in the Virtual Reality Technology Lab at the Department of Mechanical Engineering, University of Manitoba, was employed for this purpose (see Figure 6.1). The 3-D laser scanners and 3-D digitizers bring speed and accuracy coverage to computer-aided inspection. It can collect accurate coordinates at rates up to 15,360 points per second, digitizing a part in 3 dimensions. These points can be further processed to create a 3-D model.

When the ShapeGrabber is working on scanning a blade, a laser stripe sensor projects a line of laser light onto the blade while a camera views the line as it appears on the blade surface. The coordinate measuring machine moves along the blade in different orientations capturing the data rapidly and with high accuracy (within 0.001" or 25 micron).

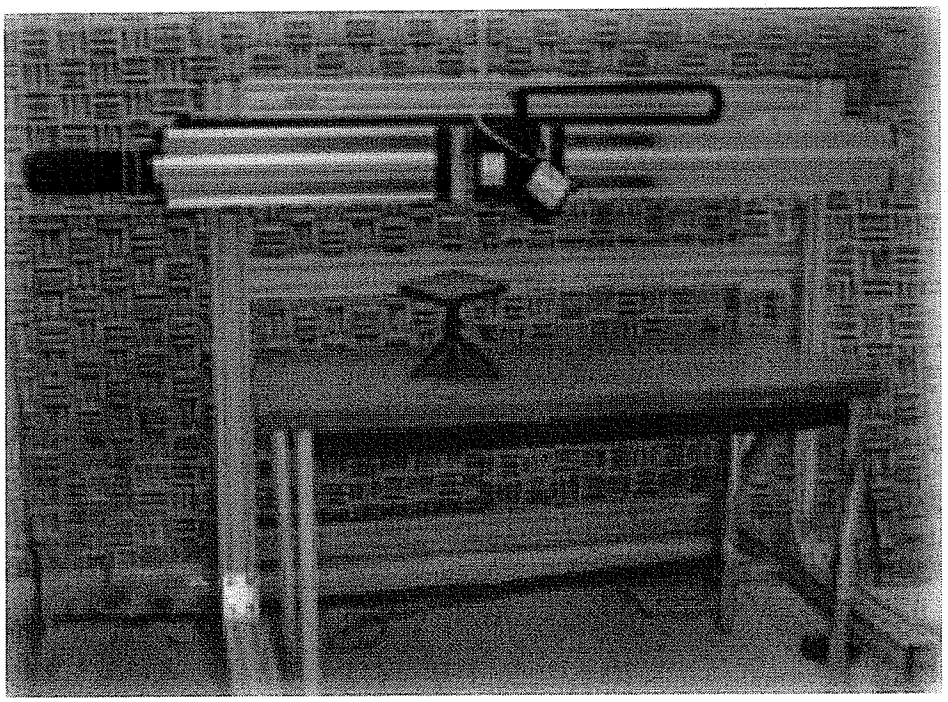

Figure 6.1 ShapeGrabber Laser Scanners System

A ShapeGrabber, like many kinds of scanning machines, uses acquisition and alignment software as a surfacing tool optimized for complex freeform design to rapidly create surfaces from the point's data. Verification tools such as color maps and deviation charts indicate where the points differ from the surfaces. The surfaces are then imported into a ProEngineer CAD/CAM package in order to create a 3-D solid model. In the case of reengineered turbine blades, the model can be used for engineering analysis. The resulting model is then used to create a part program for the machining of the new blades. The same model can also be imported into the software for the creation of coordinate measuring machines programs for the in process inspection of the machined blade features.

The ShapeGrabber has recently been used to successfully reverse engineer and measure a wind turbine blade for use in wind turbine research. The data files of the blade is produced in an IGES format, from which, the surface of blade is represented as grids similar to that shown in Figure 6.2 below.

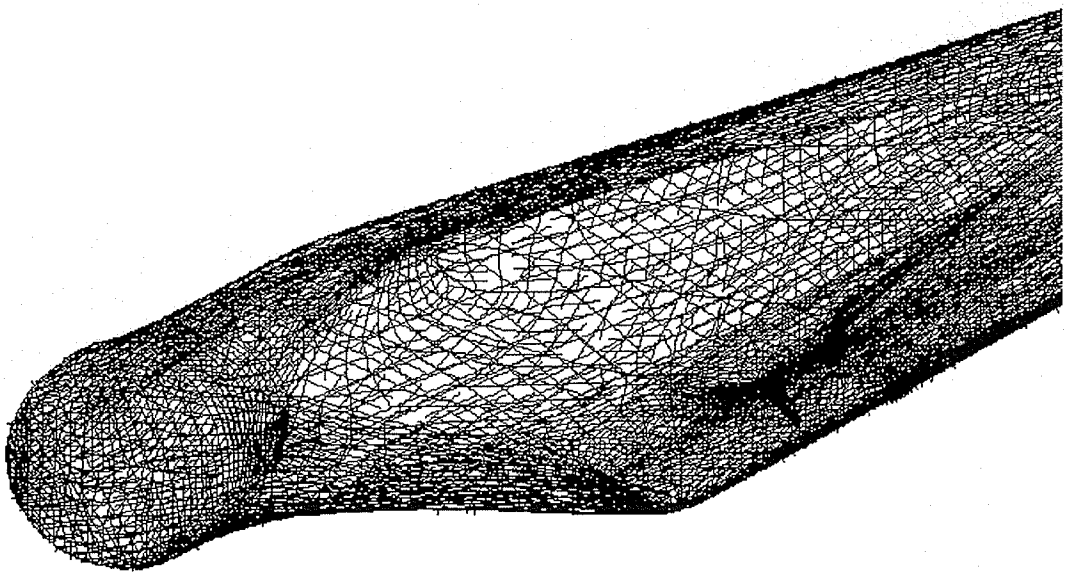

Figure 6.2 Wind Turbine Blade Represented in Grids

The IGES file can be recognized by a 3-D CAD modeling program, thus its 3-D solid model can be created. Figure 6.3 illustrates the completed 3-D solid model of the wind turbine blade in Mechanical Desktop.

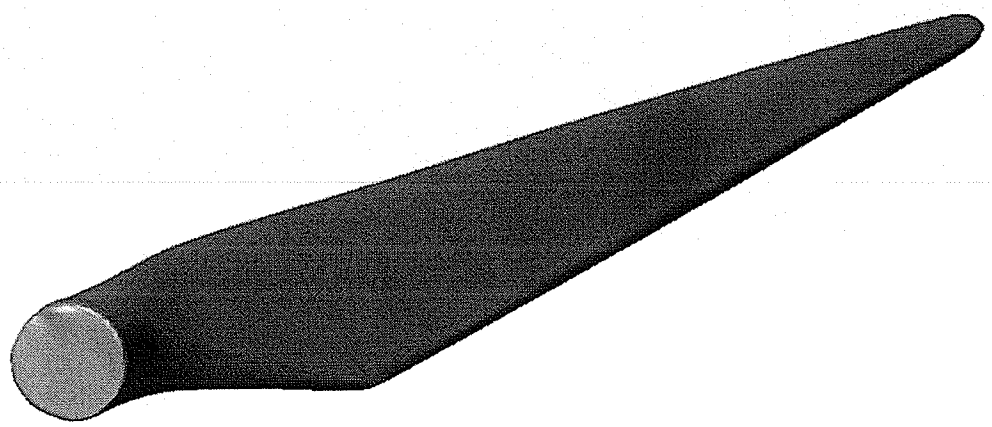

Figure 6.3 Completed Wind Turbine Blade

Although reverse engineering techniques form an important part of turbine blade research, it is obvious that the solid model created by handling surface features of the blade has less flexibility for modification and reengineering. Actually, it is difficult for a designer to deal with the complicated 3-D surface mesh to improve the performance of the turbine runner without other strategies, even if the designer works in a 3-D modeling reality. Moreover, this procedure can lead to misinterpretation of the data by the CAD operator and errors and flaws stemming from the original blade can pass on to the remodeled one. If the surface of the original blade is somehow damaged, it is difficult to restore it.

Aside from the fundamental requirement of remodeling original blades and manufacture replacements, turbine designers need a new methodology for controlling design parameters and modifying the original blade to improve the performance of the turbine. In order to meet this requirement for new turbine design, an easy-to-use method related to reverse engineering has been developed. The concept of the methodology is that a designer should never work on a 3-D surface, instead, focus on section planes of

the blade, because, as earlier mentioned, the 3-D surface of the blade can be deduced from several blade sections.

Due to the diversity and complexity of the blade sections, NACA airfoils are less flexible for alteration and are no longer appropriate for blade redesign. Indeed, it might not be possible to discover suitable curves from the NACA airfoil family matching the section curves of the scanned blade. To apply reverse engineering technology to new blade design, NURBS curves are given preference over other types of curves to define blade sections.

NURBS curves have a high level of flexibility. They are already becoming a new interactive method of designing blades that allows for blade section development and hence, forming general blade profiles. It also provides an interface and design methodology recognizable to turbine designers. Although the accessible inputs are geometric features, they are represented as familiar aerodynamic parameters. The simple interactive method allows for blade profile construction and modification. A conversion is developed which allows construction of, and interaction with, two-dimensional blade sections which are simultaneously stacked onto corresponding blade profiles. Thus, adjustment of these basic 2-D curves results in immediate changes to the 3-D blade modeling.

6.2 Reverse Engineering Methodology

After the 3-D solid model of the blade has been generated, experienced blade designers begin their design work with analysis of the density of points representing the surface of the blade. They use specialized skills to optimize the number of section planes

needed for defining blade sections and thus reducing file size. The area at the edges and over sharp contour changes having a higher density of points and puts more intersecting planes, while the area with fewer points are laid out with less ones (see Figure 6.4 below).

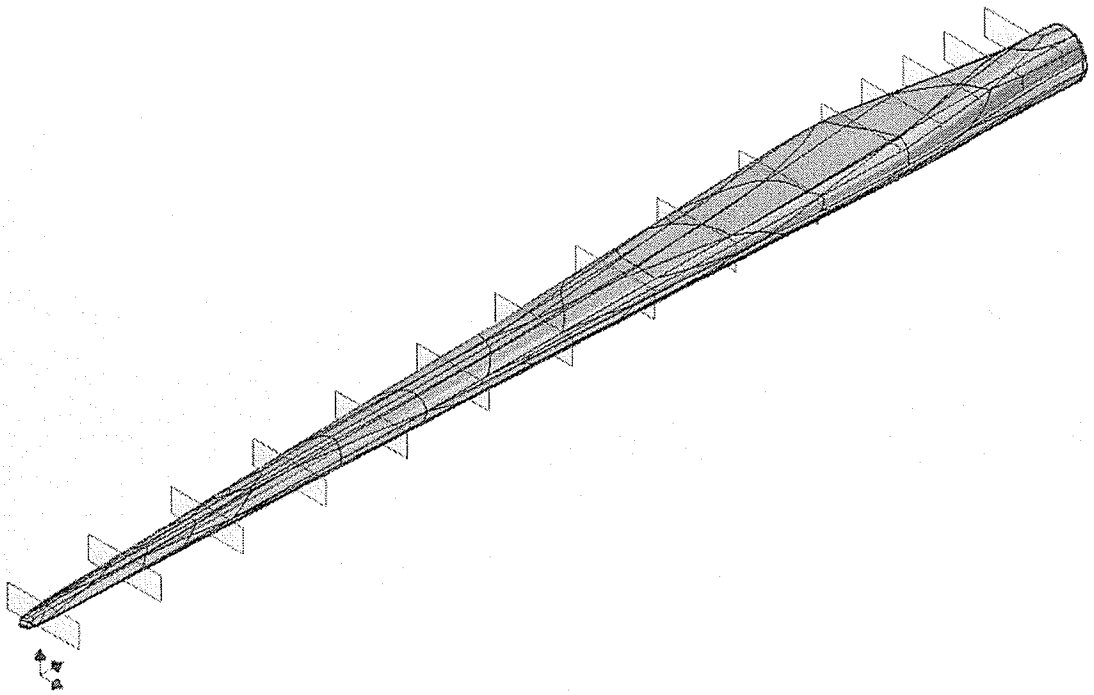

Figure 6.4 Wind Turbine Blade with Intersecting Planes

Once these planes have been set up, the corresponding blade sections can be obtained by carrying out "surface-cutting" operations in 3-D CAD modeling. One of these sections is taken as an example demonstrating how to use the geometry in blade profile (see Figure 6.5). In Figure 6.5, we can see that the outer contour of the section roughly forms a closed loop. We expect to make it a profile so that we can edit it using constrain and dimension.

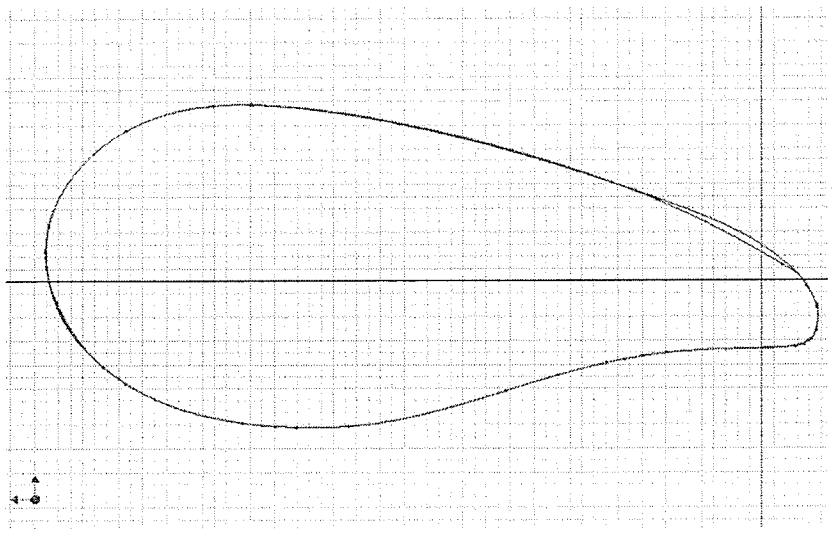

Figure 6.5 Blade Section on Intersecting Plane

Figure 6.6 shows an enlarged area of the right side of Figure 6.5. Some defects, such as kinks, corners and overlaps embedded in the curve can be seen, which are not acceptable for blade section defining.

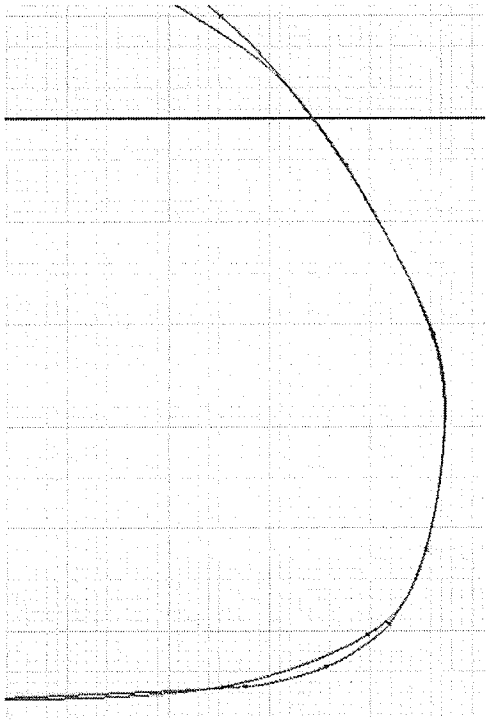

Figure 6.6 Defects in Blade Section

We must erase the overlapped segment lines, and then convert the irregular curve to NURB curve to eliminate kinks. As mentioned earlier, one very important motivation for using NURB curves is the ability to control smoothness. The NURB model allows designer to define curves with no kinks or sudden changes of direction or with precise control over where kinks and bends occur (sharp corners on NACA airfoil's trailing edge, for instance). So a NURB curve is said to have curvature continuity mathematically.

Using NURBS model, the modified curve, eliminates defects and has a high accuracy against the original one. Figure 6.7 demonstrates the revised blade section represented by a NURBS curve. Geometric constraints are handled explicitly in a sequential manner so that incompatible geometries will be signaled to the optimizer and possible corrections can be provided according to design requirements.

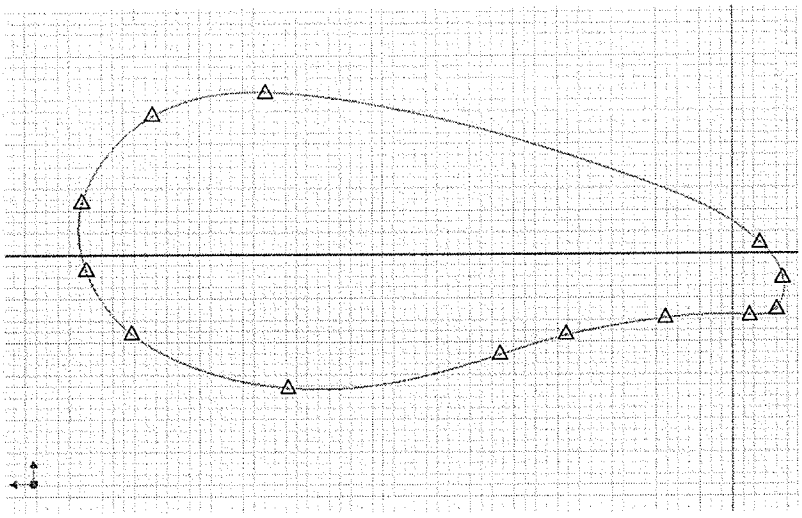

Figure 6.7 Blade Section Represented by NURBS Curve

We can see that the curve is controlled by only 13 points so that turbine designers can alter the curve's shape by simply changing the locations of those 13 control points, while maintaining the curvature continuity everywhere.

The same measures can be taken to create the rest of the blade sections, which are thus converted to a solid model through a stacking procedure as shown in Figure 6.8. A series of corresponding blade sections that are embedded in the blade model can be seen. The control points on each section curves can be utilized for design parameters. Shifting the coordinates of the points, designers can easily reengineer the blade to achieve higher performance over the original design.

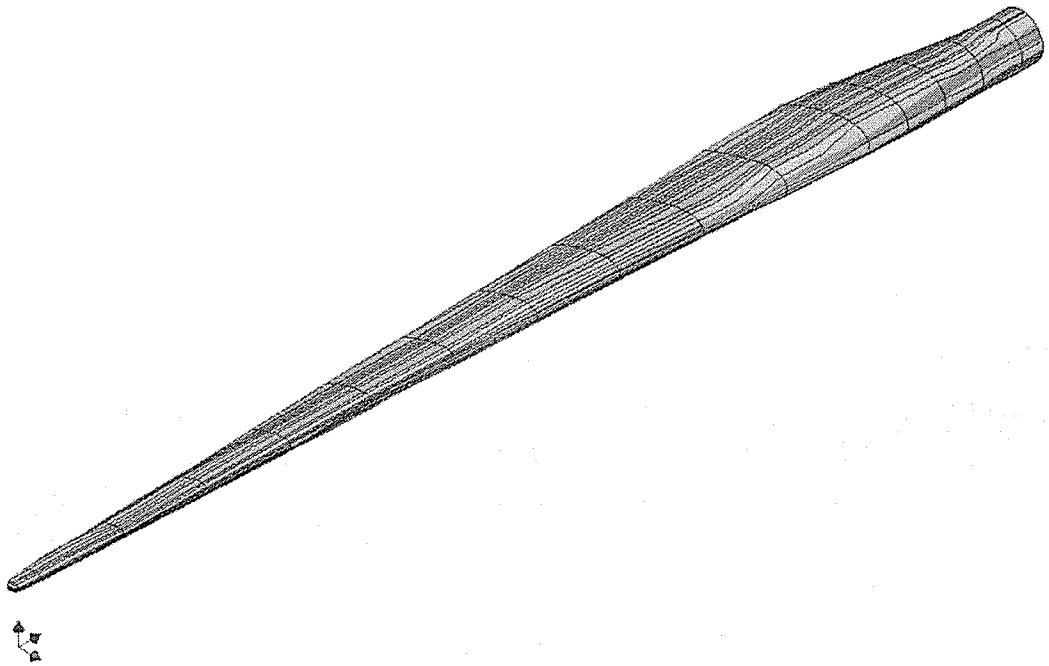

Figure 6.8 Modified Wind Turbine Blade

Another advantage of this methodology is that the size of the file has been significantly reduced by 60 percent.

6.3 Remodeling of a Propeller

Another example of an application of reverse engineering was to remodel a propeller. A data file of a propeller blade surface was obtained using ShapeGrabber and

saved in DXF format. It is perceptible that the surface has seriously been damaged and already lost its original shape as shown in Figure 6.9. The data from models of original blades can no longer be utilized to do remodeling for manufacture replacement. However, using this methodology, the shape of the propeller can be restored (see Figure 6.10).

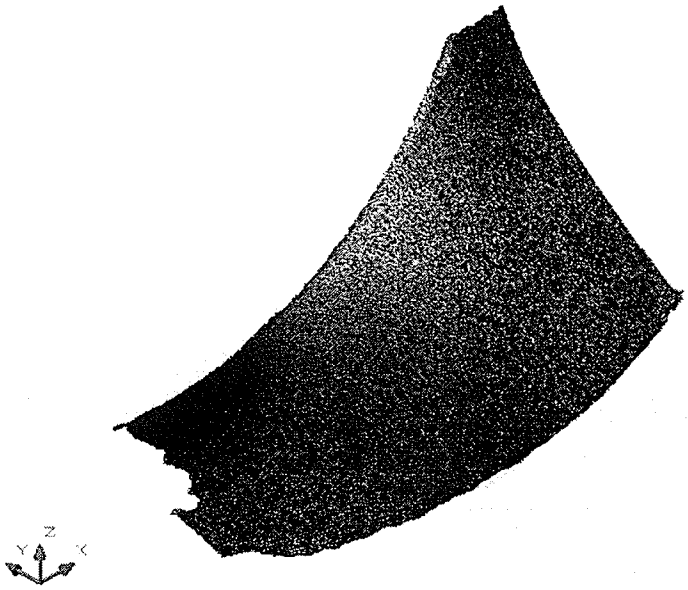

Figure 6.9 Damaged Blade Surface

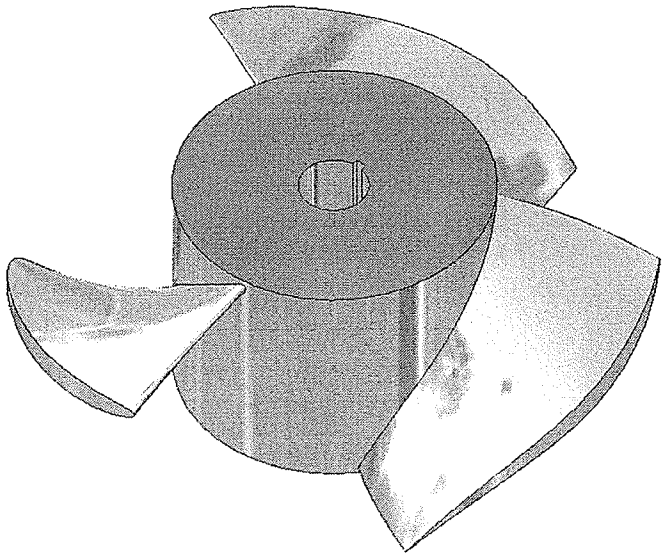

Figure 6.10 Remodeled Propeller

Chapter 7

Turbine Prototype

7.1 Depiction of the Turbine Prototype

A prototype model of the kinetic turbine has been constructed. A section view for illustrating an internal structure and a general arrangement is shown in Figure 7.1. The main components of the prototype include a turbine runner, two ball bearings, a shaft, magnetic coupling sets and a DC generator. These ball bearings can handle both radial and thrust loads as the load is relatively small.

7.2 Dynamic Rotating Seal

Initially, a mechanical coupling was designed with a dynamic sealing and flexible coupling (see Figure7.2). The flexible coupling connected the DC-generator and the drive shaft while allowing misalignment in either angular or parallel offset orientation. The coupling type is a sliding block mechanism. The rubber sliding block is slotted on shafts transmitting torque through a captured sliding disk or block. These have good shock absorption.

Alignment and motion parameters to consider when specifying flexible couplings include angular misalignment tolerance, parallel misalignment tolerance, and axial motion allowed. The angular misalignment tolerance is the maximum angular misalignment between coupled shafts that the coupling can accommodate. The parallel misalignment tolerance is the maximum parallel offset between shafts that the coupling can accommodate. The axial motion allowed refers to the relative axial motion allowed by the coupler between shafts.

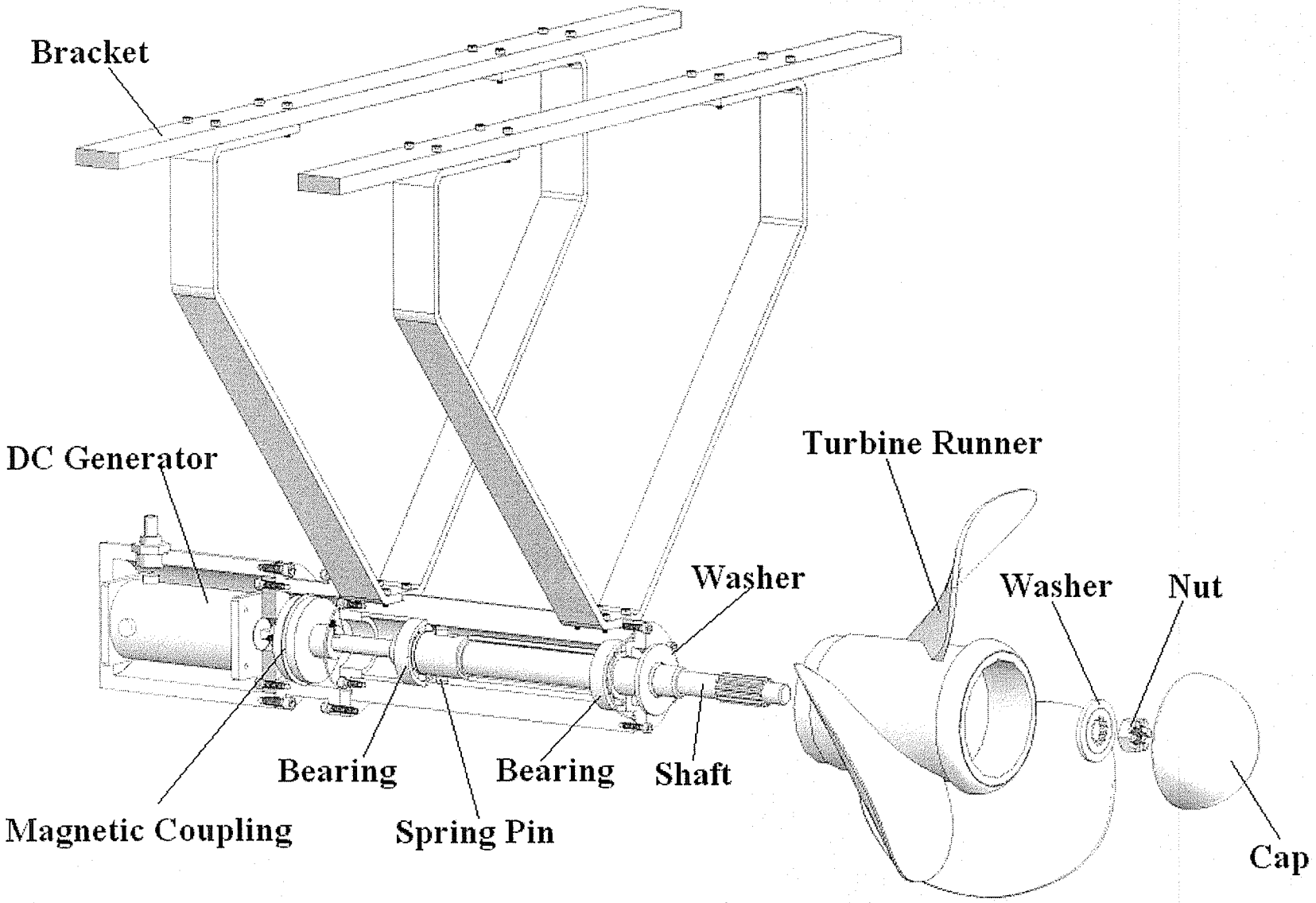

Figure 7.1 Schematic of Turbine Prototype

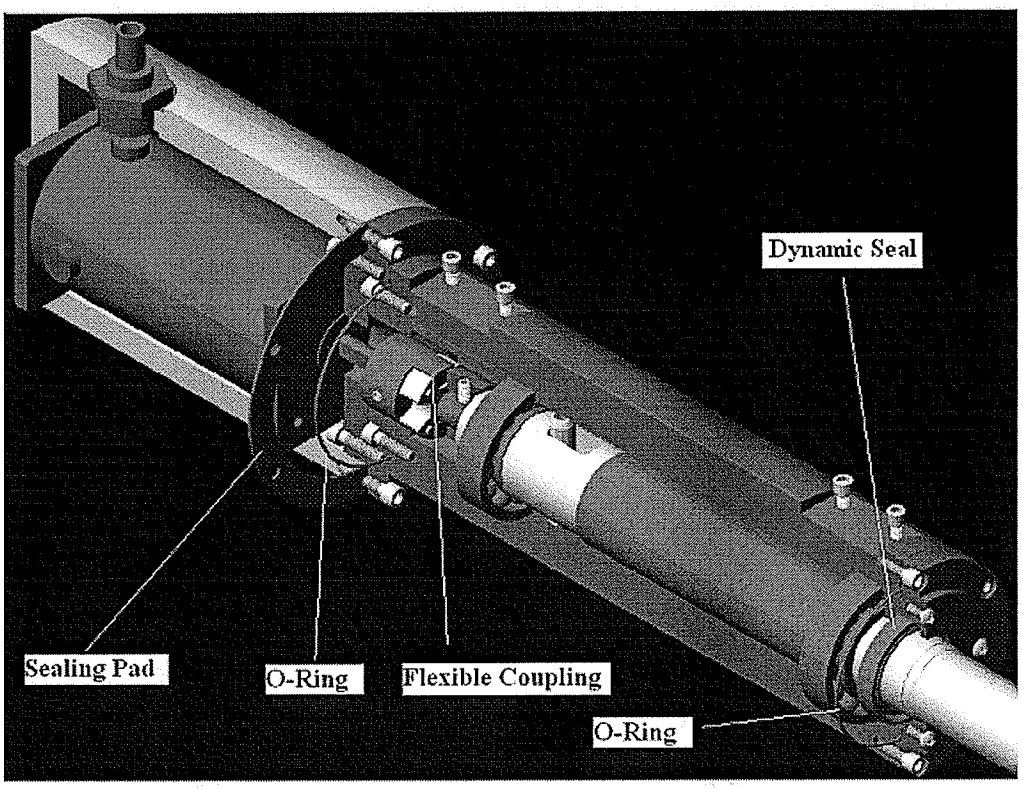

Figure 7.2 Schematic of Flexible Coupling and Dynamic Sealing

The dynamic rotating seal binds round the shaft, whereas the stationary seals, O-rings are mounted on the housing. They prevent the fluid to leak between shaft and seal and between housing and seal. The rubber lip seal (see Figure 7.6), provides a very compact and simple solution to sealing rotating shafts. The lip seal is loaded onto the shaft by a combination of the force exerted by the circumferential metal garter spring, the elasticity of the rubber and the fluid pressure. The garter spring is necessary to impart sufficient dynamic recovery. To minimize wear, the contact pressure should be as low as possible consistent with maintaining the seal. Construction material and surface finish will also affect wear rates. Shaft surface should be smooth to 0.25- 0.5μm. Seal wear will occur if the shaft is poorly finished or of inhomogeneous material such that the surface may become pitted.

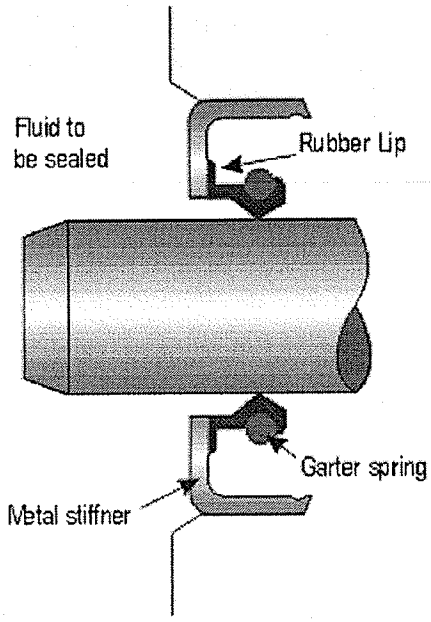

Figure 7.3 Rubber Lip Seal

7.3 Magnetic Coupling

However, due to subsequent flow leakage concerns, a magnetic coupling was developed (see Figure7.4 and 7.5). Magnetic couplings are permanent magnets mounted on shafts separated by a nonmagnetic barrier. Torque rating to 500 ft-lb (680Nm) and power to 280kw can eliminate the need for seals. Flexible links are three cantilevered beams or links arranged in a triangle, attached to hubs and torque sleeves. They can handle angular, parallel, and axial misalignment.

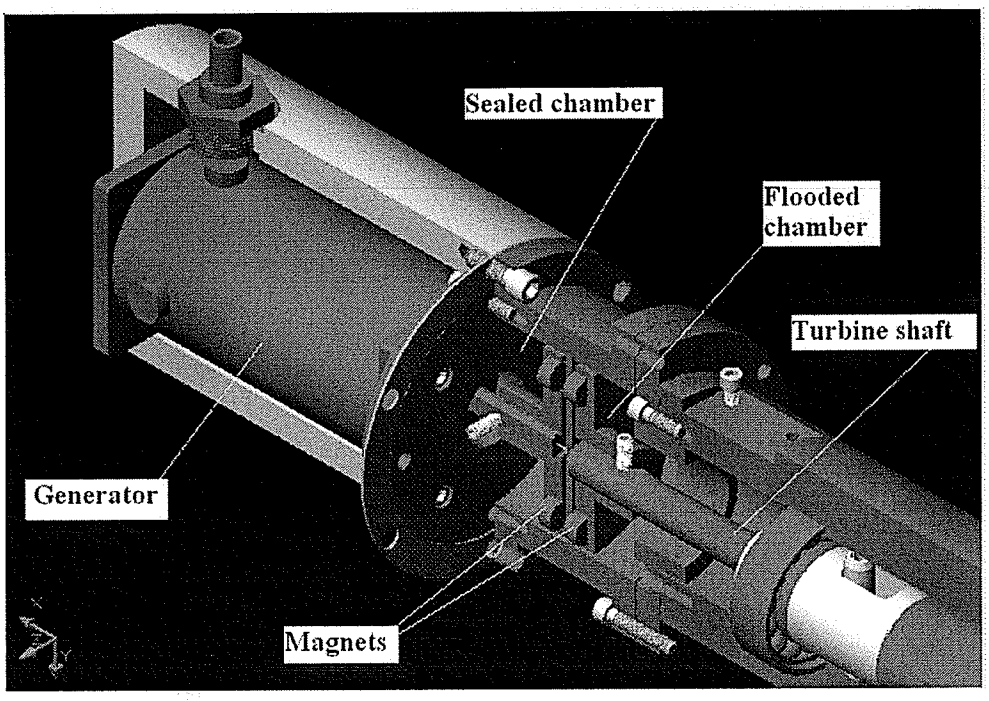

Figure 7.4 Schematic of Magnetic Coupling

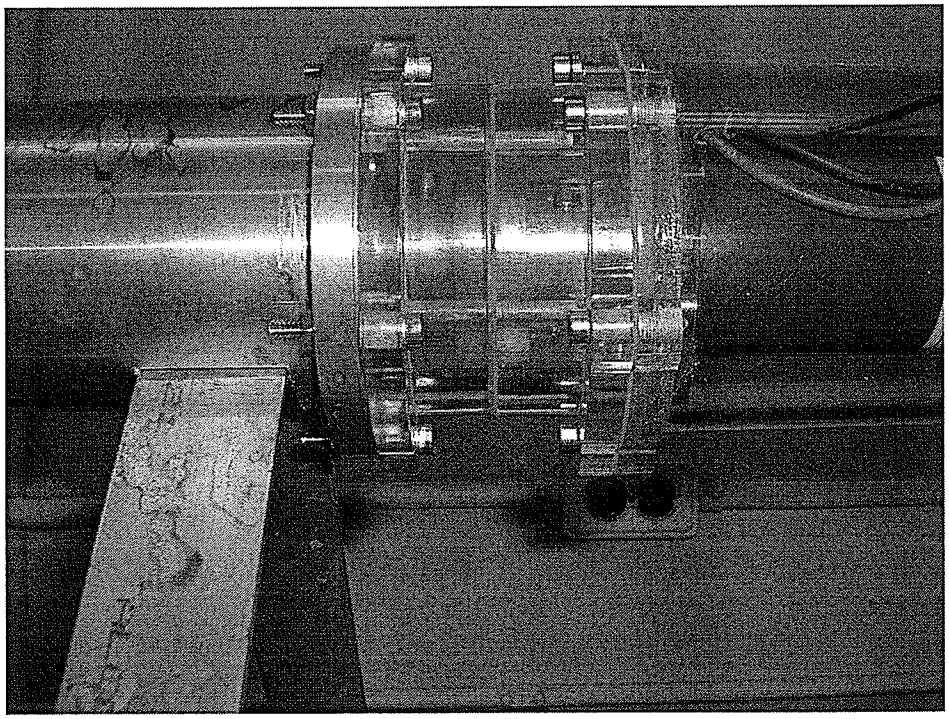

Figure 7.5 Photograph of Magnetic Coupling

The performance of the drive unit is improved with the magnetic coupling. Turbine operation in small hydro sites would convert fluid kinetic energy to electricity through the magnetic coupling. In consideration of economic feasibility, the generator places high demand on the operational safety and reliability of run-of–river hydro systems. Long delays in the purchase of electricity, due to failure of a power station, would be very expensive. As a result, leaking seals without the magnetic coupling would require expensive cleaning and be hazardous.

In contrast to a kinetic seal, the hermetically sealed metal housing can seal the generator from the water. High performance permanent magnets transfer the turbine runner torque to the generator shaft (see Figure 7.5). The magnetic coupling operates without friction. Furthermore, the magnetic coupling is as reliable and durable as the generator itself. The magnetic coupling operates without leakage, so that the generator housing remains dry. The magnetic coupling was successfully tested during operation in the water tunnel.

7.4 NACA4412 Blade

Two-dimensional flow visualization required that certain modifications were made to 3-D turbine blade profiles. 2-D NACA profiles were designed for assembly onto the turbine shaft (see Figure 7.6). The runner blades are splined onto the hub and can be rotated around their mounting point on the hub to adjust the angle of attack for various inflow angles. The 72 teeth of the spline allow for alternating the angle of attack by every five degrees.

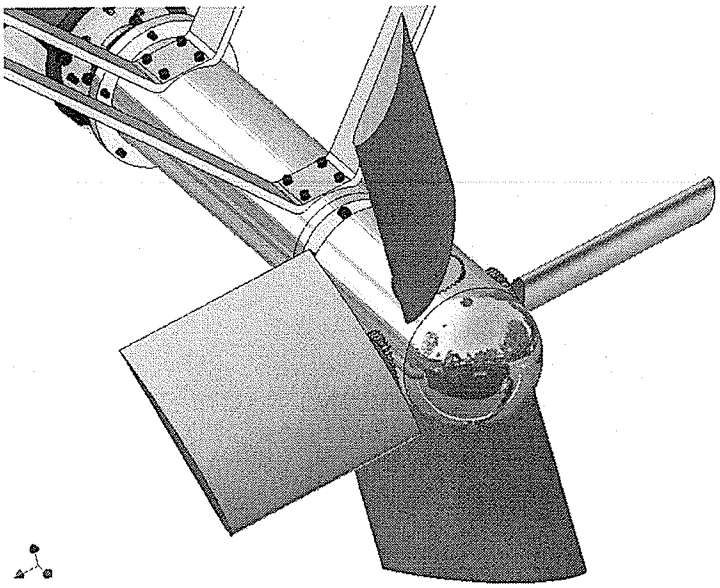

Figure 7.6 NACA Profiles on Turbine Prototype

The blades have been made from Plexiglas allowing a laser sheet to penetrate the blades and lightening particles in the region on the reverse sides. Hence, 2-D flow visualization studies with PIV could be performed (see Figure 7.7).

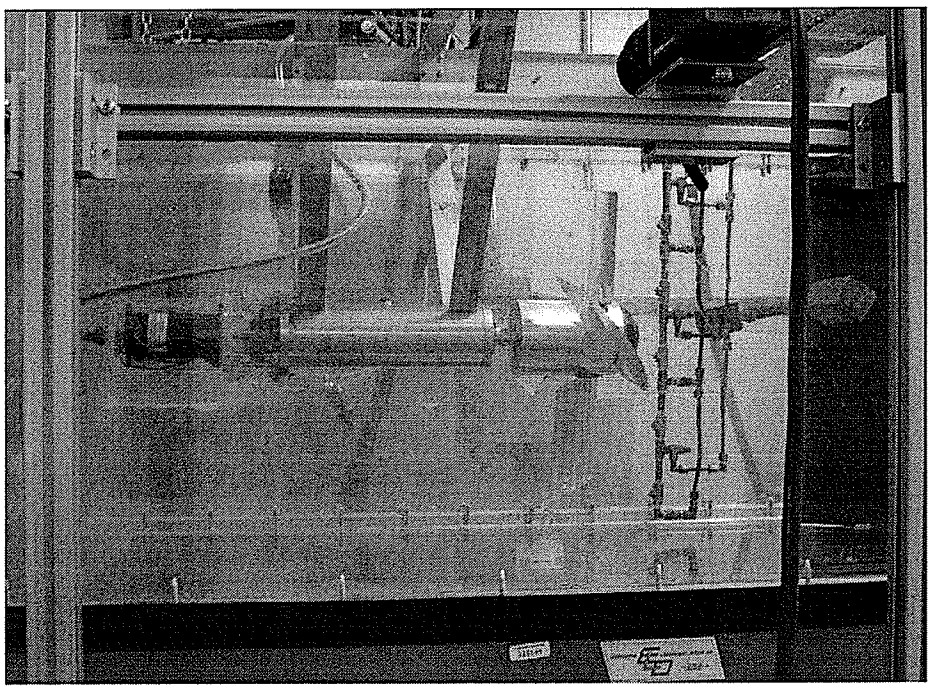

Figure 7.7 Operation of Turbine with NACA Profiles

Chapter 8

Experimental Facility

In this chapter, an experimental facility for testing blade designs from previous chapters will be described. It will be shown that these designs were developed to provide flexibility and safety specific operating parameters of the facility (such as water tunnel width). The experimental setup contains various innovative aspects to allow flow visualization in a water tunnel. For example, the magnetic coupling is shown to operate successfully without water leakage. Sample results are briefly reported in this chapter, in order to verify that the turbine prototype can operate successfully in the water tunnel.

8.1 Depiction of the Experimental Facility

A closed loop water tunnel was used to examine the performance of a prototype turbine (see Figures 8.1). The turbine prototype was mounted in the test section of the water tunnel. The test section dimensions are 70 cm (width) × 76.2 cm (height) × 182.9 cm (length). The water tunnel is a re-circulating type, with the closed loop arranged in a vertical configuration. The components of the tunnel include a test section, filtering station and a circulating pump with a variable speed drive assembly. When filled, the water tunnel contains approximately 9,463 liters of water. The test section walls (top, bottom and sides) are 1.25 inch thick acrylic Plexiglas.

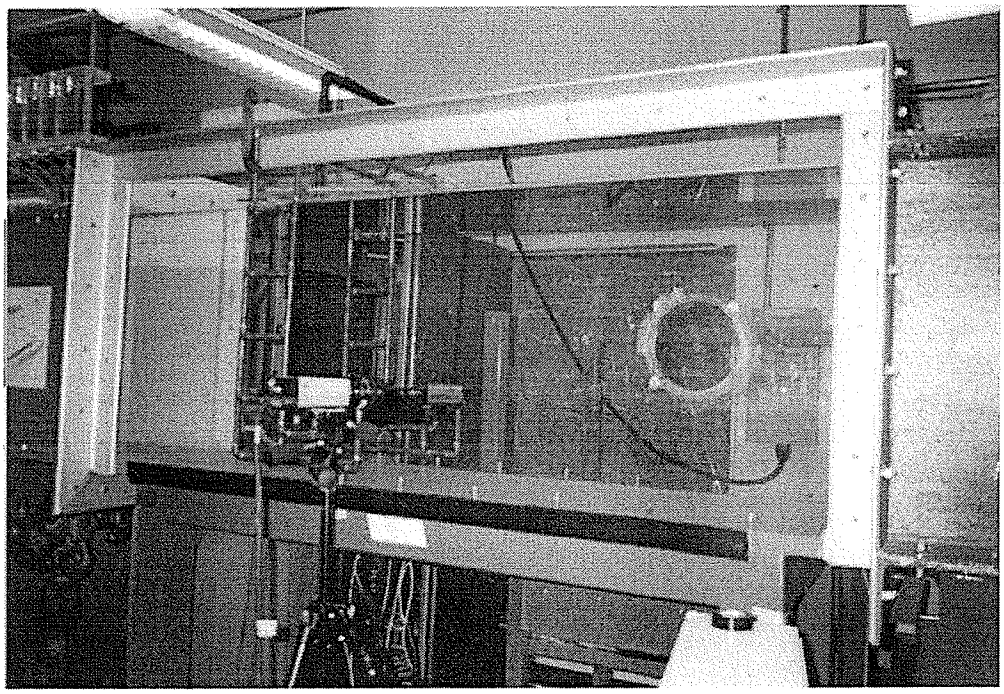

Figure 8.1 Re-circulating Water Tunnel

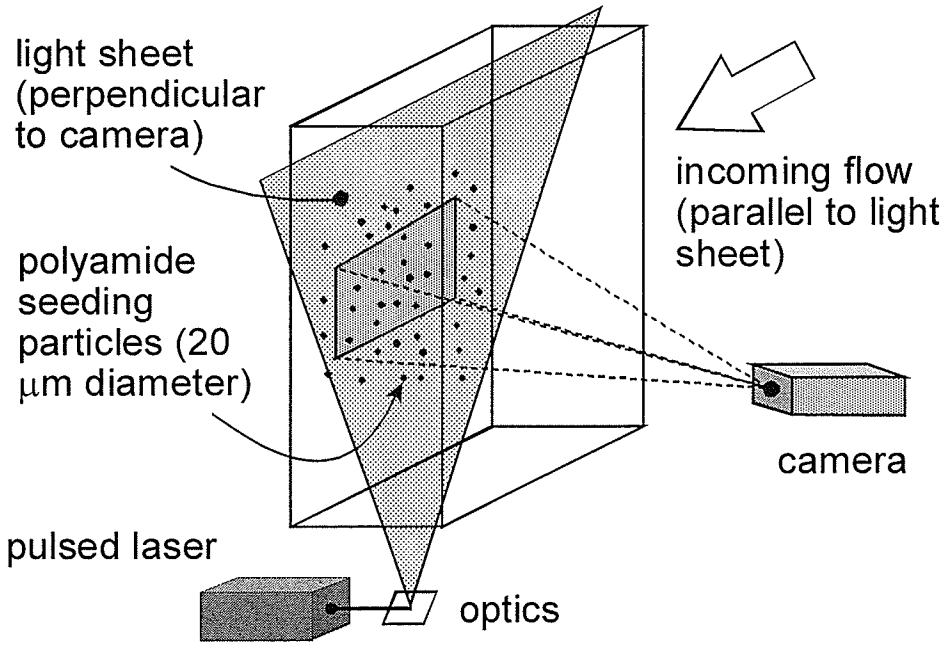

Figure 8.2 Flow Visualization with PIV / Pulsed Laser

The turbine prototype was located about 120 cm downstream of the water tunnel's contraction, thereby allowing full stabilization of the incoming flow, meaning the income flow can be treated as uniform free-flow. A 30-HP motor drives the water tunnel propeller and it is capable of generating a flow rate of 0.362 m^3/s.

This flow rate of 0.362 m^3/s corresponds to a uniform fluid velocity of 1.16 m/s across the test section. The water tunnel propeller frequency at this maximum fluid velocity is 60 Hz. Velocities are scaled down accordingly at lower frequencies. Flow visualization with Particle Image Velocimetry (PIV) and a pulsed laser can be performed in the facility (see Figure8.2). In the PIV technique, seeding particles move with the fluid stream and they are illuminated by the pulsed laser. The resulting digitized images are analyzed by Dantec FlowManager software, thereby providing whole flow field measurements. Various flow loss mechanisms, such as vortices shed from the turbine blades and wakes that may be created, can be better understood from such data.

The turbine prototype was mounted inside the water tunnel with side mounting plates (see Figure8.3).

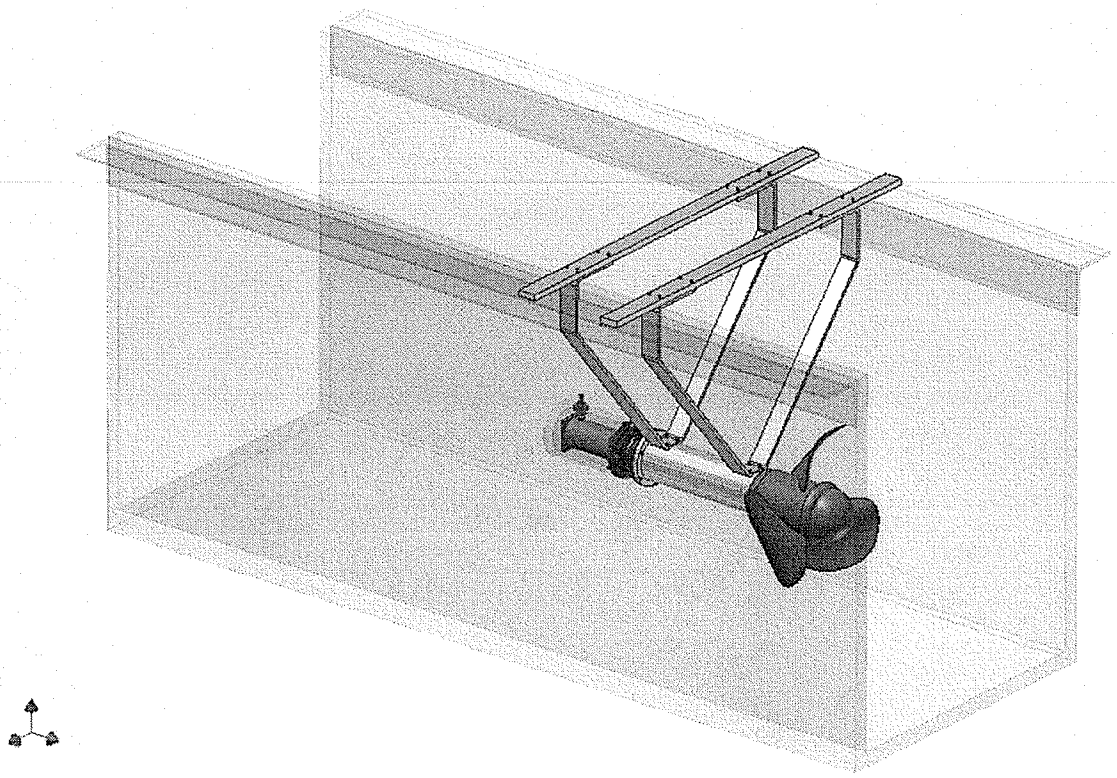

Figure 8.3 Mounting of Prototype Turbine

8.2 Results and Discussion

During operation of the turbine prototype in the water tunnel, measurements of turbine rpm were recorded (see Figures 8.4 – 8.5). As mentioned previously, the maximum fluid velocity is 1.16 m/s at 60 Hz, so fluid velocities are scaled down accordingly for lower frequencies.

Measurements of the turbine rpm were recorded with an optical tachometer (SKF TMOT1). This tachometer consists of three parts, i.e., reflective tape on the hub of the turbine runner, emitter and a collector. The tachometer is aimed at the tape on the rotating turbine hub, squeezed the triggered. The emitter sends out laser light. When the rotating hub is positioned where the tape faces the collector, the reflected laser light comes into

the collector and the signal is recorded in memory of the tachometer. Then, the rpm reading can be obtained.

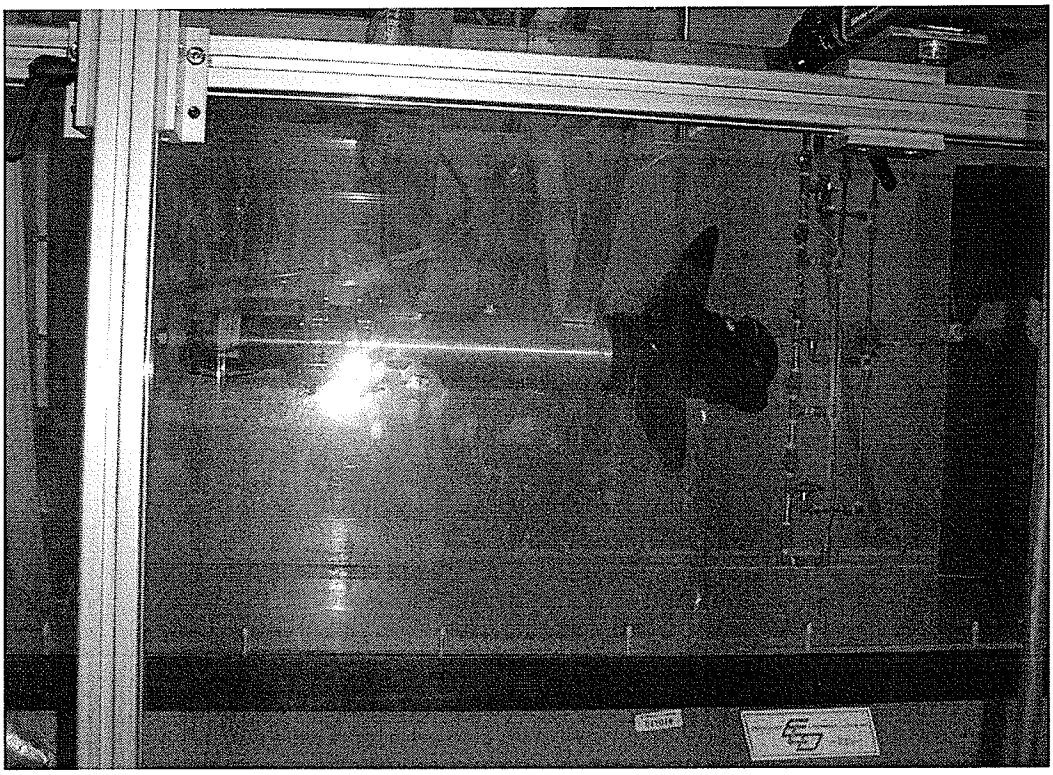

Figure 8.4 Operation of Prototype Turbine

Due to the transparency of the wall of the water tunnel, the optical tachometer can be used to remotely measure the RPM of the turbine runner. The range of possible RPM is between 3 - 99999 RPM. The maximum resolution is 0.001 RPM.

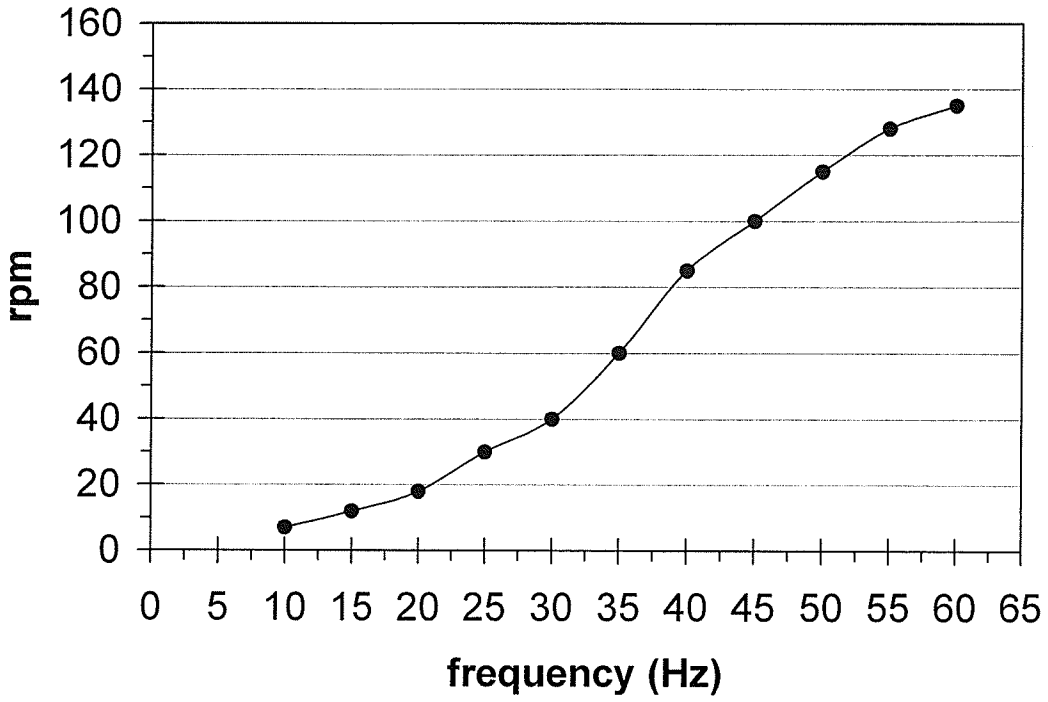

Figure 8.5 Measured RPM at Varying Frequencies

These studies are considered to have useful practical significance. For example, better understanding of flow mechanisms can lead to improved performance of turbines for small hydro applications. These applications include pumped storage or run-of-river plants. In contrast to conventional dam style hydropower plants, pumped storage plants re-use water. After water initially produces electricity, it flows from the turbines into a lower reservoir located below the dam. During off-peak hours (periods of low energy demand), some of the water is pumped into an upper reservoir and re-used during periods of peak-demand.

Run-of-river plants use little, if any, stored water to provide water flow through the turbines. Turbine designs entail different ranges of operating conditions. Although some plants store a day or week's worth of water, weather changes (especially seasonal

changes) cause run-of-river plants to experience significant fluctuations in power output. As a result, they may require some dam (small head) infrastructure.

As an example, the Tazimina Hydroelectric Project, located on the Tazimina River, about 175 miles southwest of Anchorage, has an installed capacity of 824 kW, with provision for an additional 824 kW in the future. The electricity generated will serve the towns of Iliamna, Newhalen, and Nondalton, whose electrical cooperative owns and operates the plant. Construction began in the spring of 1996 and start-up took place in April 1997. A key feature of the project is no dam. The objective was to have minimal environmental impact.

Water power resources exist worldwide and can represent a significant increase in hydropower without having to build large hydro projects. They can be deployed closer to consumers. This represents a significant energy source. Also, the installation would not require dams, although some penstock or water direction infrastructure may be necessary. From an environmental standpoint, this is ideal. Although this remains a question it would likely not affect the performance of upstream or downstream dams. Therefore, water resources, environmental and fisheries licensing requirement would be more easily met. The technology, if perfected in other locations, would be exportable and may present a feasible power generation opportunity.

Issues such as fish mortality interconnect technical issues and regulations affect the overall feasibility of water power systems. Other concerns such as frazil ice and monitoring to detect and control freezing problems may need to be addressed. Frazil ice problems decrease with increasing flow velocity, while turbine cavitation increases with increasing flow velocity.

Small hydro has been developed in various provincial jurisdictions in Canada. For example, British Columbia Hydro has connected the Hystad Creek small hydro project (a 6 MW run-of-the-river project) to the provincial electricity grid as the very first of many new independent power producers (IPP) built projects beginning to generate the green energy market. The project on Hystad Creek is one of approximately two dozen green IPP projects that BC Hydro has signed electricity purchase agreements with during the past year. With additional green energy produced by East Twin Creek Hydro Ltd. and others, BC Hydro may develop a potential 800 GW hours in new generation to meet new domestic load growth and support business ventures in BC. Owned by East Twin Creek Hydro Ltd., the project qualified in the Under 40 GW hour per year category under the initial call for IPPs. BC Hydro expects more IPP built green energy projects to begin commercial operation in the coming months.

Although Alberta primarily generates electricity from coal, there is some developed small hydro capacity. Out of approximately 855 MW of hydropower traded through the Power Pool of Alberta, 56 MW could be considered as small hydro. Contracted power sales would add to this total. As an example, Canadian Hydro Developers have four small hydro plants in Alberta with a total capacity of over 21 MW of which 12 MW is on the market.

Chapter 9

Conclusions

Increasing demand for electricity, as well as concerns about environmental degradation and global warming, has accelerated the mandate to develop kinetic hydro power. Such systems can generate utility and village scale electric power from natural underwater currents. They do not require any water impoundments, such as dams, which therefore greatly reduce environmental impacts. The core of the system is an axial-flow rotor turbine, much like underwater windmills, which convert kinetic energy from free-flowing rivers and tidal currents into electric power. In addition to delivering affordable and safe electrical energy, the systems can allow for the safe passage of fish.

The technology for kinetic turbines has been investigated in this thesis. The design of the experimental facility for kinetic turbines has been performed. Also, the general design process for turbine blades introduced. One of the most important aspects of the design is the development and determination of the blade profiles. This thesis focuses on an improvement in the methodology of new turbine runner development. The suggested approach is divided into three convenient stages. (a) the creation of preliminary blade section geometry, i.e. NACA airfoils, the Rapid Axial Turbine Design model (RATD) and NURBS curves, (b) the modifications of the various design parameters for a refined blade geometry, i.e. the chord and twist distributions, which can be practical from the manufacturing and cost points of view and (c) the construction of blade profiles by using 3-D CAD modeling. At the first stage a series of NACA curves or NURBS are developed according to optimum solution of free flow turbine blade geometry. At the

second stages, the optimum chord length scaling and twist distributions in spanwise direction are determined analytically by an approximate parabola curve. The optimum working operating condition of the blade section is considered which leads to the maximum lift-to-drag ratio. Having the aid of 3-D CAD modeling program, the blade profile along with the turbine hub was produced at the final stage. The cubic loft has been applied for creating gradual blends between the sections.

Nowadays, professional tools, such as CFX-BladeGen, are available for rapid axial turbine design; they include the complete engineering process of axial turbine conceptual design and optimization, and deliver an advanced engineering desktop solution for use in turbomachinery industry. They also provide turbomachinery designers with new options that allow rapidly evaluate influence of cavitations on turbine efficiency and performance. These new capabilities make possible to more accurate evaluate general turbine pattern by including flow dynamics parameters in the simulation. Designers can start from scratch or from an existing design using CFX-BladeGen. It offers fundamental tools to develop new blade design ideas optimize existing blade shapes or re-design blades for a different application.

Besides the normal procedures for turbine blade design mentioned in the thesis, CFX-BladeGen presents additional function. For example, increased curve control including tangential control in the meridional curvature window makes design easier; continuity and quality of the hub and shroud curves can be examined and curves created in two or more segments. A NACA profile generator is also available in CFX-BladeGen. In addition to those convenient tools, CFX-BladeGen supports:

- Completely general sculpted blades including leading or trailing edge bowing
- Radial element, axial element and user defined blades
- Dependent or independent of full blade design
- Flexible leading or trailing edge treatment
- Blade trimming or extension

This thesis has also described a new experimental facility for testing of turbines in a water tunnel. Model tests can be performed for potentially lower costs of prototypes in the development of new types of turbines in regards to kinetic small hydro. Consequently, an existing turbine's performance, particularly its efficiency and power absorbed from the water, can be improved by modification of key parameters of the turbine runners. Various design parameters can be studied in the facility, including blade performance, flow separation and loss analysis with entropy generation contours. A magnetic coupling is developed to transmit power through a magnetic coupling to a DC generator. Experimental data of rotational rpm at varying flow velocities is presented. Other data involving turbine performance can be gathered in the experimental facility. For example, this data includes rotational speed of the turbine runners, maximum output power of the turbine and mechanical efficiency of the turbine setup.

The following efforts are recommended for the research work in the future:

a. The combination of experimental and numerical simulation.

b. Professional tools, such as CFX or Fluent can be used for CFD.

c. The turbulent flow in turbine runners can be simulated by solving Reynolds-averaged Navier-Stokes equations and the standard k-* turbulence model.

d. The distribution of velocity and pressure can be predicted by using the three-dimensional turbulent flow analysis.

e. Experiments to determine the cavitation number can be performed with the models.

f. The data results from experiment can be applied for modifying the blade shape by using CAD technique

References

[1] Charles Simeons, "Hydro-Power: the Use of Water as an Alternative Source of Energy", Pergamon Press, 1980

[2] Oliver Paish, "Small hydro power: technology and current status", Renewable and Sustainable Energy Reviews, vol. 6, pp. 537-556, 2002

[3] Fraenkel P, Paish O, Bokalders V, Harvey A., Brown A., Edwards R., "Micro-Hydro Power: A Guide for Development Workers", London: IT Publications Ltd, 1991.

[4] Amiro Peter G., Jansen Hans, "Impact of Low-Head Hydropower Generation at Morgans Falls, LaHave River on Migrating Atlantic Salmon", Diadromous Fish Division, Maritimes Science Branch, Department of Fisheries and Oceans, Dartmouth, Nova Scotia, Canadian Technical Report of Fisheries and Aquatic Science No.2323, 2000

[5] Alexander N. Gorban, Alexander M. Gorlov, Valentin M. Silantyev, "Limits of the Turbine Efficiency for Free Fluid Flow", Energy Resources Technology, 2001, vol. 123 pp.311-317

[6] Ackermann, T., Soder, L., "An Overview of Wind Energy–Status 2002", Renewable and Sustainable Energy Reviews, vol. 6, pp. 67–127, 2002

[7] Iniyan, S., Jagaeesan, T. R., "Effect of Wind Energy System Performance on Optimal Renewable Energy Model - An Analysis", Renewable and Sustainable Energy Reviews, vol. 2, no. 4, pp. 327 – 344, 1998

[8] Setoguchi, T., Kinoue, Y., Kim, T. H., Kaneko, K., Inoue, M., "Hysteretic Characteristics of Wells Turbine for Wave Power Conversion", Renewable Energy, vol. 28, pp. 2113 – 2127, 2003

[9] Ocean Wave Energy, Kelly J. Kimball, "Embedded Shoreline Devices and Uses as Power Generation Sources", 2003

<http://classes.engr.oregonstate.edu/eecs/fall2003/ece441/groups/g12/>

[10] Kim, T. H., Setoguchi, T., Kaneko, K., Raghunathan, S., "Numerical Investigation on the Effect of Blade Sweep on the Performance of Wells Turbine", Renewable Energy, vol. 25, no. 2, pp. 235 – 248, 2002

[11] Setoguchi, T., Santhakumar, S., Takao, M., Kim, T. H., Kaneko, K., "Effect of Guide Vane Shape on the Performance of a Wells Turbine", Renewable Energy, vol. 23, no. 1, pp. 1 – 15, 2001

[12] Maalawi, K. Y., Badawy, M. T. S., "A Direct Method for Evaluating Performance of Horizontal Axis Wind Turbines", Renewable and Sustainable Energy Reviews, vol. 5, no. 2, pp. 175 – 190, 2001

[13] Grassmann, H., Bet, F., Ceschia M., Ganis, M. L., "On the Physics of Partially Static Turbines", Renewable Energy, vol. 29, no. 4, pp. 491 – 499, 2004

[14] Grassmann, H., Bet, F., Cabras, G., Ceschia, M., Cobai, D., DelPapa, C., "Partially Static Turbine – First Experimental Results", Renewable Energy, vol. 28, no. 11, pp. 1779 – 1785, 2003

[15] Thakker, A., Dhanasekaran, T. S., "Computed Effects of Tip Clearance on Performance of Impulse Turbine for Wave Energy Conversion", Renewable Energy, vol. 29, no. 4, pp. 529 – 547, 2004

[16] Thakker, A., Hourigan, F., "Modeling and Scaling of the Impulse Turbine for Wave Power Applications", Renewable Energy, vol. 29, no. 3, pp. 305 – 317, 2004

[17] Mansouri, M., Mimouni, M., Benghanem, B., Annabi, M., "Simulation Model for Wind Turbine with Asynchronous Generator Interconnected to the Electric Network", Renewable Energy, vol. 29, no. 3, pp. 421 – 431, 2004

[18] Bahaj, A. S., Myers, L. E., "Fundamentals Applicable to the Utilisation of Marine Current Turbines for Energy Production", Renewable Energy, vol. 28, no. 14, pp. 2205 – 2211, 2003

[19] Guy Dauncey, "The Call of the Moon- Earth's New Season",

<http://www.commonground.ca/iss/0301138/12_dauncey.shtml>

[20] Hartono, W., "A Floating Tied Platform for Generating Energy from Ocean Current", Renewable Energy, vol. 25, no. 1, pp. 15 – 20, 2002

[21] Setoguchi, T., Santhakumar, S., Takao, M., Kim, T. H., Kaneko, K., "A Modified Wells Turbine for Wave Turbine for Wave Energy Conversion", Renewable Energy, vol. 28, no. 1, pp. 79 – 91, 2003

[22] Setoguchi, T., Santhakumar, S., Maeda, Takao, M., Kaneko, K., "Review of Impulse Turbines for Wave Energy Conversion", Renewable Energy, vol. 23, no. 2, pp. 261 – 292, 2001

[23] Blue Energy: Market Drivers

<http://www.bluenergy.com/marketdrivers.html>

[24] Blue Energy: Tribute to Barry Davis

<http://www.bluenergy.com/barrydavistribute.html>

[25] Renewable Energy/ Underwater Electric Kite

<http://uekus.com/index.html>

[26] Lindsay M.K. Melvin, "Small Hydro in Manitoba", University of Manitoba, Master Thesis, pp. 43, 2004

[27] Wasserrad und Turbine,

< http://www.udo-leuschner.de/basiswissen/SB107_03.htm>

[28] <http://www.engr.utexas.edu/uer/tidal/body.htm>

[29] Arne Kjølle, "Hydropower in Norway----Mechanical Equipment", Norwegian University of Science and Technology, Trondheim, 2001, pp.9.4-9.5

[30] Instream Energy Generation Technology,

<http://www.verdantpower.com/Tech/lowimpact.shtml>

[31] Alexander Gorlov, Kenneth Rogers, "Helical Turbine as undersea Power Source", Sea Technology, pp.39-40, 1997

[32] Ron Shannon, "Water Wheel Engineering",

<http://www.rosneath.com.au/ipc6/ch08/shannon>

[33] Abbott, Ira H. and Von Doenho., Albert, E, "Theory of Wing Sections", Dover Publications, Inc., 1959

[34] John Dreese, "The Totally FREE Airfoil Primer", <http://www.dreesecode.com/other/aflprimer.pdf>

[35] David F. Rogers, "Aerodynamic Characteristics of Airfoils", <http://web.usna.navy.mil/~dfr/wtlab3.pdf>

[36] Christophe Leclerc, Christian Masson, Idriss Ammara, Ion Paraschivoiu, "Turbulence Modeling of the Flow Around Horizontal Axis Win Turbines", Wind Engineering, Multi-Science Publishing Co. Ltd, 1999, pp279-294

[37] Dennis, B. H., Dulikravich, G. S., and Han, Z., "Constrained Shape Optimization of Airfoil Cascades Using a Navier-Stokes Solver and a Genetic/SQP Algorithm," ASME Paper No. 99-Gt-441, 1999,

[38] Pritchard, L. J., "An Eleven Parameter Axial Turbine Airfoil Geometry Model," ASME Paper No. 85-GT-219, 1985,

[39] Mansour T., Ghaly W., "An Implicit Geometric Representation of Turbine Blades Using NURBS", Proceeding of the 11th Annual Conference of the CFD Society of Canada, Department of Mechanical and Industrial Engineering, Conordia University, Montreal, QC, Canada, pp. 232 – 237

[40] Darrell W. Sproles, "Computer Program to Obtain Ordinates for NACA Airfoils", National Aeronautics and Space Administration Langley Research Center • Hampton, Virginia 23681-0001, 1996

[41] D.M. Somers, M.D. Maughmer, "Theoretical Aerodynamic Analyses of Six Airfoils for Use on Small Wind Turbines", National Renewable Energy Laboratory,

NREL/SR-500-33295, June 2003

[42] Philip J. Schneider, "NURB Curves: A Guide for the Uninitiated", <http://www.mactech.com/articles/develop/issue_25/schneider.html>

[43] German Aerospace Center, <http://www.pagendarm.de/trapp/programming/java/profiles/NACA4.html>

[44] Hanley's VisualFoil NACA, <http://www.hanleyinnovations.com/vfnaca.html>

Appendix -CAD Modeling of Blade Design

• Using AutoLisp

The following is the AutoLisp source codes written for creating NACA 3505.

```
(defun c:naca ()
  ;              Initialization and read data from the files
     (setq ptlst nil)
     (setq datafilex (open "c:/naca3505x.txt" "r"))
     (setq datafiley (open "c:/naca3505y.txt" "r"))
  ; opens file in read mode
               (repeat 198
               (setq px (read (read-line  datafilex)))
               (setq py (read (read-line  datafiley)))
               (setq pp (list px py))
               (setq ptlst (append ptlst (list pp)))
              ); end of the repeat loop
              (command "pline" (foreach pt ptlst (command pt)))
     (redraw)  (princ)
  ); end of defun
```

The graphic of the NACA 3505 produced by the codes is shown in Figure A-1. We notice that the curve approximately represented by a sequence of line segments has a relatively high resolution.

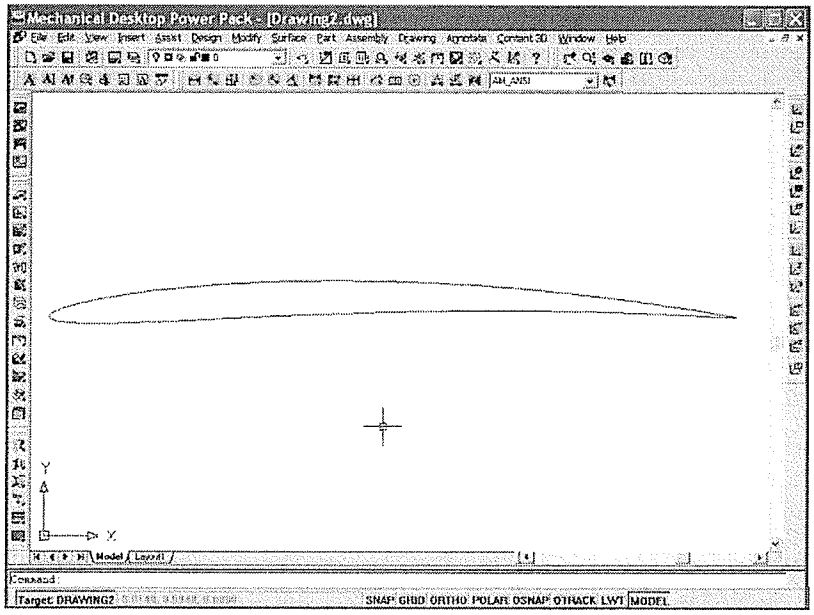

Figure A-1 NACA 3505 Curve Created by AuotoLisp

The rest NACA airfoils that will be distributed on multiple planes may be produced in the same way. They are illustrated in Figure A-2.

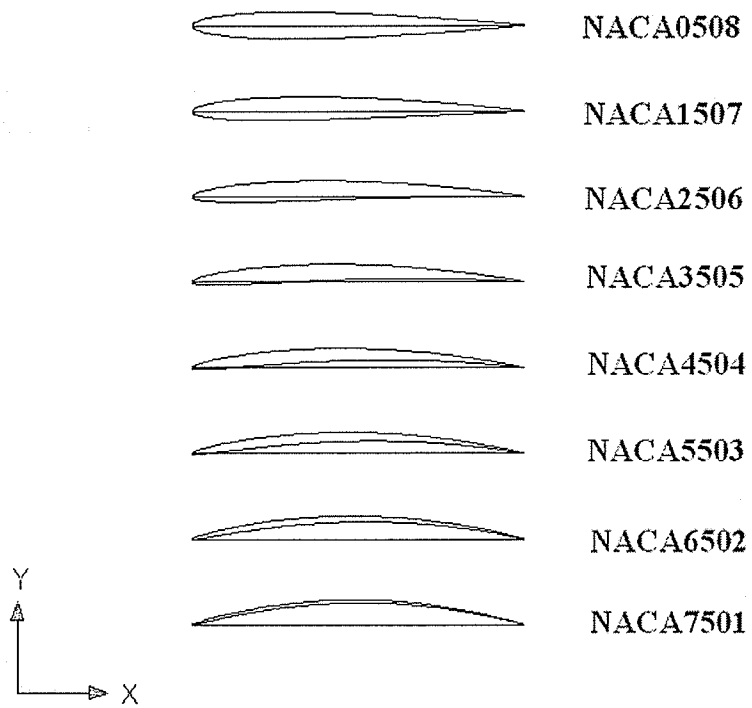

Figure A-2 NACA Curves Created by AuotoLisp

Provision is made for camber, center of camber, chord, skin thickness, spar and leading edge dimensions (in inches or millimeters).

• Modification of NACA Airfoils

There are several factors relating to the determination of the blade shape. By evaluating existing designs and testing results, it was found that the shape of the blade is the most important factor affecting the performance of the turbine runner. In addition to the blade section, other parameters are involved in the blade design, such as the attack angle of the individual airfoil, which usually vary in terms of different successive planes,

the distribution of space of the successive planes in the spanwise direction, the thickness transition from root to top, and the locations of blade sections related to the Cartesian coordinate. Generally, to effectively work on blade design, the following principles can be applied.

a) Airfoil Rotation

For a 3-D blade profile the attack angle of the airfoils vary on different cross-sectional planes. In blade design, those airfoils usually have a uniform distribution in terms of rotation angles, meaning equivalent angle between two successive airfoils. The airfoil can be rotated by choosing a base point and a relative or absolute rotation angle. Specify a relative angle to rotate it from its current orientation around the base point by that angle. Specify an absolute angle to rotate it from the current angle to a new absolute angle. The base point is specified as the midpoint of the chord.

Once a series of airfoils are rotated, the rest is to make their base points coincide. The result is shown below, in Figure A-3.

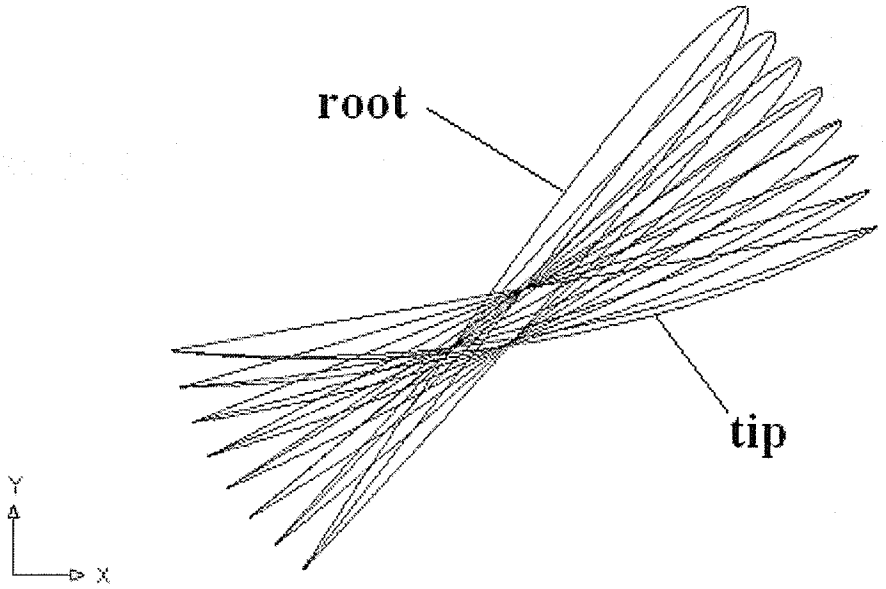

Figure A-3 Rotated NACA Curves

b) Chord Extension

The shape of a propeller blade rotated usually gives fan-shaped sector. The lengths of the chords gradually increase from root to tip. Although the NACA airfoils have less flexibility for modification, as mentioned earlier, some simple adjustments are allowed for optimization of the blade section. We can extend the length of a chord while keeping a constant thickness to constitute a fan-shaped blade. The scale factor essentially remains constant during the operation so that the length of the chord can evenly be enlarged in the spanwise direction and the surface of the blade can have a smooth transition from section to section. Figure A-4 shows a series of chord-scaled NACA profiles. We can see from the figure that the one on the root remains unchanged. The rests have increased chord lengths.

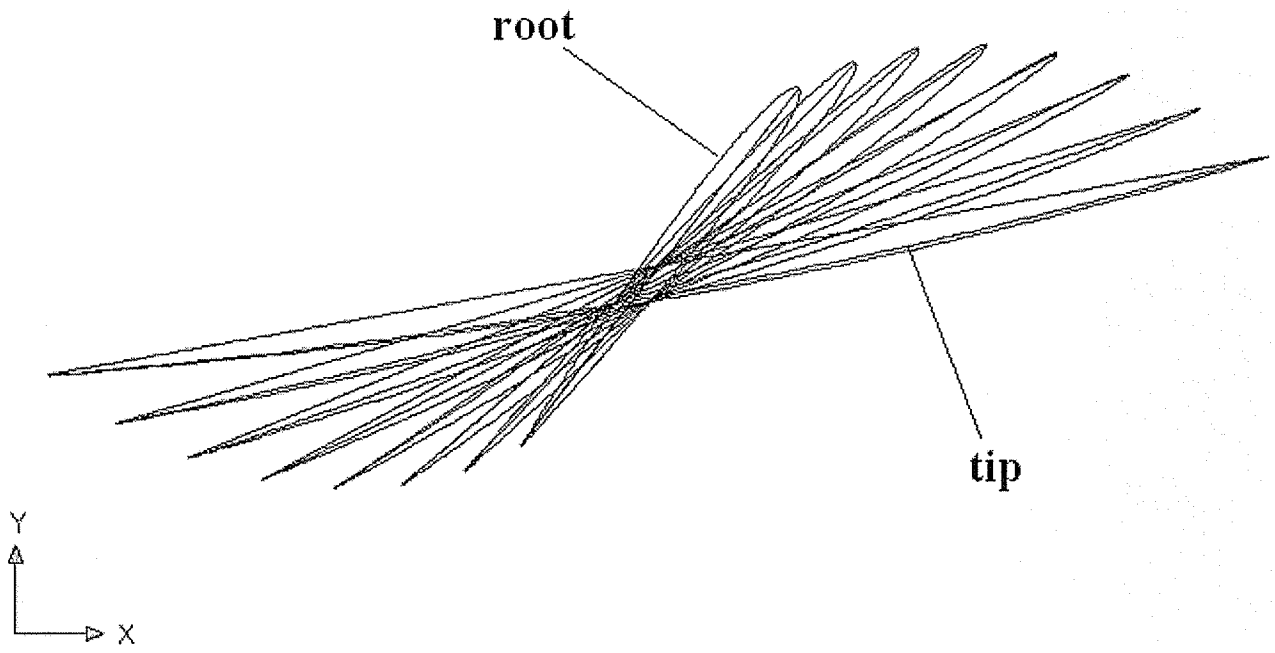

Figure A-4 NACA Curves Scaled in Chord Direction

c) Airfoil Realignment

Unlike compressor blades, run-of –the –river turbine blades can have very diverse shapes depending on the design requirements. For example, the location of the sections on X-Y plane can be changed instead of maintaining the original position. The objective of this work is to enhance the incline with respect to the rotation plane to confine the flowing water through the turbine runner and achieve higher performance.

The airfoils reposition in y direction in proper order, and remain the midpoints of the chords on the center line. The range for the realignment can be arbitrary depending on the technical specifications. However, the appropriate position must be where the distribution of the trailing edges of the airfoils constitutes a smooth curve, usually defined as a parabola. The rearranged airfoils are illustrated in Figure A-5. The smooth transition among the airfoils can be seen.

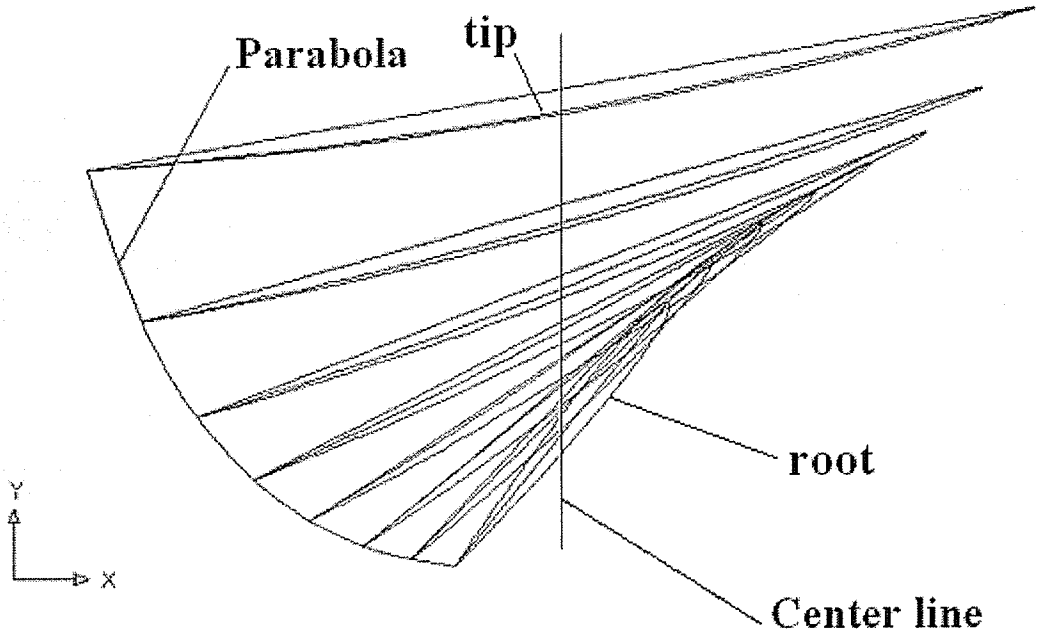

Figure A-5 Repositioned NACA Curves

• **Composition of Section Planes**

The numbers of the section planes are identified by the airfoil's numbers. The space is determined by the diameter of the turbine runner and the diameter of the hub, respectively. These planes have a uniform space and disperse in the spanwise direction orthogonal to the turbine axis. Once the section planes are built up, the airfoils will take up their individual positions. Figure A-6 shows the locations of the airfoils relative to the hub in 3-D space.

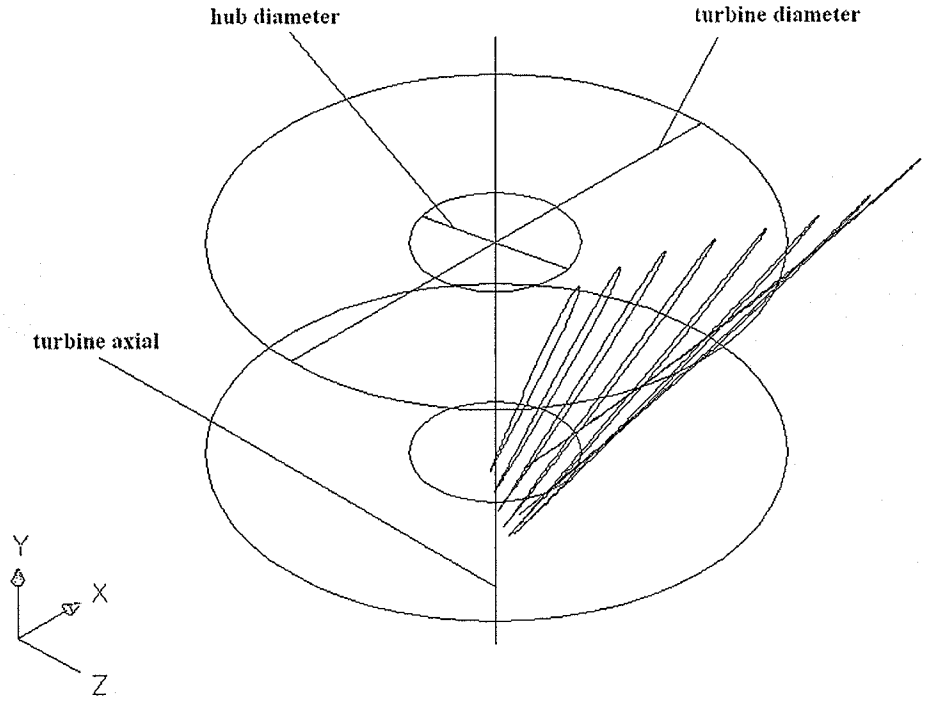

Figure A-6 Airfoils on Section Planes

• **Composition of Blade Surface**

After the blade sections are constructed they are converted to the corresponding blade surface in 3-D Cartesian space via the stacking procedure mentioned above. Thus when the blade section is defined in the two-dimensional X-Y space and located in their

individual planes, there are exact equivalent blade sections that lies directly on the blade surface (see Figure A-7).

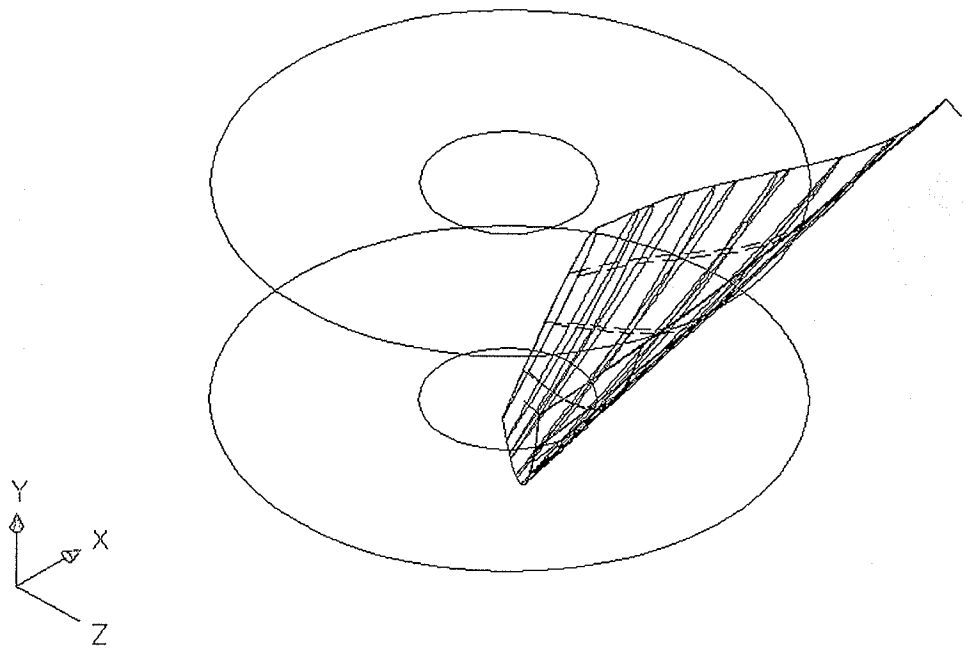

Figure A-7 Blade Section Conforming to 3-D Surface

In order to make the design of the blade as simple and effective as possible, we consider the cubic loft, the most powerful loft type, for design of the blade surface for the following reasons. (1) It gives the designer the most control over the shape and the start and end sections of the loft you are creating. (2) It creates gradual blends between the sections. (3) Its structure and shape are simple and easy to make. (4) It is possible to model and analyze the turbulence and cavatation process for a turbine runner by using related computer aided software, such as CFX and Fluent.

• **Surface Modification**

The blade surface created in a way is not suitable for practicable conditions hence necessary modifications are needed. In this case, it is obvious that the contour of the blade surface does not fit the turbine runner. A simple approach for the adaptation is to trim it to obtain a desired shape of the blade. Another surface that intersects the original blade surface is created in a very simple method. We can begin with creating of a closed loop via splines on a plane vertical to the turbine axis, and then extrude them in the axial direction. The surface created in this way is a 2-D surface and has uniform sections on truncated planes parallel to the plane the loop formed on. The 2-D surface is defined as a cutting edge at which we want to trim the blade surface as shown in Figure A-8.

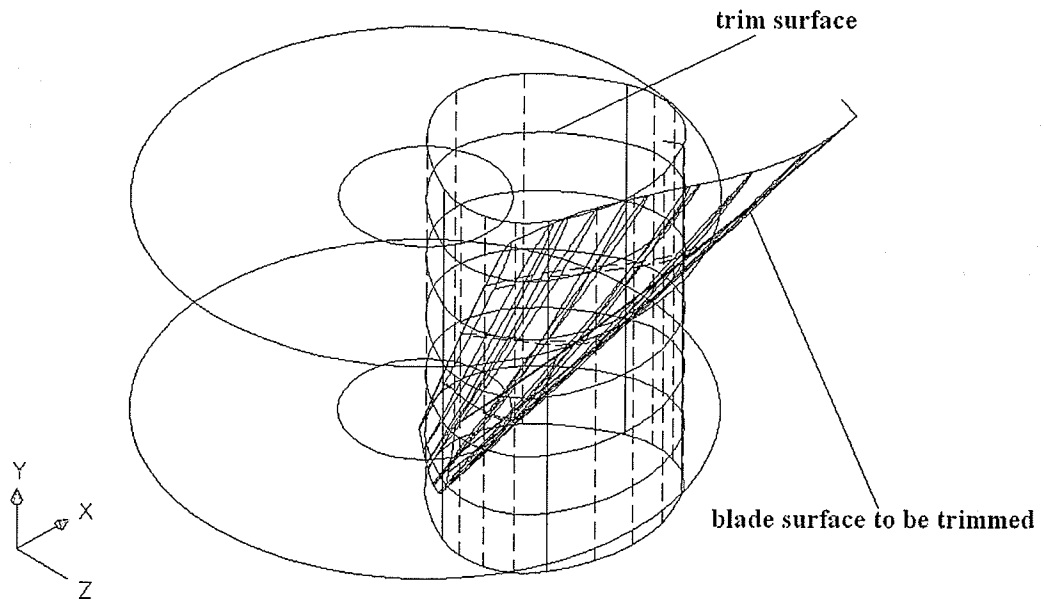

Figure A-8 Blade Surface to be Trimmed

Figure A-9 shows that TRIM projects the cutting surface and the blade surface to be trimmed onto the *X-Z* plane of the current user coordinate system.

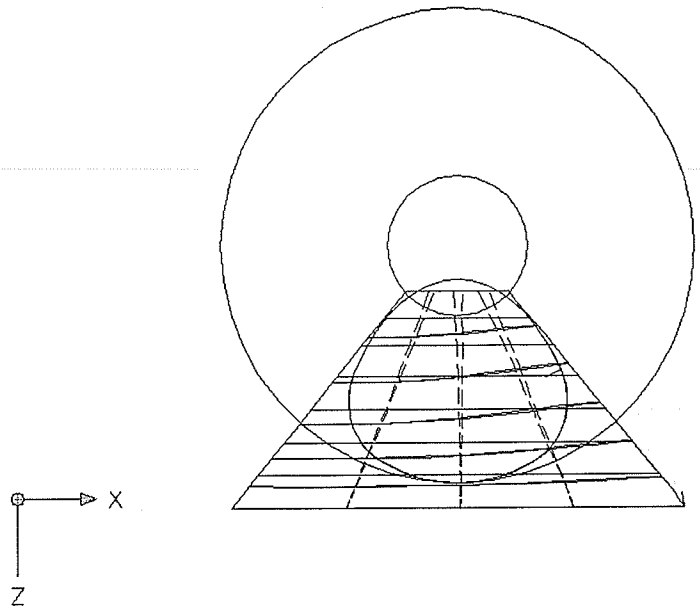

Figure A-9 Top View (Projections of Cutting Surface and Blade Surface)

Figure A-10 demonstrates a 3-D virtual model of the blade profile after the TRIM operation has been done.

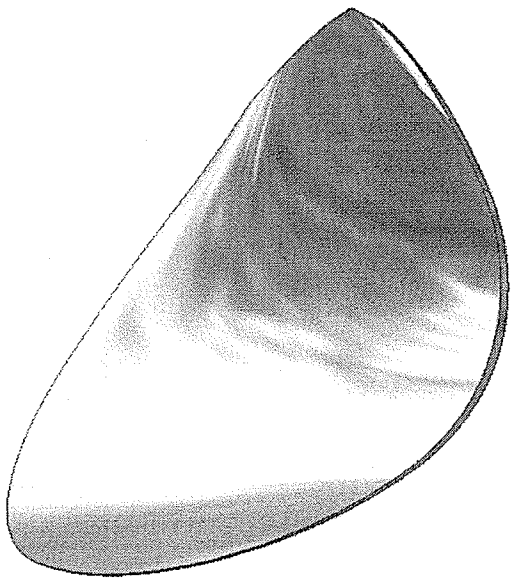

Figure A-10 Blade Profile Modeling